Preparation and Evaluation of a Thermosensitive Hydrogel for the Nasal Delivery of Insulin

Hamde Nazar

The thesis is submitted in partial fulfilment of the requirements for the award of the degree of Doctorate of Philosophy of the University of Portsmouth.

February 2012

Contents

List of Figures

Chapter One: Introduction

Chapter Two

Chapter 3

Chapter Four

List of Tables

Glossary of Terms

AFM	Atomic Force Microscopy
ATR	Attenuated total reflectance
BET	Brunauer-Emmett-Teller
BJH	Barrett-Joyner Halenda
Calu 3	Human airway epithelial cell line
DQ	Degree of quaternisation
DSC	Differential scanning calorimetry
G*	Complex modulus
G’	Elastic or storage modulus
G”	Viscous or loss modulus
GP	Glycerphosphate
IR	Infra-red
MCC	Mucociliary clearance
MTR	Mucociliary transport rate
NMR	Nuclear magnetic resonance
PEG	Poly(ethylene) glygol
SDS PAGE	Sodium dodecyl sulfate polyacrylamide gel electrophoresis
SNES	Simulated nasal electrolyte solution
SPH	Superporous hydrogel
SPHC	Superporous hydrogel complex
TEER	Transepithelial electrical resistance
TMC	N-trimethyl chitosan chloride
XRD	X-ray diffraction

Declaration

Whilst registered as a candidate for the above degree, I have not been registered for any other research award. The results and conclusions embodied in this thesis are the work of the named candidate and have not been submitted for any other academic award.

Word Count: 33,559.

Acknowledgements

'If you knew what you were doing, it wouldn't be research'.

Einstein

I wish I had known this at the beginning, middle or anytime during my PhD, it might have been reassuring!

To those who were my Einsteins along my journey I would like to thank first and foremost my PhD supervisors: Marisa van der Merwe, Marta Roldo, Dimitris Fatouros and John Tsibouklis. You have provided me with guidance, support, and advice that has been most valued and appreciated. Other members of the Faculty to whom I would like to extend my gratitude for their moral and technical advice and support are to: James Smith; Eugene Barbu; Brian Carpenter and Michael Norris.

I would also like to extend thanks to those who helped with experiments that would have otherwise not been possible: Prof Paolo Caliceti and his research colleagues, University of Padua, Italy, for the *in vivo* diabetic studies; Prof Abdullah El-Mallah and his research colleagues, Beirut Arab University, Lebanon, for the *in vivo* nasal clearance studies; Assistant Prof Nikolas Bouroupolous and G. Avgeropoulos, Institute of Chemical Engineering and High Temperature Chemical Processes and the University of Patras, Greece, for the data pertaining to the XRD, TGA and porosity.

Thanks also go to Christopher Young, Chun Fu Lien, Dimitris Lamprou, and Eva Molnar as fellow PhD students and post-doctorates that provided technical, knowledgeable and moral advice and support.

The kind assistance of the technicians in the Faculty of Pharmacy to perform NMR and provided training and supervision on equipment and procedures: Jill Rice, Val Ferrigan and Darren Gullick.

Motivational wellbeing has been largely due to the care of many of the academics previously mentioned, but also to fellow researchers: Sarah Upson and Petr Toman, and to the external network of friends who were always happy to listen to the trials and tribulations and share the highlights and successes of this PhD.

Lastly, I would like to express my gratitude to my parents, brothers and sister who were always encouraging and supporting me to continue and persevere and helped me in all aspects of my life.

Dissemination

Publications

H. Nazar, D. Fatouros, S. van der Merwe, M. Roldo, J. Tsibouklis. Hydrogels for Mucosal Delivery. Therapeutic Delivery (2012) 3(4) 535-555.

H. Nazar, D. Fatouros, S. van der Merwe, N. Bouropoulos, G. Avgouropoulos, J. Tsibouklis, M. Roldo. Thermosensitive hydrogels for nasal drug delivery: The formulation and characterisation of systems based on *N*-trimethyl chitosan chloride. European Journal of Pharmaceutics and Biopharmaceutics (2011) 77(2).

Conference presentations

H. Nazar, D. Fatouros, S.M. van der Merwe, M. Roldo: Thermosensitive hydrogel formulations containing N-trimethylchitosan (TMC) chloride for nasal drug delivery. In: 36th Annual Meeting and Exposition of the Controlled Release Society, Copenhagen, Denmark (2009) Oral presentation.

H. Nazar, D. Fatouros, S.M. van der Merwe, M. Roldo: Thermosensitive and mucoadhesive hydrogel formulations containing *N*-trimethylchitosan chloride (TMC) for nasal drug delivery. In: 7th World Meeting on Pharmaceutics, Biopharmaceutics and Pharmaceutical Technology, Valletta, Malta (2010) Oral presentation.

H. Nazar, D. Fatouros, S.M. van der Merwe, M. Roldo: *In vitro* investigations of a thermosensitive, mucoadhesive hydrogel based on *N*-trimethylchitosan chloride for nasal drug delivery. In: Recent Advances in Pharmaceutical Research and Technology International Conference, Beirut Arab University, Lebanon (2010) Oral presentation.

H. Nazar, D. Fatouros, S.M. van der Merwe, M. Roldo, J.Tsibouklis: *In vitro* and *in vivo* investigation of a thermosensitive, mucoadhesive *N*-trimethylchitosan chloride (TMC) based nasal hydrogel. In: 8th World Meeting on Pharmaceutics, Biopharmaceutics and Pharmaceutical Technology, Istanbul, Turkey (2012) Poster presentation.

General Abstract

Towards the development of a drug delivery vehicle for the nasal delivery of insulin, *N*-trimethyl chitosan has been co-formulated with poly(ethylene glycol) and glycerophosphate into a thermosensitive hydrogel structure, the sol-to-gel transition properties of which occur at physiologically relevant temperatures over optimally brief timescales. *In vitro* experiments mimicking those of the nasal environment have indicated the dual capability of the formulation to affect the opening of tight junctions and to release its therapeutic content in a controlled manner, while spectroscopic and analytical investigations have indicated the structural integrity of the incorporated insulin. The *in vivo* potential of this *in situ* thermogelling nasal formulation to act as a once-a-day dosage form for the intranasal delivery of insulin has been demonstrated in the diabetic rat model.

Chapter One: Hydrogels in Mucosal Delivery

Hydrogels in Mucosal Delivery

Abstract

The concept of mucoadhesion and the molecular design requirements for the synthesis of mucoadhesive agents are both well understood, and as a result hydrogel formulations that may be applied to mucosal surfaces are readily accessible. Nano-sized hydrogel systems that make use of biological recognition or targeting motifs, by reacting to disease-specific environmental triggers and/or chemical signals to effect drug release, are now emerging as components of a new generation of therapeutics that promise improved residence time, faster response to stimuli and trigger release.

1.1. Mucosal membranes

Mucosal surfaces are rendered attractive for the delivery of drugs by their: high degree of vascularisation; generally thin layers of epithelial cells; large surface-area to volume ratios; and, with exception of the oral route, avoidance of the first-pass metabolic effect. The impetus for research in transmucosal drug delivery is provided not only by the ongoing drive to improve the delivery of existing low-molecular-weight drugs and therapeutic macromolecules [1] but also by the need to evolve effective dosage forms for the delivery of emerging biologics. It has been suggested that the efficacy of many therapeutic agents may improve if they were to be delivered specifically through the nasal [2-5], pulmonary [6], buccal [7-10], oral [11-13], vaginal [14-16], rectal [17] or ocular [18, 19] routes.

Human mucosal membranes have a collective surface area of 400 m^2 [20], and consist of a thin layer of differentiated epithelial cells that are attached basally to the basement membrane, which separates the epithelium from the underlying connective tissues (*lamina propia*). The basal cells of this basement membrane are packed closely, forming a robust barrier to most microorganisms but also to drug absorption. Some of the physiological features characterising each mucosal membrane are presented in Table 1.

Table 1. Physiological features of mucosal membranes and the associated barriers to penetration.

Mucosal membrane	Cells of the epithelia	Surface area	Mucus	Additional barriers	Temp/ °C	pH	Refs
Ocular	Corneal epithelium: 5-6 layers of cells; basally columnar with tight junctions (TJ) that differentiate as flattened polygonal cells with microvilli. Cornea impermeable to molecules > 5kDa. Conjunctival epithelium: 5-7 cell layers, including goblet cells. TJ at surface. Conjunctiva is permeable to macromolecules <20 kDa.	16.3 cm^2	Daily production, 2-3 µL; mucus turnover, 15-20 h; pre-corneal film (10 µL) made up of a superficial lipid layer, a central aqueous layer and an inner mucus layer (3-10 µm thick).	Nasolacrymal drainage consisting of secretory, distributive and collection parts. Tears spread over surface; collection at canaliculi, lacrimal sac, nasolacrimal sac and nasolacrimal duct leading to nasal passage. Basal tear flow, *ca*. 1.2 µL/min; turnover rate 16%/min, but highly sensitive to reflex stimulation (up to 100-fold).	34	7.4 with diurnal changes from acid to alkaline	[21-23]
Buccal	Buccal: non-keratinised stratified squamous epithelium, 40-50 cell layers thick (500-600 µm); blood flow 2.4 mL/min. Sublingual: non-keratinised stratified squamous epithelium, *ca*. 100-200 µm thick; blood flow 0.97 mL/min.	Oral cavity 100 cm^2. Buccal 50.2 cm^2	Thickness, 40-300 µm. Mucus turnover 12-24 h. Saliva film, *ca*. 70 µm thick; resting flow rate, 1-2 mL/min.	Permeability barrier due to membrane-coating granules (MCGs), which cause membrane thickening, cell adhesion, deposition of a coating on the cells, and cell desquamation. Salivary scavenging and accidental swallowing. Residence time < 5-10 min.	32-37	Average: oral, 6.78, buccal, 6.28	[7, 8, 24-26]
Gastro-intestinal	Single layer of columnar epithelium, with TJ. Also present: Peyer's patches of the gut-associated lymphoid tissue (GALT); these are lined with specialised epithelium-containing microfold (M) cells.	Small intestine 200m^2	Two forms in stomach: insoluble mucus protects underlying cells from gastric acid; soluble mucus is derived from degraded insoluble mucus.	High rate of mucus turnover, broad transit time, enzymatic degradation, hepatic first-pass metabolism, luminal degradation.	Oesophageal approx. 37	Stomach, pH1-3; intestine pH6-7	[11, 23, 27-29]
Nasal	Anterior: stratified, keratinised, non-ciliated squamous cells with sebaceous glands. Olfactory (found posteriorly): ciliated olfactory nerve cells, 200-400 mm^2. Respiratory: ciliated and non-ciliated columnar cells; goblet and basal cells. Polar drugs <1 kDa are transportable *via* a paracellular mechanism.	150 cm^2	Resting-state daily production at 75-150 mL; mucus blanket, *ca*.5µm thick.	Mucociliary clearance (MCC) *ca*. 4-6mm/min; dimensions of nasal cavity restrict volume to 100-500 µL; enzymatic activity.	32-35	6	[3, 5, 30-33]
Pulmonary	Bronchi: ciliated and goblet cells. Bronchioles: ciliated cuboidal cells; fewer goblet cells. Alveolar: simple squamous; no mucus; 0.1-0.5 µm thick.	100 m^2	Tracheobronchial (TB) region: thickness, 0.5-5 µm; absent in alveoli.	TB region with MCC removing particles and dissolved drugs entrapped in mucus within a few hours.	Trachea 34-37	Exhaled breathing condensate 7.6	[34-38]
Vaginal	Non-cornified, stratified squamous epithelial cells (thickness, 200-300µm); no goblet cells. Extends from uterus to the external genitalia.	6-10 cm (length) × *ca*. 2 cm (width). Holds 2-3g of liquid	Flow rate of vaginal fluid, 2-3 g/day.	Rapid removal from the site of application *via* discharge; poor spreading of administered mucoadhesive.	37.2	3.5-4.5 influenced by age, menstrual cycle, infections, and sexual arousal	[23, 39-41]

1.2. Absorption pathways

- ### Types

The effective permeability of each type of mucosa varies according to the type of cells that make up the epithelia that cover the basement membrane. Four possible mechanisms of transport across mucosal membranes have been identified: simple diffusion (transcellular and paracellular); carrier-mediated diffusion; active transport; and, pinocytosis or endocytosis [27]. It is generally accepted that the key mode for the transference of materials is passive transport, but this is highly influenced by the nature of the permeant molecule (structure, conformation, charge, lipophilicity). Transcellular transport is primarily favoured by small lipophilic molecules, which diffuse through the cells from one side of the barrier to the other. Large, charged, hydrophilic molecules may be transported paracellularly. In general, however, the free flow of material from the apical lumen into the blood stream is inhibited by tight junctions and the associated junctional complexes that are localised between neighbouring cells [27]. Consequently, drug-delivery strategies often attempt the transient disruption of the conformation of protein subunits to allow the passage of drug molecules that would otherwise be excluded.

- ### Barriers to penetration across the mucosa

The common feature shared by mucosal membranes (basement membrane, the associated layers of epithelial cells and the overlying layer of proteinaceous-glycol mucus) is the barrier to absorption. Additional specialised protective and/or locomotive mechanisms may also operate within each mucosal membrane, Table 1.

• Mucus

Apart from water (>95 %), mucus is comprised mainly of exceptionally high molecular weight glycoproteins (mucins; 2-14 x 10^6 g/mol) and relatively small proportions (*ca*. 1%) of proteins, mucopolysaccharides, lipids and inorganic salts [42, 43]; it is the glycoproteins that impart gel-like characteristics to mucus [42]. The mucus glycoproteins may be considered as graft polymers consisting of a protein backbone and pendent oligosaccharide chains comprised of sugar residues (fucose, galactose, *N*-acetylgalactosamine, *N*-glucosamine and sialic acid) [7]. Owing to their low pK_a, sialic acid and sulphated sugar moieties exist in their fully ionised forms at physiologically relevant acidic conditions, rendering mucus negatively charged [44]. The barrier properties stem from the dense glycoproteinic component, which bestows mucus with significant water-holding capacity and imparts resistance to proteolysis [7].

Mucus is secreted by goblet cells, which are glandular epithelial cells found in all mucosal linings that may become exposed to the external environment. The mucins are stored in goblet cells and in submucosal cells where their negative charges are counterbalanced by the reservoir of calcium ions to form a tightly packed structure. Secretion into the lumen is accompanied by an outflux of calcium ions and the consequent establishment of intramolecular electrostatic repulsions, which stem from the negative charges that are localised along the mucin molecule. This results in a *ca*. 400-fold expansion in molecular size, but chain entanglement and the structuring of water around individual mucin molecules give mucus its characteristic viscoelastic gel structure [43].

In addition to acting as a barrier to solids, mucus functions as a permeable lubricating gel that maintains hydration and allows the transfer of gases and nutrients to the underlying epithelium [43].

1.3. Mucoadhesion

- ### Interactions facilitating mucoadhesion

Bioadhesion is the adherence of a material to a biological surface for an extended period of time; if that biological surface is covered with a layer of mucus, the term mucoadhesion is used [8, 42, 43, 45]. Owing to the complexity of the process of mucoadhesion, several theories have been proposed to explain its mechanism [7, 8, 43, 45], Fig. 1. These are the: electronic theory, in which adhesion is explained in terms of the electron transfer across the double layer of electrical charge that is established at the interface of two interacting surfaces; adsorption theory, where the dominant surface forces are considered to be van der Waals' interactions and hydrogen-bond formation; wetting theory, which assumes the interaction between mucus and mucoadhesive to be a process that is dominated by structural similarity, complementary degrees of cross-linking and the surface-tension-lowering action of surfactants; diffusion theory, in which chain interpenetration is regarded as the main mode of interaction between the mucus and the mucoadhesive; and, fracture theory, where the adhesive force between the interacting systems is treated as consequential to the interfacial energy [43, 45].

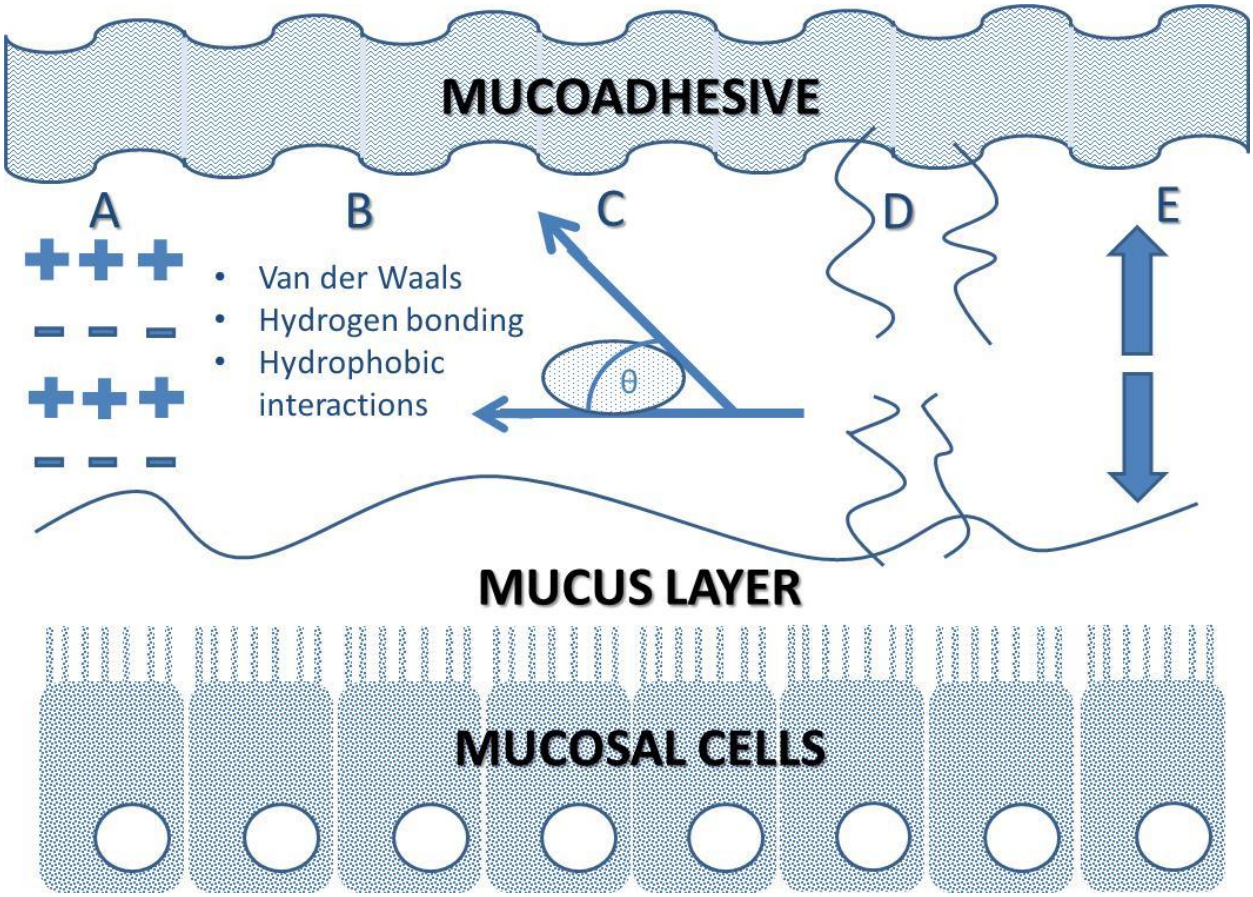

Figure 1. Schematic representation of mucoadhesive behaviour: A) electronic theory; B) adsorption theory; C) wettability theory; D) diffusion theory, and E) fracture theory.

- ## Factors influencing mucoadhesion

Mucoadhesive drug delivery has been rationalised in terms of its potential to maintain a therapeutic molecule at a mucosal site for a prolonged period of time [23]. The concept of mucoadhesive interactions evolved from a suggestion by Ishida *et al*. [46] who demonstrated the increased bioavailability of a polymer-containing intranasal peptide preparation, and further suggested that polymers may be used in formulations of anti-inflammatory treatments for ankle injuries or in those for the local treatment of cervical cancer. Since mucoadhesive behaviour is determined both by the nature of the bioadhesive polymer and by that of the aqueous medium that is necessary for its

delivery to the mucosal surface, each mucoadhesive delivery system needs to be optimised according to the local environment of the target mucoadhesive surface [45].

- ## Functional group contribution

It is well accepted that polymers possessing functional groups that can interact with the glycoprotein component of mucins *via* hydrogen bonding (carboxyl, -COOH; hydroxyl, -OH; amino, $-NH_2$; and sulphate groups, $-SO_4H$) are effective mucoadhesive agents [43]. The archetypal mucoadhesive agent is poly(acrylic acid), which interacts with mucus not only by the hydrogen bonds that form between the carboxyl groups of poly(acrylic acid) and the sialic residues of mucin glycoproteins but also by favourable interactions of the van der Waals' type. Hagesaether and Sande [47] examined the significance of hydrogen bonding within the process of mucoadhesion by considering the effects of added urea, a well-accepted hydrogen bonding disruptor, to mucus/pectin mixtures: the considerable reduction in mucoadhesive behaviour was manifested as a decrease in cohesion and as loss of rheological synergy [47]. Additional to the instantaneous contributions of ionic, hydrogen and van der Waals' interactions, the time-dependent establishment of covalent bonding may also play a role in certain, appropriately functionalised mucoadhesive systems [48]. It has been suggested [48], within the context of mucus-turnover time, that such covalent interactions strengthen mucoadhesion.

- ## Degree of hydration

It has been observed that mucoadhesion is facilitated by the ready hydration and the capacity of a mucoadhesive polymer to swell rapidly but to a limited extent [8, 49]. The wetting theory accounts for this observation in terms of the associated water-induced decrease in the barrier to rotation of the hydrated polymer and the consequent enhancement of its capacity for chain interpenetration with the underlying mucus [23, 43]. The significance of rapid but limited swelling is exemplified by the work of Xiang *et al.* [50] who investigated the relationship between hydrophilic-lipophilic

balance (HLB) and mucoadhesive behaviour for a range of poly (acrylic acid-polyethylene glycol monomethylether monomethacrylate dimethylaminoethyl acrylate). It was observed that above a certain degree of hydration, polymers adopt an extended chain structure that inhibits their propensity to establish mucoadhesive interactions by limiting their capacity to become entangled with mucus glycoproteins.

- ## Structural characteristics of polymeric mucoadhesives

The mucoadhesive behaviour of a polymeric mucoadhesive is sensitive to its average molecular weight, chain length, conformation and degree of crosslinking [49, 51]. Whilst a high average molecular weight is a general prerequisite to macromolecular-chain entanglement, excessively crosslinked polymer structures may become too rigid to form such interactions with mucus molecules [43]. The optimal range of average molecular weight is unique to each polymeric mucoadhesive: poly (acrylic acid) is reported to be optimally mucoadhesive at *ca*. 750 kDa, whilst poly(ethylene oxide) interacts most efficiently with mucus if it has an average molecular weight of *ca*. 4,000 kDa. In the case of chitosan, there is a direct relationship between average molecular weight and mucoadhesive efficiency [52], whilst dextran exhibits the same bioadhesive strength at *ca*. 19,500 kDa as it does at 200 kDa (this has been explained in terms of the shielding of the potential bioadhesive sites of the higher molecular weight structure as a result of its coiled-helix conformation) [43].

- ## Charge and pH

Although it is generally accepted that non-ionic polymers are not as mucoadhesive as ionisable structures, this needs to be considered within the context of the pH of the physiological environment within which the polymer must display its mucoadhesive behaviour. In view of the toxicity that is sometimes associated with polycationic structures, polyanions are considered as the bioadhesive materials of choice for all such applications [8, 43]. Studies on poly(acrylic acid)s have

shown that these materials, although optimally mucoadhesive in their fully protonated form, continue to exhibit mucoadhesive behaviour under all physiologically relevant pH environments [23, 43].

- ## Polymer concentration

The physical state of the delivery system, and consequently the concentration of the mucoadhesive polymer in the formulation, is of some significance [51], especially in semi-solid dosage forms [43]. Concentration at the site of action is also of significance, as is exemplified by the work of Madsen *et al*. [53] who reported that the optimal polyacrylic acid concentration for ocular preparations is in the range 0.05-0.2% w/v. Andrews *et al.* state that for a semi solid state, an optimum concentration exists for the polymer beyond which reduced adhesion occurs due to fewer polymer chains available to interpenetrate with mucus. In solid dosage forms an increase in polymer concentration can result in increased adhesive strength as is demonstrated by buccal tablets.[54]

- ## Environmental factors

The physiological environment (mucus thickness, pH, mucus turnover) are all factors influencing mucoadhesive behaviour [5], Table 2 [43, 45].

Table 2. Environmental factors influencing mucoadhesive behaviour

Factors	Comments
pH	The extent of protonation is proportional to the electrical charges localised along the mucus backbone, which in turn impact upon the strength of the mucoadhesive interaction.
Mucin turnover	The residence time of a mucoadhesive drug delivery system may in some cases be limited by mucus turnover, which may in turn reflect circadian rhythms.
Disease states	Certain conditions (e.g. common cold, cystic fibrosis, gastric ulcers, ulcerative colitis, inflammation) alter the physicochemical properties of mucus.
Mucus thickness and viscosity	Thick layers favour polymer/mucus bond formation but greater thickness presents a more robust barrier to drug absorption. Low-viscosity mucus is associated with weak mucoadhesive interactions; increased viscosity augments the barrier to drug diffusion.

1.4. The assessment of mucoadhesive behaviour

Since no standard test methods are recognised for the evaluation of mucoadhesion, researchers normally report the relative mucoadhesion efficiencies of materials in terms of a ranking order that is specific to the *in vitro* or *in vivo* method used for the determination. Although there are considerable variations within the relative mucoadhesive efficiencies reported by different research groups, the ranking positions of individual classes of mucoadhesive materials do not appear to be sensitive to the methodology adopted for the evaluation.

- ***In vitro* methods**

The most widely used method for the assessment of mucoadhesion involves the determination of the force, and the associated work of adhesion, that is required to detach a material from a biological substrate. In an early attempt to quantify mucoadhesion, Smart *et al.* [55] studied a range of polymers using an adaptation of the Wilhelmy plate technique, a technique that provides a measure of the work done on passing a plate coated with a mucoadhesive polymer through the mucus/air interface [56].

A readily accessible means for the evaluation of mucoadhesion is tensile testing. The use of dual tensiometers has been claimed to allow the modelling of the effects of the shear stresses that operate at the site of administration [57], while the use of texture analysers has allowed the study of the relationship between mucus/mucoadhesive contact time and force of adhesion [58]. Experiments in which a mucoadhesive is brought into contact with excised biological mucosa and the force of detachment is measured are now considered routine in the assessment of the mucoadhesive potential of a material [44, 50, 59].

The rheological profile of the polymer-mucin mixture is a powerful *in vitro* model of mucoadhesive behaviour [53]. The development of rheological synergism in such mixtures is a pre-requisite to mucoadhesive interaction [43]. The concept was pioneered by Hassan and Gallo [60] who studied the mucoadhesive capacity of a range of polymers by comparing the rheology of binary polymer/mucus mixtures with those of mono-component mucus and polymer systems. Work by Madsen *et al.* [53] has demonstrated the importance of polymer type and concentration in the development of synergistic effects with mucus. Further work by the same group established that the mucus mixtures of polymers capable of mucoadhesive behaviour exhibit rheological profiles that are characteristic of a weakly cross-linked gel network, and that gel strengthening is influenced by the acidity of the local biological environment [42]. Consequent to these findings, the rheological evaluation of mucus-mucoadhesive mixtures is considered integral to the study of such systems [61, 62].

Comparative studies of tensile mucoadhesive testing and shear rheological tests using three poly(acrylic acid)-based polymers and reconstituted mucus have shown that the two techniques give the same rank order of mucoadhesion, highlighting the complementarity of the two techniques in the evaluation of this property [63-65].

The use of fluorescent probes has found some applications in the evaluation of ocular [43] and oesophageal [66] formulations. Infrared spectroscopy in attenuated total reflectance (ATR) mode

[67] has provided evidence in support of the theory of chain interpenetration at the poly(acrylic acid)/mucin interface. The same mucus/mucoadhesive system has been studied by Patel *et al*. [68] who have reported that combined data from infrared, ^{1}H and ^{13}C nuclear magnetic resonance (NMR), X-ray photoelectron spectroscopy (XPS) and differential scanning calorimetry (DSC) studies support the hypothesis that in such mixtures the mucus tends to encapsulate the mucoadhesive agent, and that there are fewer H-bonded interactions between the interacting materials than within the bulk of the pure mucoadhesive polymer. The same workers have provided spectroscopic evidence that the pH of the medium influences the structures of both the poly(acrylic acid) and the mucus, which, in turn, determine the nature and the extent of mucoadhesive interactions.

Following earlier atomic force microscopy (AFM) work by Sriamornsak *et al*. [69], Joergensen *et al*. [70] employed the techniques of AFM and surface plasmon resonance (SPR) to assess the mucoadhesive characteristics of pectins. Esposito *et al.* [71] and Lehr *et al*. [72], who investigated the relationship between surface energy and mucoadhesive behaviour, report a direct correlation with corresponding results from the tensile testing of adhesive strength. Since a correlation was unmasked between the fractional surface polarity of the substrate (pig small intestine mucus gel) and the mucoadhesive (polycarbophil), it has been concluded that the consideration of surface energy data needs to be integral to strategies for the development of improved mucoadhesive materials, not least because of their effect on the control of spreading processes [71, 72].

A method that monitors the zeta potential of the suspension formed when mucin powder is added to solutions of methylated N-aryl chitosan derivatives has been developed by Takeuchi *et al.* [73], who report that the change in the zeta potential of mucin particles correlates with increased interactions between the substrate and the mucoadhesive [74].

Using a polyether-modified poly(acrylic acid), Cleary *et al.* [75] combined data from AFM, tensiometric force measurements and advancing contact angle determinations to assess adhesion to mucin as a function of pH and ionic strength. The results again highlighted the relative significance of

the combined effects of hydrogen-bond formation, van der Waals' interactions and electrostatic forces on the process of mucoadhesion [75].

- ***In vivo* methods**

Some work has been done in the *in vivo* testing of mucoadhesive systems, with much of the effort focusing on nasal and oral dosage forms [43].

The non-invasive technique of choice for the evaluation of mucoadhesion involves the monitoring of gamma-emitting radiolabelled polymers *via* gamma scintigraphy, as is exemplified by human clearance studies of radiolabelled chitosan and starch microspheres, and chitosan solution [76]. It was reported that the chitosan solution had a clearance that was double that of the control; starch microspheres of more than triple and the chitosan microspheres were retained for four times as long as the control. These results supported the hypothesis that chitosan delivery systems can reduce the rate of clearance from the nasal cavity and thereby increase the bioavailability of drugs incorporated into these systems [74]. The technique has also been employed by Richardson *et al*. [77] for the study of the distribution of technetium-labelled microspheres of a hyaluronic acid derivative (HYAFF) in the genital tract of sheep.

The technique of magnetic resonance imaging has been employed by Albrecht *et al.* [78] to localise the point of release of thiolated polymers from dosage forms and to determine residence time in the intestinal mucosa of rats.

Donovan *et al.* [79] has demonstrated a simple technique for monitoring nasal clearance. The method involved the timed collection of nasally instilled microspheres (non-absorbable FluoSpheres® of sulphated latex particles) *via* swabbing of the back of the oral cavity.

Riley *et al*. [80] have employed the rat model to determine the *in vivo* gastrointestinal distribution profiles of three ^{14}C -labelled poly(acrylic acid)s with differing degrees of crosslinking, and hence

different average molecular weights. These structural features were found to be of little influence to the overall gastrointestinal transit of the materials under consideration. Within the first hour from administration, a smaller proportion of the lower molecular weight polymer, as compared with the higher molecular weight materials, was seen to be retained in the stomach but after this time the observed profiles for all three polymers became essentially identical. After four hours, irrespective of the material utilised, the stomach was free of all polymer; at six hours from ingestion, all polymers were found to concentrate in the caecum with only small amounts of material present in the ileum or in the lower large intestine. No evidence for the systemic absorption of poly(acrylic acids) could be identified following the scintillation counting of NaOH-digested samples of liver, kidneys, blood, and urine.

Roldo *et al.* [81] determined the *in vivo* (rat) gastrointestinal distribution profile of orally administered millimetre-sized particles, prepared from ^{14}C-radiolabelled poly(acrylic acid) that had been crosslinked with 4-4'divinylazobenzene, Figure 2. The work has shown the capability of these particles to swell progressively along the gastrointestinal tract (GIT) and develop into colon-specific hydrogel coatings that exhibit prolonged residence and mucoadhesion specificity. Additionally, the efficacy of the selected material as a protective coating for the colonic mucosa has been tested in a hapten-reactivated *in vivo* model of inflammatory bowel disease. Seven days after reactivation of the condition, the myeloperoxidase activity of animals that had received doses of the selected azopolymer was determined to be at the same level as that of healthy animals or that of the negative control group, highlighting the therapeutic promise of this material.

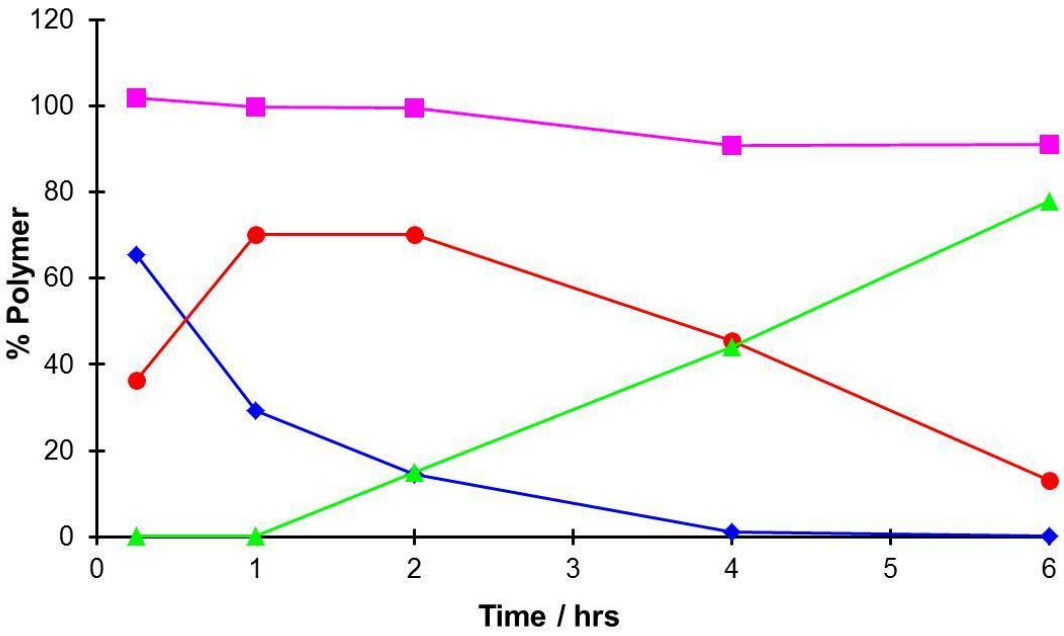

Figure 2. GIT distribution profile of azocrosslinked polyacrylic acid (◆ stomach; ● small intestine; ▲ caecum/colon; ■ total); radiolabelled polymer appeared in the faeces after 24 hours from oral administration (Based on data from Roldo et al. [81])

1.5. Formulation design

The concept of mucoadhesive drug delivery systems was first conceived in 1980 as a means of overcoming physiological barriers in sustained and targeted drug delivery by placing the formulation in intimate contact with the absorption site [82]. The complexities for the design of an effective mucoadhesive formulation are highlighted by the multitude of performance demands that such a system must meet before it can be considered appropriate for clinical testing. A therapeutically relevant mucoadhesive must display [83]:

- rapid but limited swelling, wetting and spreading on contact with aqueous media;
- adhesiveness to the mucosal layer;
- capacity to exhibit prolonged residence at the site of administration;
- pK_a values that are appropriate to the physiological environment of interest;

- viscoelastic behaviour;
- controlled release of the loaded active;
- biocompatibility; and,
- efficient clearance from the site of administration and/or biodegradability to molecular entities that do not cause adverse effects.

The search for mucoadhesive drug delivery systems that meet these demands has considered a range of systems, including patches, tablets, gels, pastes, inserts and nanoparticles [82].

• Hydrogels

Ever since they were first introduced in the 1960s, hydrogels have continued to be investigated for a multitude of therapeutic applications [84]. These cross-linked polymeric networks are capable of imbibing water and of acting as semi-solid dosage forms for drug delivery and as supporting materials that promote tissue regeneration. In their swollen state they share some of the physical properties that characterise biological tissues: soft consistency, which minimises their capacity to act as irritants; high affinity for water and biological fluids, which in addition to increasing biocompatibility inhibits the adsorption of proteins and cell, and hence reduces the likelihood of a negative immune response; and, they are deformable, which allows them to adapt to the shape of the underlying mucosa of the target organ [85].

• Pharmaceutical considerations

Hydrogels have been classified into entangled networks, covalently cross-linked networks, and networks formed by physical interactions [86] but very few systems conform with the pure definition of each class [87]. Consequently, attempts have been made to describe hydrogels in many ways. The nature of side groups (neutral or ionic) or mechanical and structural features can be used to differentiate types. The hydrogel can be described by its method of preparation (homo- or co-polymer). The physical structure (amorphous, semi-crystalline, hydrogen-bonded, supermolecular,

and hydrocolloidal) can be used to classify the systems. Also if appropriate hydrogelscan be defined by their responsiveness to physiological environmental stimuli (pH, temperature, ionic strength, electromagnetic radiation and redox potential) [88]. The reasons for the lack of a universally acceptable system for the classification of hydrogels are exemplified. In a review of chitosans, Dash *et al.*[89] describe the variety of hydrogel types that this naturally occurring polymer is capable of forming. Firstly, physical association networks which are maintained through non-covalent interactions. Ionic complexes are stabilised by electrostatic interaction between cationic and anionic species and analogous to ionic complexes are polyelectrolyte complexes maintained by stronger inter-ion interactions since they involve large charged molecules. Polymeric blends consist of physical admixtures and irreversible cross-linked networks formed through chemical cross-linking or by appropriately formulated interpenetrating networks. Lastly, stimuli sensitive thermo-reversible hydrogels are described which exhibit temperature-triggered sol-to-gel transitions. The application of oscillatory rheological methods, has allowed Hunt *et al.* [90] to classify alginate structures as true gels (viscoelastic solids) or as concentrated polymer solutions (viscoelastic liquids), suggesting that rheology [91, 92] may be a readily accessible tool for the classification of such systems irrespective of the mechanism that governs their formation.

The capability of a hydrogel to act as a drug delivery device is determined by the combined effects of the two parameters that define its swollen state, namely, polymer volume fraction, which measures the amount of fluid a hydrogel can absorb, and the average number of constitutional repeat units between each cross-linking point along the polymer backbone, which determines the structure of the network mesh and hence the average pore size, and impacts upon mechanical strength, degradability and the diffusivity of a loaded molecule [93]. Typically, biomedical hydrogels in their swollen state have pore sizes in the range 5 - 100 nm, which are considerably larger than that of the majority of small-molecule drugs and renders them inappropriate for the delivery of such agents [85]. The use of hydrogels is thus limited to applications demanding the sustained release of macromolecular drugs that are characterised by large hydrodynamic radii, such as peptides, proteins

and oligonucleotides. Lü *et al*. [94] have reported the release of BSA, a protein with a hydrodynamic diameter of 7.2 nm, which is smaller than the average pore size of the oxidised carboxymethylcellulose/*N*-succinyl-chitosan carrier hydrogel: an initial Fickian diffusion of the incorporated BSA (which has been explained in terms of the progressive swelling of the hydrogel and the consequential increase in hydrodynamic radii) is reported to have been followed by a stage of zero-order release that appeared to be governed by the degradation profile of the hydrogel.

The mechanism for the release of a loaded drug from a hydrogel is influenced by chemical structure, mesh size and the swelling properties of the carrier system, Table 3.

Table 3. Possible mechanisms for the release of a loaded drug from a hydrogel

Drug release	Mechanisms
Diffusion controlled	Drug diffusion is dependent upon hydrogel mesh sizes. Normally modelled using Fick's law of diffusion.
Swelling controlled	Drug diffusion is faster than hydrogel swelling. Modelling involves moving boundary conditions where molecules are released at the interface between rubbery and glassy phases of swollen hydrogels.
Chemically controlled	Drug release is dependent upon chemical reactions occurring within the gel matrix, e.g. hydrolytic or enzymatic degradation of polymer chains.

A range of hydrogels has been explored for the controlled delivery of many actives, ranging from small molecular weight drugs to nucleic acids, peptides and proteins [95-97]. Loading with low molecular weight drugs normally involves the placement of the fully formed gel into a medium that has been saturated with the therapeutic agent. Macromolecular therapeutics are normally incorporated into the polymer mix before the onset of gelation. In a typical example, Wu *et al*. [4] formulated a range of thermosensitive hydrogels for the release of insulin by mixing systematically varied proportions of the active with N-[(2-hydroxy-3-trimethylammonium) propyl] chitosan chloride (HTCC) and polyethylene glycol, before the addition of αβ-glycerophosphate, the gel-network facilitator, and heating to 37° C. The work has shown that the proportion of loaded insulin is limited

by its capacity to participate in hydrogen bond formation with PEG and/or HTCC, which strengthens the network and inhibits release [4].

Following *in vivo* administration both loading methods are characterised by a burst release stage, which precedes the onset of controlled-release behaviour – this has been explained in terms of the time lag for the equilibration of the concentration gradient between the hydrogel and the surrounding environment [27]. The normal formulation strategy for the minimisation of drug loss during the burst-release stage involves the linking of the active to the polymer *via* labile covalent bonds that are susceptible to degradation (enzymatic, redox, acid mediated) at the local biological environment [85]. This has been carried out with a number of small molecular weight drugs, such as paclitaxel, dexamethasone and fluvastatin [98-101]. The covalent conjugation has afforded drug release to be extended from weeks to months. The thermosensitive polyphosphazene-paclitaxel conjugate gel was reported to sustainably release paclitaxel for up to one month. A degradable lactide bond was used to conjugate dexamethasone to a photoreactive mono-acrylated polyethylene glycol (PEG) in order to facilitate osetogenic differentiation of human mesenchymal stem cells [100].

Table 4 summarises the design variables that need to be balanced in order to maximise the effectiveness of drug-carrying hydrogel formulations.

Table 4. Design variables that influence the effectiveness of hydrogel formulations

Design criteria	Design variable
Drug molecule	Molecular weight and size Ionic charge and functional groups Drug-loading method: post or *in situ* loading
Hydrogel properties	Average molecular weight of polymer Cross-linking density Polymer-drug interactions Biodegradability Sensitivity to stimuli Biocompatibility

2. Mucoadhesive polymers for hydrogel formulation

Owing to their capacities to form crosslinked structures that retain water, the most commonly utilised hydrophilic polymers are polyacrylates: poly(acrylic acid), PAA; poly(methacrylic acid), PMA; poly(hydroxyethylmethacrylate), PHEMA; and, poly(acrylamide), PAM [85]. Other hydrogel-forming polymers include: poly(ethylene glycol), PEG; poly(vinyl alcohol), PVA; cellulose derivatives; starch; chitosan; hyaluronic acid; pectin; sulphated polysaccharides; sodium alginate; and gelatine. The water sorption capacities of these polymers vary from a fraction to several thousand times their own weight. Polymeric structures with ionisable moieties are generally more mucoadhesive than non-ionic macromolecules, Table 5.

Table 5. Commonly used mucoadhesive polymers.

Charge	Polymer	Application	Reference
Anionic	Poly(acrylates)	Insulin vaginal gel	[102]
	Poloxamer and polycarbophil	Vaginal gel for immunisation	[103]
	Polycarbophil	Vaginal gel for candidiasis	[104]
	Carbopol and hydroxypropyl gel	Oral ointment	[46]
	Hydroxypropyl cellulose/ carbopol 954P/ poloxamer 407	Metoclopramide nasal gel	[105]
	Hydroxyethyl methacrylate	Diclofenac sodium buccal gel	[106]
	Ethyl (hydroxyethyl) cellulose and surfactant	Timolol ocular gel	[107]
	Poloxamer 407, hydroxypropyl methylcellulose and Gantrez S-97 (polymethylvinylether-co-maleic anhydride)	Buccal delivery of 5-fluorouracil	[108]
	Hydroxypropyl cellulose; methyl cellulose; methylcellulose/Tween 80; hydroxyethyl cellulose; hydroxyethyl cellulose/Tween 80	Ciprofloxacin nasal gels	[109]
	Poloxamer-hyaluronic acid	Sustained protein delivery	[110]
	Pluronic F127 and Pluronic F68	Moxifloxacin ocular gel	[111]
	Poloxamers and hyaluronic acid	Acyclovir ocular gel	[62]
Cationic	Chitosan and polyethylenimine blend	Gene transfection agent	[112]
	Chitosan-g-PEG	Delivery of a bioactive bone protein	[113]
	Chitosan-pluronic UV cross-linked system	Delivery of growth factors	[114]
	Chitosan cross-linked with glutaraldehyde	Used in breast cancer therapy	[115]
	Chitosan-polyethylene oxide semi-IPN hydrogel	Oral delivery of antibiotics to the stomach	[116]
	Chitosan	Nasal insulin-loaded hydrogel	[117]
	N-[(2-hydroxyl-3-trimethylammonium)propyl] chitosan chloride and PEG and αβ-glycerophosphate	Insulin nasal gel	[4]
Non-ionic	Pectin	Ketorolac tromethamine nasal gel	[118]
	Carrageenan and acrylic acid	Oral delivery of insulin	[119]

To effect systemic absorption of incorporated actives, mucoadhesive formulations are often co-formulated with penetration enhancers. In addition to the opening of tight junctions [3], the mechanisms of penetration enhancement are as diverse as drug solubilisation or stabilisation [120],

the inhibition of enzymatic action [121], the extraction of a membrane protein, and the removal of the outer layer of mucous membrane [122], Table 6.

Table 6. The role of penetration enhancers in mucoadhesive formulations.

Mechanism	Example
Alters mucus rheology: reduces the viscosity and thickness of mucus and/or saliva.	N-Acetyl cysteine effects a reduction in the viscosity of mucus and facilitates the diffusion of FD-4 across the intestinal mucosal membrane [123]; Poloxamer reduces the viscosity and elasticity of mucus and disrupts the lipid membrane allowing leakage of lipids and proteins [105].
Increases the fluidity of the lipid bilayer: disturbs intercellular packing through interactions with lipid and/or protein components.	Above the critical micelle concentration, sodium dodecyl sulphate (SDS) increases the *in vitro* penetration of caffeine through porcine buccal mucosa [124]. Micelles disrupt barrier properties by extracting mucosal lipids [125].
Acts at the tight junctions: mimics desmosomes to disrupt membrane integrity.	Confocal imaging has shown the opening of tight junctions of intestinal epithelial cells by N-trimethylated chitosan chloride to enhance the penetration of ^{14}C mannitol, fluorescently-labelled dextran 4400 and ocreotide [126].
Overcomes enzymatic barrier: inhibits peptidases and proteases present within the mucosa.	Morishita *et al*. [127] used the *in situ* loop method to co-administer aprotonin and insulin to the duodenum, the jejunum, the ileum and the colon. The most pronounced hypoglycaemic effect was observed in the ileum.

- ## Anionic mucoadhesive polymers

Carboxyl- or sulphate-functionalised polymers have pK_a values that are suitable for applications within the living host and combine good mucoadhesion properties with low toxicity, which renders them potential candidates for mucoadhesive drug delivery [43]. The good mucoadhesive properties of poly(acrylic acid) and its weakly cross-linked derivatives (carbomers, polycarbophils) and those of sodium carboxymethylcellulose have been attributed to the formation of strong hydrogen bonds with mucin [128]. A comparative study by Madsen *et al*. [42] has shown that while both these classes of polymers exhibit rheologically synergistic interactions with mucus, those of the poly(acrylic acid)s are most pronounced over the pK_a range 4.9-6.7, where the polymers are in their partially

deprotonated form. The pH-independent rheologically synergistic behaviour of carboxymethylcellulose (CMC), which has been explained by the potential of CMC to retain its coiled conformation due to the non-disruption of hydrogen bonding across the pH range [42], has been confirmed by Rossi *et al*. [64].

Sriamornsak *et al*. [44] have studied the rheological interactions between mucin and pectin, an anionic polymer at neutral pH. In simulated gastric fluid (pH 1.2), and in accord with the behaviour of poly(acrylic acid)s, at pH values $<pK_a$ (3.2-4.3) the carboxyl groups of pectin are fully protonated, as are the sialic acid moieties of mucin, effecting extended hydrogen bonding and demonstrating rheological characteristics that indicate entanglement of the pectin with the mucin: the G" (dissipative loss modulus) exceeded G' (elastic storage modulus), and a substantial decline at low frequencies. As the pH is increased to near-neutral (6.8), both the carboxyl moieties of pectin and the sialic acid groups of mucin become ionised, leading to the destruction of the hydrogen bonded network. The mucoadhesive interactions between the two anionic species are significantly weaker since the hydrogen-bonding component of the mucoadhesive interaction is replaced by electrostatic attractions that require the involvement of cations present within the aqueous medium.

- ## Cationic mucoadhesive polymers

Properties of biocompatibility, biodegradability and low toxicity make chitosan – a linear polysaccharide derived from the deacetylation of chitin sourced from crustaceans – and its derivatives the most extensively used cationic hydrogel polymers [43, 129]. Of significance in mucoadhesive drug delivery are the capacity of the primary amino groups of chitosan to participate in ionic interactions with the sialic acid and sulphonic acid moieties of mucus and the capability of the material to promote the systemic absorption of co-formulated large hydrophilic molecules [5, 43]. It has been suggested that the penetration-enhancement properties of chitosan are due to its capacity to counterbalance the fixed anionic charges of tight junctions, which effects the transient

opening of these junctures and allows the transit of otherwise excluded molecules *via* the paracellular route [5, 43]. Accordingly, Boonyo *et al*. [130] have demonstrated the increased capability of the more positively charged trimethylated chitosan (TMC; 40% derivatised) to enhance antigen uptake in mice, as compared with its non-quaternised precursor molecule. However, in the design of mucoadhesive TMC-based formulations, the increasing capability of the progressively more highly quaternized polymer to enhance penetration must be balanced against the corresponding reduction in the capacity of the material to adhere to mucosal surfaces [131].

- ## Site-specific mucoadhesive polymers

Given the need for drug delivery at regions distal to administration and the effects of mucoadhesive clearance associated with mucus turnover, attempts have been made to address the non-selectivity of conventional mucoadhesive systems through the development of cytoadhesive polymer platforms [43, 45, 51]. Prime examples of the cytoadhesive component of such platforms are the lectins. These naturally occurring proteins play a fundamental role in biological recognition through reversible binding to specific carbohydrate residues [27, 43]. On binding to the mucosal surface, the lectins can either remain on the cell exterior or, as is the case with receptor-mediated adhesion, become internalised *via* endocytosis. Although endocytosis offers the opportunity for the active cell-mediated uptake of macromolecular drugs [51], the toxicological and immunological profile of lectins places caution on their suggested deployment in drug delivery systems [27, 43].

The use of polyacrylic acid that had been covalently attached to bacteria (pathogenic *E. coli*) that are known to adhere to the GI mucosal membrane has been shown to effect a significant increase in bioadhesion, *in vitro*, relative to the polymer control [132]. Lee *et al*. [23] extended the idea of polymer-fimbriae adhesion complexes to the adhesion of bioadhesive microspheres to epithelial surfaces as an alternative means of facilitating adhesion of hydrogels to mucosal membranes.

An approach to improved mucoadhesive strength has involved the chemical functionalisation of hydrophilic polymers (chitosan, polyacrylates or deacetylated gellan gum) to their thiolated derivatives. The approach has been rationalised on the basis of the principle that thiols imitate the natural behaviour of secreted mucus glycoproteins, which become covalently anchored to the mucus layer through the formation of disulphide linkages. On mixing, the thiol groups form covalent bonds with the cysteine component of mucus, increasing residence time and improving bioavailability [43]. *In vitro* experiments by Roldo *et al.* [133] have shown that the attachment of thiolated chitosan to mucosal surfaces, as evaluated by total work of adhesion measurements, is two orders of magnitude stronger than that of its precursor molecule. It has been claimed that, owing to the covalent nature of their interactions with mucus, thiolated structures are less susceptible to the effects of changes in ionic strength and/or pH than other mucoadhesive materials [43].

Sajeesh *et al*. [134] have reported the surface functionalisation of poly(methylacrylic acid)-based hydrogel microparticles with thiol groups. The modified particles although more mucoadhesive exhibited reduced swelling capacity and lower insulin encapsulation efficiency. Pritchard *et al*. [135] have shown that the incorporation of thiol functionalities to a polyethylene glycol hydrogel promoted cell adhesion due to the increase of interactions involving cysteine groups. A hydrogel that is responsive to the presence of human neutrophil elastase, and hence degradable at sites of inflammation, has been prepared by Aimetti *et al*. [136] *via* the functionalisation of polyethylene glycol with photopolymerisable thiol-ene groups.

1.6. Mucoadhesive-hydrogel drug delivery systems

The mechanism proposed to explain the mucoadhesive behaviour of hydrogels [137] considers the miscibility of the mucoadhesive material with the mucus layer in terms of its capability to participate in interpolymer interactions. Key to the establishment of such interactions is the capacity of the

mucoadhesive to become hydrated at a rapid rate but to a limited extent; all patented mucoadhesive materials, Table 7, exhibit this property.

Table 7. Examples of recently patented hydrogel formulations

Function of the gel	Active	Gelling agents	Reference
Teething gel	Benzocaine	Sodium carboxymethylcellulose, sodium alginate and xanthan gum	[138]
Gel for dental pain	Diclofenac sodium and chlorhexidine gluconate	Carboxymethylcellulose, acrylic acid copolymer and copolymer of methyl vinyl ether and maleic anhydride	[139]
Hormonal vaginal gel	Estriol	Acrylic acid crosslinked with allyl surface or divinyl glycol	[140]
Anti-fungal vaginal gel	Econazole nitrate	Hydroxyethylcellulose	[141]
Nasal/oral/vaginal pain-relief gel	Diclofenac sodium	Xyloglucan and glycerol	[142]
Immunostimulating gels	An immune response modifier	Polyethylene glycol, hydroxyethyl cellulose, hydroxymethyl cellulose, hydroypropyl cellulose	[143]
Protective gel for injured, inflamed or surgically repairing tissue of the ear/nose/throat/limbs/spinal cord		Chitosan, oxidised polysaccharides (e.g. methylcellulose)	[144]
Resistant hydrogel for mucosa or natural tissue, e.g. cartilage, bone		Thiolated chitosan with oxidising agent and external crosslinking agent	[145]

- ## Stimuli-responsive hydrogels

The simplest example of a site-specific hydrogel formulation is provided by Nazar *et al.* [146] who formulated a TMC-based hydrogel that may be useful for the intranasal delivery of insulin. The

material may be administered into the nasal cavity as a solution which undergoes a sol-to-gel transition at the physiologically relevant temperature to a structure that is capable of acting as a device for the controlled release of co-administered insulin. Systematic variations of the proportions and chemical nature of the polymeric component allows the fine control of the gelation temperature to that appropriate to the target site, as has been demonstrated with not only the system described by Nazar *et al.* [146] but also with those developed by Khan *et al.* [147] (chitosan, glycerophosphate and hydroxyl propyl methyl cellulose gel for the intranasal delivery of ropinirole), Ved *et al.* [148] (poloxamer 407, phosphatidylchonine and n-tridecyl-(-β-)maltoside gel for the intranasal delivery of zidovudine), Nguyen *et al.* [149] (poly(amidoamine)-poly(ethylene glycol)-polyamidoamine) triblock copolymer hydrogels for oral drug delivery), and Shastri *et al.* [111] (poloxamers Pluronic F127 and F68 gel for the ophthalmic delivery of moxifloxacin hydrochloride).

To synchronise the drug-release profile of carrier systems with variations in the physiological environment, much research work has focussed on systems capable of modulating their release profile by sensing changes at the target site [150]. Such systems may adjust their swelling behaviour, permeability, network structure or mechanical strength [85] by reacting to internal or external stimuli [84].

Sharma *et al*. [151] have described the development of stimulus-responsive drug release systems that exhibit pulsatile release. Such hydrogels may prove useful in the treatment of diseases that require on-demand or rhythmic medication (amongst others hypercholesterolemia, asthma, cancer, duodenal ulcer, arthritis, diabetes, neurological disorders, cardiovascular diseases, and irritable bowel syndrome). Driven by this demand hydrogel devices have been formulated that respond to levels of glucose, enzymes, antibodies or pH.

Several glucose-sensitive hydrogels have been investigated. The systems reported to date are categorised into those that: respond to the variations in pH that accompany the enzymatic oxidation of glucose to H_2O_2 (based upon glucose oxidase [152]); depend on the competitive binding of glucose

(concanavalin A [153]); form a reversible complex with glucose (phenylboronic acid [154]); and, are based on a glucose-binding protein [155].

Enzyme-responsive hydrogels have been reviewed by Roy *et al.* [156]. Most promising appear to be those that employ protein- or peptide-based crosslinkers that become hydrolysed on exposure to proteases, leading to gel degradation and the consequent release of the therapeutic component. Miyata *et al*. [157] have developed an antigen-responsive hydrogel for the pulsatile release of protein. This system is designed such that competitive binding of free rabbit IgG antigen with antibodies in the hydrogel compromise the antigen-antibody crosslinks within the antigen-antibody semi-interpenetrating network leading to reversible swelling of the system and to the release of the active.

Since at pathological conditions there is often interplay of more than one stimulus, early work on stimulus-responsive hydrogels has been superseded by the quest for multi stimuli-responsive systems. An example of a dual-stimulus responsive biodegradable hydrogel is provided by a network of gelatin and dextran: incorporated lipid microspheres acting as drug micro-reservoirs are released by the combined action of α-chymotrypsin and dextranase, but not by either enzyme acting in isolation [158]. Another example is provided by Guo *et al*. [11] who have reported the co-formulation of carboxymethyl chitosan and poly(N-isopropylacrylamide) to a pH- and temperature-sensitive amphoteric polyelectrolyte hydrogel for the oral delivery of drugs.

Blanchette *et al*. [27] have investigated the effects of copolymer composition and pH of the surrounding medium on the network structure of a series of hydrogels. Of the systems investigated, an equimolar hydrogel of poly(methacrylic acid) (PMA) and ethylene glycol (EG) exhibited the greatest pH-dependent change in mesh size. It has been suggested that, since the acidic environment of the stomach would maintain a collapsed network that inhibits the release of the active, this responsiveness may be useful for the enteric delivery of oral actives [27]. Wang *et al*. [159] have developed a multi-stimulus responsive hydrogel formulation by utilising a copolymer that

had been prepared from the pH and temperature-sensitive (2-dimethylamino)ethyl methacrylate and the glucose-sensitive 3-acrylamidephenylboronic acid. The high specificity and capacity to respond to physiological changes that are specific to each disease state render stimulus-responsive hydrogels the delivery systems of choice for further development. However, before such systems can be adopted in the clinic, considerable advances are needed in the design of synthetic formulations that are capable of adapting their properties in a pre-specified manner and in accordance with specific interactions with biomolecules or with other markers characterising a disease state [156].

Drug release is most frequently observed during the swelling of the hydrogel structure. However, drug release may occur as the gel contracts and liquid along with dissolved drug are expelled from the formulation. Such hydrogels have been shown, by Gutowska *et al.* [160], to respond to changes in temperature and/or pH and to be amenable to formulation into systems that exhibit controlled swelling-deswelling kinetics.

- ## Self-assembling peptide nanofibre hydrogels

Upon introduction to electrolyte solutions, certain peptides comprising of alternating hydrophobic and hydrophilic amino acids self-assemble into interconnected nanofibers (diameter 10-20 nm), which become then organised into highly hydrated hydrogels with pore sizes in the range 5-200 nm. Due to their peptide composition, these structures are assumed to be more biocompatible and to have a lower potential to induce adverse effects than conventional hydrogels. The sol-gel transition occurs at physiological conditions and the high internal hydration provides an environment that can accommodate bioactive molecules and/or cells [161, 162]. A recent example is provided by a self-assembling peptide hydrogel that has been shown to effect the localized delivery of curcumin over sustained periods of time [163]. In another example, the sustained and controlled drug release of docetaxel has been effected from a hybrid hydrogel composed of Fmoc-diphenylalanine (Fmoc-FF)

peptide, konjac glucomannan (KGM) and b-mannanase [164]. In addition to their application in drug delivery, and because of their capability to support cell adhesion, self-assembling peptide hydrogel scaffolds have been applied to tissue engineering functions, including bone and cartilage reconstruction, heart-tissue regeneration, and angiogenesis [165, 166], but their efficacy in mucosal drug delivery has yet to be determined.

- ## Superporous hydrogels and complexes, and interpenetrating networks

The need for mucoadhesive hydrogels that exhibit rapid swelling to equilibrium dimensions has provided the impetus for the development of open-channelled network structures: superporous hydrogels (SPH) and SPH composites (SPHC) [167-169]. The improved aqueous permeability and biocompatibility of SPH systems relative to those of other hydrogel structures is counterbalanced by poor mechanical strength, which is markedly improved in SPHC structures, such as those prepared by adding croscarmellose sodium (Ac-Di-Sol) to the hydrogel mix [169, 170]. The impact of mechanical properties on the performance of such systems has been studied by Dorkoosh *et al*. [171, 172] who suggested that the opening of tight junctions is caused by the mechanical pressure produced by the swelling of SPH and SPHC polymers.

Attempts to improve the mechanical properties and resilience of SPHs and SPHCs have led to the development of interpenetrating networks (IPNs). These systems are formed through the mixing of cross-linked polymer networks at the molecular-segment level: if only one polymer is cross-linked and the other is linear, the system is termed semi-IPN; if both polymers are cross-linked, the system is described as full-IPN [170].

Tang *et al*. [169] has shown that SPHCs containing Carbopol adhere more rapidly to intestinal mucosa and demonstrate higher mucoadhesive capacity than congeners prepared in the absence of this carbomer. Work by Kim *et al.* [173] has led to the development of third generation SPHs: poly(acrylic acid-co-acryl-amide)/poly(ethylenimine), P(AA-co-AM)/PEI, semi-IPNs that possess good

mechanical strength (comparable with that of SPHCs), which is claimed to be bestowed by the high degree of molecular entanglement between the cationic PEI and the anionic PAA. Yin *et al.* [174] have synthesised SPH-IPNs of poly(acrylic acid-co-acrylamide)/carboxymethyl chitosan that are claimed to display an enhanced loading capacity for insulin, and improved *in vitro* mucoadhesive and mechanical properties as compared with previous generation materials.

Verestiuc *et al*. [175] have prepared a series of optically transparent semi-IPN networks by the free radical polymerisation of *N*-isopropylacrylamide (NIPAAm) in the presence of chitosan (CS) using tetraethyleneglycoldiacrylate (EGDA) as the crosslinking agent. Up to a plateau CS/NIPAAm ratio of 0.46, the proportion of chitosan that could be incorporated into the matrix was found to increase as the crosslinking density of the network was increased. Also, it was observed that as the chitosan content and crosslinking density increased, the phase transition temperature of the hydrogels became less well defined and shifted towards lower temperatures and that the degree of swelling of the hydrogel fluctuated from *ca*. 100% at basic pH to over 2000% at acidic pH. Reinforced biocompatible systems, such as those obtained *via* the formulation of SPHCs with IPNs, exhibit improved biocompatibility without compromising the stability and mechanical strength of the hydrogel.

- ## Micro- and nano-gels

Potential applications in injectables, and the demand for drug-delivery systems that respond rapidly to stimuli and exhibit trigger release, have led to the development of small-sized gel systems. Structures ranging between 50 nm and 5µm in average diameter [176] are being investigated for their potential in peptide and protein drug delivery, with much of the work focusing on those that exhibit stimuli-dependent transitions; systems that exhibit responsiveness to temperature, electrostatic environment, metabolic processes and products, external fields (light, ultrasound, magnetic), and degradation have all been considered [177]. Such miniaturised drug-carrying vehicles

are claimed to be minimally invasive if administered *via* the oral or nasal routes, or if injected into patients [93].

Drug delivery by means of hydrogel nanoparticles (nanogels; <200 nm) [178] has received considerable attention [1, 178-180]. Such materials are considered to possess the combined features of hydrogels and nanoparticles: hydrophilicity, flexibility, versatility, high capacity to accommodate water, biocompatibility, long circulation time, and the potential to be targeted actively or passively to the site of action [88]. These properties are often tuneable to the demands of each drug-delivery application by altering proportions of cross-linking density, chemical functionalisation, surface-active components and stimuli-responsive constituents [178]. Vinogradov *et al*. [179] who investigated a cross-linked cationic polymer nanogel network for the delivery of an active form of a cytotoxic anticancer drug claims that the formulation achieved a 90% protection of the drug from enzymatic degradation and a fourfold increase in transcellular transport across Caco-2 cell monolayers while enhancing drug targeting and internalisation at the desired site. Prego *et al*. [1] have shown that chitosan-coated nanogels display a significant capacity to enhance the intestinal absorption of salmon calcitonin in the rat, which renders them candidate structures for the treatment of hypercalcemia. In another example, Nukolova *et al*. [181], who loaded cytotoxic drugs into folate-decorated nanogels and tested them on an animal model of ovarian cancer, report that these delivery systems improve the anti-tumour action of the chemotherapeutant and reduce its side effects as a result of the combined benefits imparted by high loading capacity, steric-stabilisation and tumour specificity.

Li *et al.*[182], in their effort to design a system for the delivery of paclitaxel (an anticancer drug of poor aqueous solubility), prepared a micellar nanogel formulation by cross-linking Pluronic F127 with polyethylenimine and poly(butylcyanoacrylate). This formulation exhibited improved blood-plasma stability and a more sustained drug release profile than corresponding micelles of Pluronic F127.

Rationalised by the principle that the hydrophobic internal cavity of cyclodextrins (CDs) renders it a suitable host for certain drug molecules, Kettel *et al.* [183] have incorporated reactive CDs into aqueous nanogels. The inclusion complexes that formed exhibited excellent colloidal stability in water, and were found to be amenable to regulation of their nanogel size (hydrodynamic radius) through variations in the ratio of incorporated CD.

Barbu *et al*. [184] prepared hybrid nanoparticles (10–70 nm) that combine the temperature sensitivity of *N*-isopropylacrylamide or the good swelling characteristics of 2-hydroxyethyl methacrylate with the susceptibility of chitosan to lysozyme-induced biodegradation, and the materials have been investigated for their capability to act as controlled release vehicles in ophthalmic drug delivery. Studies on the effects of network structure upon swelling properties, adhesiveness to mucosal surfaces and biodegradability, coupled with *in vitro* drug release investigations employing ophthalmic drugs with differing aqueous solubilities, have identified nanogel compositions for each of the candidate drug molecules.

1.6. Conclusions

As compared with other structures such as liposomes or micelles, polymeric hydrogels are more stable, simpler to prepare and to scale-up, and offer considerable promise as systems for controlled drug release. Additional to biodegradability, loading capacity, immunogenicity and toxicity, the choice of the polymeric matrix is dictated by its capability to respond to physiological stimuli and/or exhibit mucoadhesion. The organic nature of hydrogel-forming polymers offers the advantage of allowing blending with other polymers (such as in the formation of interpenetrated networks) or conjugation with molecules (such as azoreducible crosslinkers), which in turn afford a significant degree of control over the drug release profile and impart targeting specificity. Also, the internal porosity may be manipulated such that hydrogels meet specified criteria that influence drug release profiles.

1.7. Future Perspective

Recent progress in nanoformulation has seen the promise of hydrogel structures that may help the incorporated active to cross biological barriers, such as those of the eye, but the challenges of nanogel design for such applications are integral to those associated with the detailed appreciation of specific disease-induced changes in the structure and functionality of the target barrier. Early work utilising lectins has highlighted the potential for the combination of specific materials and cell-based delivery strategies (e.g. complexation with antibodies, cell-penetrating peptides or cell-specific ligands) and may evolve into another tactic for improved organ or even cell targeting. Hydrogel systems that are formulated from biocompatible polymers are now being customised by tailoring their physicochemical characteristics not only to the demands for efficient drug incorporation and controlled release but also to those for site specificity, by building into the hydrogel structure response mechanisms that are only triggered by the target physiological environment. The design of hydrogel formulations that release therapeutic agents only once they have sensed a disease-specific biomarker represents the next stage of development.

1.8. Aim and objectives

Towards the development of a drug-delivery vehicle for the nasal delivery of insulin, a systematic series of *N*-trimethyl chitosan will be co-formulated with poly(ethylene glycol) and glycerophosphate into a thermosensitive hydrogel structure. Rheological evaluations will allow the optimisation of the sol-to-gel transition properties such that they occur over optimally brief timescales and at physiologically relevant temperatures. *In vitro* experiments will allow the evaluation of the capacities of the formulation to affect the opening of modelled tight junctions and to release its therapeutic content under conditions that mimic those of the nasal environment. In parallel, spectroscopic and analytical investigations will assess the structural integrity and conformational

order of the incorporated insulin over a specified time scale. Finally, the *in vivo* potential of the *in situ* thermogelling nasal formulation to act as a once-a-day dosage form for the intranasal delivery of insulin will be investigated in the diabetic-rat model.

Chapter Two: Thermosensitive hydrogels for nasal drug delivery: the formulation and characterisation of systems based on *N*-trimethyl chitosan chloride.

Thermosensitive hydrogels for nasal drug delivery: the formulation and characterisation of systems based on *N*-trimethyl chitosan chloride.

Abstract

Towards the development of a thermosensitive drug delivery vehicle for nasal delivery, a systematic series of *N*-trimethyl chitosan chloride polymers, synthesised from chitosans of three different average molecular weights, have been co-formulated into a hydrogel with poly(ethylene glycol) and glycerophosphate. Rheological evaluations have shown that hydrogels derived from *N*-trimethyl chitosan with a low degree of quaternisation and high or medium average molecular weight exhibit relatively short sol-gel transition times at physiologically relevant temperatures. Also, the same hydrogels display good water-holding capacity and strong mucoadhesive potential, and their mixtures with mucus exhibit rheological synergy. An aqueous hydrogel formulation, derived from *N*-trimethyl chitosan of medium average molecular weight and low degree of quaternisation, appears particularly promising in that it exhibits most favourable rheological and mucoadhesive behaviour and a sol-gel transition that occurs at 32.5 °C within 8 min.

2.1. Introduction

Nasal drug delivery for systemic effects is an historic administration route [185], and owing to the avoidance of the first-pass effect, the nasal mucosal membrane presents a potentially useful site for the delivery of proteins and peptides [186-190]. However, there are drug-delivery challenges that need to be overcome if intranasal drug delivery is to become the method of choice for the delivery of therapeutic agents, namely: mucosal membranes pose a substantial barrier to the absorption of macromolecules [191]; proteolytic enzymes in nasal secretions impact upon the bioavailability of proteins and peptides [185]; and, nasal residence, as determined by mucus turnover time, is limited to approximately 15 - 20 minutes [30, 185]. Drug-delivery strategies that have been explored in efforts to overcome these challenges are as diverse as the modification of the peptide structure [192], the inhibition of the ciliary beat frequency [185], the employment of permeation or absorption enhancers, and the utilisation of mucoadhesive polymers [105].

Research efforts into the employment of mucoadhesive viscoelastic hydrogels in nasal drug delivery are rationalised in terms of their potential for prolonging the residence time of the active on the mucosal surface. Such systems lend themselves to administration as sprays or drops and may be designed such that they undergo a sol-gel transition at the temperature of the site of deposition (32 – 35 °C, table 8) [31, 32], with the implication that the increased viscosity and rheological synergy of the resulting mucus/mucoadhesive system effects prolonged residence at the site of action [4, 23, 43, 53, 193].

Table 8. Distribution of temperature in the nasal passageway during quiet breathing at room temperature (25 °C, 8.06 mg H_2O/l)[32], and the areas of dosage form deposition by nasal drops and spray [194]

Location	Inspiration temperature °C	Expiration temperature °C	Deposition of nasal dosage forms
Nasal vestibule	25.3	34.2	
Nasal valve	29.8	35.1	
Anterior turbinate area	32.3	35.1	Targeted by nasal sprays and drops
Nasopharynx	33.9	36.2	More deposition by nasal drops

Amongst the mucoadhesive viscoelastic hydrogels studied to date, those structured around chitosan – a biocompatible and biodegradable natural polysaccharide – have shown particular promise since they facilitate the paracellular transport of large molecules across the mucosal surface by opening tight junctions [195-199]. In particular, the thermosensitive chitosan/glycerophosphate gels, developed by Chenite *et al.* [200], were shown to be suitable for the delivery of sensitive biological materials such as proteins and gene-based therapeutics. However, despite promising results, chitosan presents limitations in that it is only soluble and active in acidic environments, when in its protonated form [126]. For this reason, and due to the fact that the chitosan-based thermosensitive gels so far developed undergo only a slow sol-gel transition at physiological pH [201], chitosan has been substituted by its positively charged derivative *N*-trimethyl chitosan chloride (TMC) [202]; this retains the key qualities of the parent polymer but presents improved solubility profile, enhanced mucoadhesive properties and a significant absorption enhancing effect over a wide pH range [203] as well as enhancing the properties of the thermosensitive formulations [4, 200, 204]. TMC/GP hydrogels have been previously studied for parenteral drug delivery [201, 205]. However, there are scarce reports on their use for intranasal administration. Therefore, the current work aims at investigating this specific application, studying the effect of molecular weight (MW), degree of

quaternisation (DQ) of TMC, and hydrogel composition on the thermosensitivity and rheological behaviour of nasal formulations. The objective is to optimise a system able to undergo a sol-gel transition in the temperature range 32-35 °C, thereby allowing a stable liquid state to be maintained at storage temperature and prior to usage, easing administration via nasal spray or drops. This system should gel at 32-35°C, representative of the nasal environment [31], and provide a synergic effect in contact with the nasal mucus that can guarantee prolonged residence time and show the required rheological characteristics. These have been identified to be specific apparent viscosity (350 mPa s) and viscoelasticity (200 Pa) values that significantly reduce the mucociliary transport rate (MTR) [206].

2.2. Materials

Chitosans (low viscosity, 150 kDa, degree of deacetylation (DD) 95 - 98 *%*; medium viscosity, 400 kDa, DD 84 - 89 *%;* and, high viscosity, 600 kDa, DD 75 - 85 *%*), poly(ethylene) glycol 4000 (PEG) and poly(acrylic acid) (PAA) were obtained from Fluka, UK. Glycerophosphate (GP; equimolar mixture of *α* and *β* isomers), tristearin (TRIS) and porcine-stomach mucin were purchased from Sigma-Aldrich Inc., UK. Methyl iodide and 1-methyl-2-pyrrolidinone were sourced from Acros Organics, Belgium. All other chemicals were obtained from Fisher Scientific, UK, and used as received.

2.3. Methods

2.3.1. Synthesis and characterisation of *N*-trimethyl chitosan chloride

TMC was synthesised *via* the reductive methylation of chitosan of three different average molecular weights (low, L; medium, M and high, H) according to the method described by Sieval *et al.* [202]. Different degrees of quaternisation were obtained by employing a one and a two step synthesis method (e.g. L1 or L2) as described by Hamman *et al.* [207].

Briefly, chitosan (2 g) and sodium iodide (4.8 g) were dissolved in 1-methyl-2-pyrrolidinone (80 ml) by stirring for 30 min in a water bath at 60°C. Sodium hydroxide (11 ml, 15% w/v) and methyl iodide (11.5 ml) were added to the solution and stirred for 1 h. The product was precipitated using ethanol and diethyl ether and isolated by centrifugation. The precipitate was washed with ethanol:ether 3:1 (30ml x 3). For the one step synthesis the product was dissolved in NaCl solution (40ml, 10%) and

stirred over night. On subsequent precipitation with the two solvents and centrifugation the material was dissolved in 40 mL of deionised water and dialysed for 72 h before freeze-drying.

The two step synthesis differs in the later stage as the initial precipitate was again dissolved in 1-methyl-2-pyrrolidinone (80 ml) with sodium iodide (4.8 g). Once dissolved methyl iodide (7 ml) and sodium hydroxide (11 ml, 15% w/v) were added and stirred in a water bath at 60 °C for 30 min. An additional 2 ml of methyl iodide and 0.6 g of NaOH pellets were also added and left for 1h stirring. The material produced was washed and isolated as before.

The degree of quaternisation was calculated from corresponding ^{1}H NMR spectra (D_2O; 80 °C; Jeol 400 MHz spectrometer, Bruker, Japan) using Eq. (1) [208]:

Equation 1. Degree of quaternisation.

$$DQ\ \% = \frac{(\int 3.4)}{(\int 4.7{-}5.4)} \times \frac{1}{9} \times 100 \qquad (1)$$

where *DQ* is the degree of quaternisation, and $\int$3.4 and $\int$4.7 - 5.4 are the respective integrals of the trimethyl amino group absorption (3.4 ppm) and of the collective ^{1}H resonances in the range 4.7 - 5.4 ppm [202] respectively. Infrared spectra were recorded using a Varian 640-IR FTIR (Varian Inc, Palo Alto, USA; 400 – 4000 cm^{-1}, absorbance mode, 4 cm^{-1} resolution, 32 scans). Thermogravimetric analysis (TGA) was performed using a TGA-Q50 (TA Instruments, New Castle DE, USA; N_2 atmosphere, 10-600 °C, 10 °C min^{-1}). The crystalline order of dry TMC polymers was examined using an X-Ray diffractometer (Bruker D8, Karlsruhe, Germany; Ni-filtered Cu$K\alpha_1$, wavelength (λ) = 0.154059 nm at 40 kV, 40 mA, scan speed =1 deg min^{-1}, 2θ range 2-50°). Fourier Transform Raman (FT-Raman) spectra were recorded using a Bruker EQUINOX 55 spectrometer (Karlsruhe, Germany) equipped with a (D) FRA-106/S attachment: Raman excitation was by means of a A R510 diode pumped Nd:YAG laser operating at 1064 nm (with a maximum output power of 500 mW); optical filtering reduced the Rayleigh elastic scattering and, in combination with a CaF_2 beamsplitter and a high sensitivity liquid N_2-cooled Ge-detector, allowed the Raman intensities to be recorded over the range 50 - 3300 cm^{-1} in the Stokes side.

2.3.2. Formulation and characterisation of hydrogels

For each synthesised TMC polymer, four TMC solutions with a concentration of 4.5 % w/v and a total volume of 4 mL were prepared in deionised water. To the TMC solutions, PEG 4000 (270 mg) was added with stirring until a clear solution was obtained. In parallel, a series of aqueous GP solutions of specified concentrations (6.25, 12.5, 25 and 50 % w/v) was also prepared. All solutions were

placed in an ice bath for 10 min. Hydrogels were prepared by the dropwise addition (under stirring) of 1 mL aliquots of the cold GP solution to each of the cold TMC/PEG solutions, gel compositions are given in table 9

Table 9. The composition of TMC hydrogel formulations

Component	Final concentration (% w/v)
TMC (L1, L2, M1, M2, H1, H2)	3.6
PEG 4000	5.8
GP	1.25, 2.5, 5, 10

- ## Visual determination of sol-gel transition time

The sol-gel transition time was determined by visual inspection, using the inversion method [209]: TMC/PEG/GP solutions (5 mL) were incubated in a water bath at 35 °C, or left at room temperature for the duration of the test, and at 30 s intervals the vials were inverted to assess the flowage of the sample; the sol and gel phases were respectively characterised by the sample exhibiting liquid-like flow or becoming immobile. All experiments were carried out in quadruplicate.

- ## Rheological investigations

Rheological analysis (cone and plate geometry; cone dimensions 2° and 60 mm diameter) was performed using an AR2000 controlled-stress rheometer (TA Instruments, Leatherhead, Surrey, UK) interfaced to TA Rheology Data Analysis software (V.5.1.42, TA Instruments, Leatherhead, Surrey, UK). Aliquots of test samples were loaded onto the rheometer platform and allowed to equilibrate (5 min) at the temperature of the experiment. Strain sweep measurements at 1 Hz (n=1) allowed the determination of the linear viscoelastic region (LVR); where appropriate, further rheological investigations were performed within this region.

- ## Assessment of *in vitro* sol-gel transition time and temperature

To assess the physiological relevance of the sol-gel transition time of TMC hydrogels, rheological evaluation tests were performed at 15 °C and at 35 °C; temperatures that respectively correspond to that of cool storage and that of the surface of the nasal mucosa [31]. For formulation M1-2.5GP, the experiment was also carried out at 25, 27, 29, 31, and 33 °C, to study the effect of temperature on

gelation time. A multiwave frequency test allowed the determination of the frequency-independent gelation time from the intersecting curves tan *δ versus* time. A time sweep (1 °C min^{-1}) was performed over the 10 °C – 40 °C temperature range, at a fixed frequency (0.01 Hz) and a fixed amplitude of applied stress (0.02 Pa). The gelation temperature was determined by monitoring the variations in the elastic (G') and viscous (G") moduli: gelation temperature was identified by the transition from a prevalently viscous state (G" > G') to one that is prevalently elastic (G' > G"). All experiments were carried out in quadruplicate.

2.3.3. Preparation of mucus/hydrogel systems

Since the capability of hydrogels to form true blends with mucus is a property of some importance to the *in vivo* mucoadhesion behaviour of the system and also its influence upon the mucociliary transport rate (MTR), hydrogel/mucus mixtures for rheological and other investigations were prepared by mixing the hydrogel formulations with simulated nasal electrolyte solution (SNES: 7.45 mg mL^{-1} NaCl; 1.29 mg mL^{-1} KCl and 0.32 mg mL^{-1} $CaCl_2.2H_2O$; adjusted to pH 5.5 with 1M aqueous HCl and mixed with 1 mg mL^{-1} aqueous mucin in the 5:1 (w/w) ratio). Controls were provided by similar, 5:1 (w/w), mixtures of hydrogel and water and also of water and mucin.

- **Viscosity, viscoelasticity and rheological synergy**

Frequency sweeps (10 - 0.01 Hz, 20 readings) at 35 °C on hydrogel/mucus mixtures allowed the determination of the complex modulus, G*; evaluation studies confirmed there was no significant difference between the 20 readings of G*. Measurements of G' and G" were also averaged over 20 readings. The synergistic effect of hydrogel and mucin mixtures was evaluated using Eq. (2) [61]:

Equation 2. Relative G'.

$$Relative\ G' = \frac{G'_{Mix} - (G'_{Hyd} + G'_{Muc})}{G'_{Hyd} + G'_{Muc}} \quad (2)$$

where G'_{Mix}, G'_{Hyd}, G'_{Muc} represent the respective elastic moduli of hydrogel–mucin mixtures, hydrogel, and mucin; relative G" was calculated similarly.

The apparent viscosities (η) of the hydrogel and of the hydrogel-mucin samples were monitored for 1 min under constant shear rate (100 s^{-1}); experiments were repeated four times, and measurements are reported as the average of those taken during the final 30 s of each measurement period. Oscillatory measurements (40 - 0.01 Hz; constant applied stress, within the

LVR) allowed the investigation of the effects of frequency on the dynamic moduli, G' and G", and provided the means for the assessment of rheologically synergistic effects.

2.3.4. Water-holding capacity of hydrogel formulations

The capacity of the hydrogels to hold absorbed water was evaluated as a function of molecular weight and the degree of quaternisation. Discs were cut (diameter 15 mm, cross-sectional thickness 5 mm) from freeze-dried hydrogel and dried at 60°C for 24 h. These were placed into dissolution baskets, which were then immersed into pH 5.5 SNES-mucin (20°C) for specified periods of time. The baskets were lifted out of the solution and each weighed following the repetitive wiping of excess surface liquid (filter paper) until three consecutive readings gave identical mass readings. The water-holding capacity (WHC) was calculated from Eq. (3):

Equation 3. Water holding capacity.

$$WHC = \frac{M_{Max} - M_0}{M_0} \quad (3)$$

where M_{Max} is the maximum mass of the hydrated gel, and M_0 is the mass of the dry gel at time 0.

2.3.5. Mucoadhesive behaviour

A TA-XT2 Texture Analyser (Stable Micro Systems, Surrey, UK) in adhesion mode allowed the determination of the total work required to detach the lyophilised hydrogels from isolated rat intestinal mucosal tissue [210]. Positive and negative controls were provided by samples of poly (acrylic acid) and tristearin, respectively. Test materials or controls were attached to the lower tip of the texture-profile-analyser probe using double-sided adhesive tape. The substrate was Wistar rat intestinal mucosa that had been isolated surgically and kept under mucin solution (pH 5.5). For force measurements, the tip was lowered onto the surface of the mucosa, a force of 0.02 N was applied for 2 min, to ensure intimate contact between the mucosal surface and the hydrogel sample, and the probe was raised at a constant speed of 5.00 mm s^{-1} to a return distance of 300 mm. The total work of adhesion (TWA) was calculated from the area under the force *versus* distance curve and reported as the average of four measurements. Data collection and manipulation was by means of an interfaced XTRA Dimension software package.

2.3.6. Statistical Analysis

The statistical significance of the differences between rheological and mucoadhesive parameters of the range of TMC/PEG/GP hydrogel formulations was tested by one-way analysis of variance (ANOVA) and further by the multiple comparison Tukey-Kramer test. Differences were considered to be significant if $p < 0.05$.

2.3.7. Physicochemical characterisation of hydrogels

The porosity and surface area of the lyophylised hydrogels were determined using the Brunauer-Emmett-Teller (BET) method. The specific surface area (S_{BET}), the pore volume (V_P) and the pore size distribution of the samples were determined (Quantachrome Autosorb-1 instrument; Boynton Beach, FL, USA) from the adsorption/desorption isotherms of nitrogen at -196 °C. The surface area was obtained following the BET (Brunauer–Emmett–Teller) procedure with six relative pressures of nitrogen in the range 0.05 p_0 – 0.3 p_0. Pore size distribution was estimated using the BJH (Barrett, Joyner and Halenda) method. Total pore volume was determined (out-gassed samples; room temperature, 10 h, vacuum) at P/P_0 = 0.995. The surface morphology and internal structure of hydrogels were visualised by scanning electron microscopy (SEM; JEOL SEM (JSM-6060LV, JEOL Ltd, Japan; working distance 12 - 14 mm at 10 Kv, spotsize 35 µm): flat surface cross-sections of dried samples were prepared using a sharp blade and imaged under vacuum after 3 min of palladium/gold sputtering; displayed images are at 3000× magnification.

2.4. Results and Discussion

2.4.1. TMC synthesis and characterisation

Consequent to the quaternisation reaction, vibrational spectra exhibited the features that differentiate TMC polymers from their precursor chitosans. Indicative of the destruction of residual amidic linkages during the quaternisation reaction, Raman spectra (Fig. 3) showed that the intense CH_3 absorption of acetamide groups (1380 cm^{-1}), the amidic carbonyl band (1657 cm^{-1}) and the weak amidic N-H strech (3367 cm^{-1}) all disappeared on quaternisation [211, 212]. Infrared spectra (Fig. 3) showed the characteristic band (3300 - 3500 cm^{-1}) that is consistent with the presence of hydrogen bonded $–NH_2$ and –OH functionalities. As expected, the intensity of the amino group bend, at 1597

cm^{-1}, weakened on quaternisation. Indicative of the specificity of the reaction, primary and secondary alcohol absorptions (1102 - 1082 cm^{-1}) appear little changed following quaternisation [204]. Consistent with the introduction of methyl moieties, the C-H stretching bands (2900-3000 cm^{-1}) and bending deformations (1470-1500 cm^{-1}) appeared to become more intense with increasing degree of quaternisation.

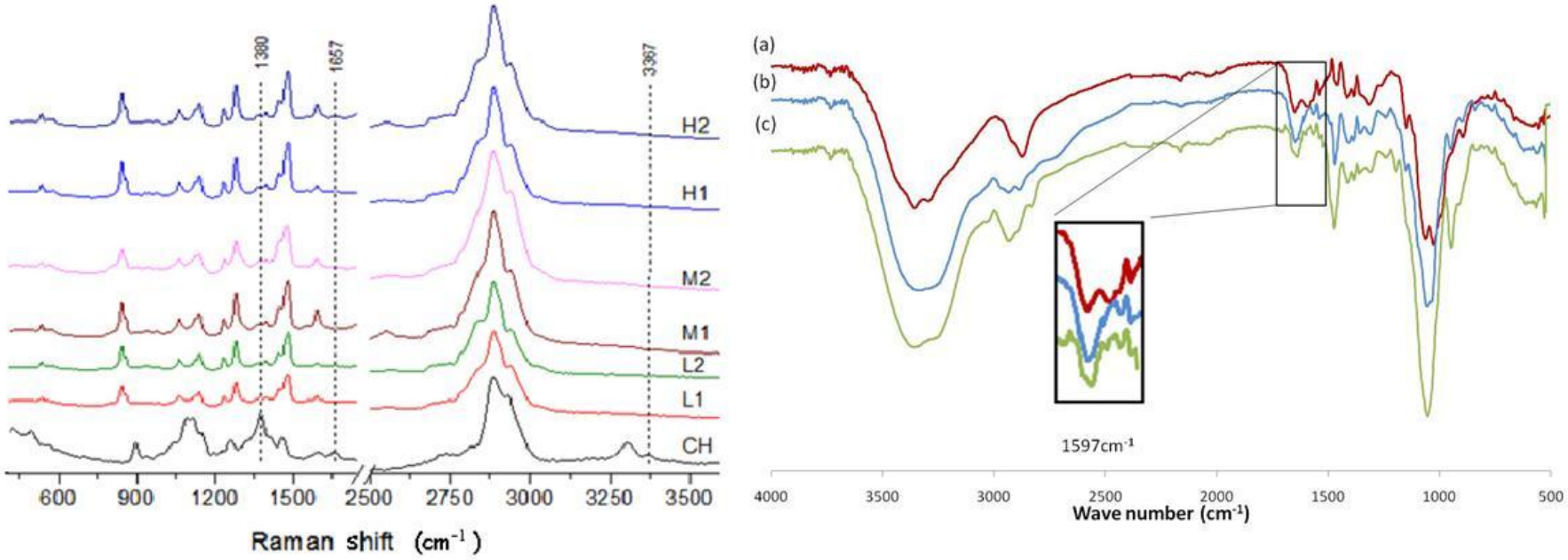

Figure 3. Left: FT-Raman spectra of chitosan (CH) and TMC polymers (L, low; M, medium and H, high molecular weight; 1, one step synthesis and 2, two step synthesis). Right: FTIR spectra of (a) low molecular weight chitosan, (b) L1 and (c) L2.

The DQ of the synthesised TMC polymers, as calculated from ^{1}H-NMR experiments [202], is presented in Table 10, along with $T_{50\%}$ values from thermogravimetric investigations. In accord with expectation [213], higher DQ polymers exhibited increased thermal stability relative to their respective congeners; a similar trend of increasing thermal stability was observed with increasing average molecular weight.

Table 10. Degree of quaternisation of N-trimethyl-chitosan chloride polymers synthesised and the temperature required to reduce the respective weight by 50%, $T_{50\%}$, as derived via thermogravimetric analysis. The indexes 1 and 2 refer to the number of steps employed in the synthesis of chitosan.

TMC	Chitosan average molecular weight	DQ %	$T_{50\%}$ / °C
H1	High	25.6	356
H2		53.9	380
M1	Medium	32.8	323
M2		61.3	383
L1	Low	37.0	308
L2		54.6	322

Consistent with the thermal-stability effects, XRD experiments showed the increased crystalline order in TMC samples relative to that of their precursor chitosans, as is indicated by the appearance of pronounced bands at 2ϑ 19.4°, 23.4° and 32.0°, Fig. 4, and the corresponding disappearance of the characteristic chitosan peak at 2ϑ = 11° [214, 215].

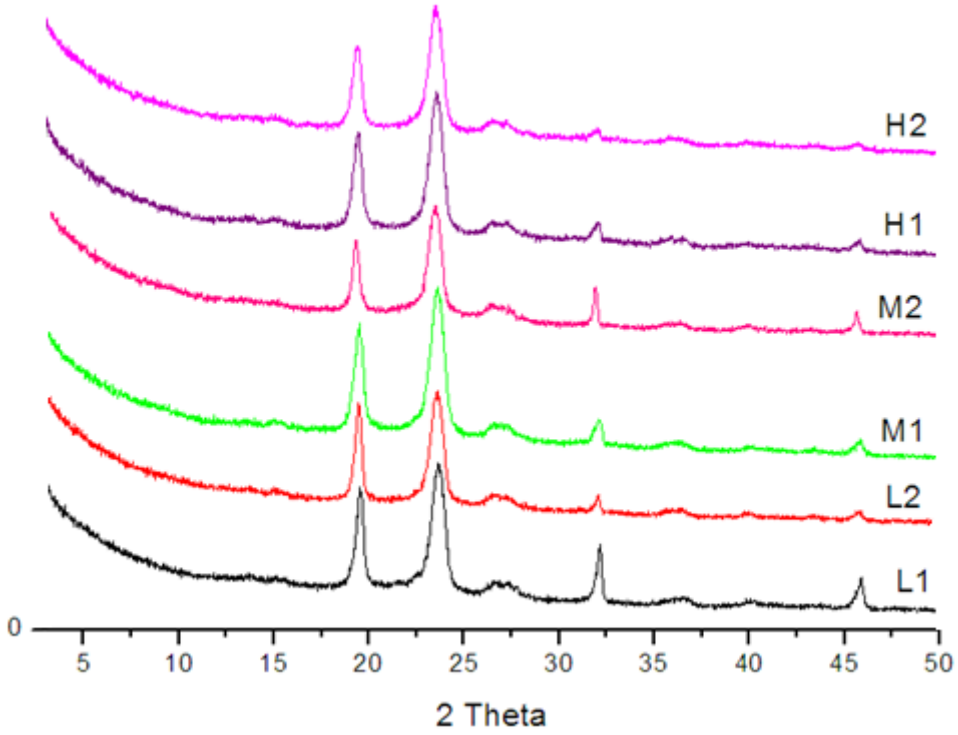

Figure 4. XRD patterns of TMC polymers (H, M and L denoting high, medium and low Mw respectively and 1 and 2 denoting one or two step synthesis respectively)

2.4.2. Characterisation of hydrogel formulations

- ### Determination of gelation time and temperature

The performance criteria of the nasal-delivery formulations are imposed by the physiological temperature of the nasal cavity (32 - 35 °C [31]) and by the mucociliary clearance time (half life *ca*. 21 min [76]), which correspondingly specify the temperature range and time limits for the sol-gel transition. The application of the inverted-tube test coupled with rheology investigations allowed the determination of the influence of GP concentration on gelation temperature and gelation time, Fig. 3.

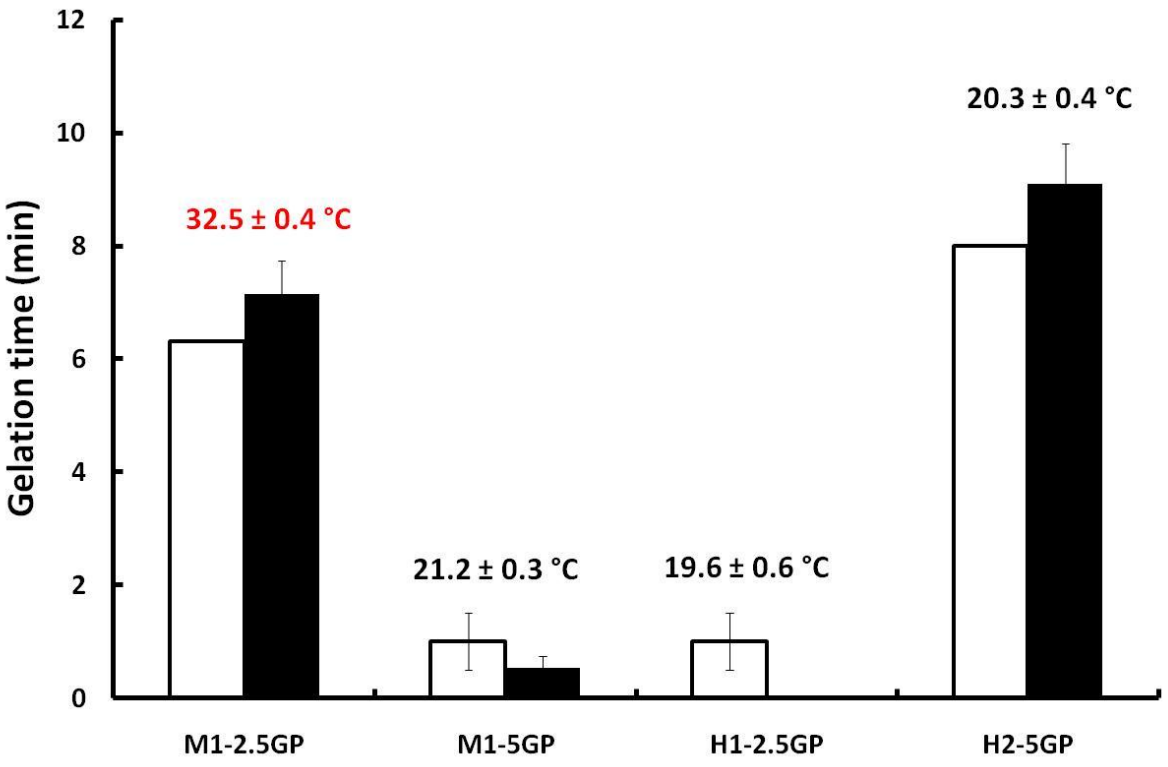

Figure 5. Rheological (black) and observational (white) gelation time, and rheological gelation temperature of TMC/PEG/GP hydrogel formulations (e.g. M1-2.5GP, hydrogel formulated with medium molecular weight TMC, synthesised by one step procedure and containing 2.5% GP). Results are given as mean ± SD (n=4).

The data for TMC formulations based on low MW chitosan are not shown as they do not exhibit gel-like behaviour over the investigated range of GP concentrations, due to the short polymeric chain which offers limited chances of physical entanglement and hydrophobic interactions. The co-formulation of PEG molecules imparted considerable improvement on the capacity of networks to form gels. Amongst the formulations tested, only hydrogel M1 (2.5 % w/v GP) exhibited its sol-gel transition at a physiologically relevant temperature (32.5 ± 0.4 °C; Fig. 5). The gelation time of the same formulation has been determined at 6.3 ± 0.6 min, which is well below the time for mucociliary clearance. The gelation time of this formulation was tested in the 25-35 °C range to ascertain that it would be effective even if the temperature of the nasal cavity was different (Table 11).

Table 11. Effect of temperature on the gelation time of M1-2.5GP formulation.

Temperature (°C)	Gelation time (min)
29	49.6 ± 3.4
31	16.5 ± 1.9
33	9.3 ± 1.6
35	6.3 ± 0.6

The formulation underwent sol-gel transition in a time shorter than the half life of the mucociliary clearance at all temperatures above 29 °C. The polyol, GP, provides protective hydration of TMC, maintaining the polymer chains stretched in solution, as the inter- and intra-molecular crosslinking within the system is reduced [4]. Upon raising the temperature to 35°C, the increased kinetic energy favours the formation of hydrophobic interactions between chains. The addition of PEG allows the formation of an even more extensive gel network by providing extra sites for hydrogen bonding [4]. Gelation was accompanied by a significant change in viscoelasticity, G* (Fig. 6a). Apparent viscosity increased with increasing temperature; this increase was not statistically significant for formulation H2 (5 % w/v GP), (Fig. 6b). The effect of temperature was most pronounced for formulation M1 (2.5 % w/v GP), which displayed the most significant differences, $p < 0.0001$, in both viscosity and viscoelasticity. Hydrogel H1 (2.5 % w/v GP) exhibited the lowest gelation temperature and the fastest gelation time (19.6 ± 0.6 °C, 13 ± 4 s), since the long polymer chains formed extensive hydrophobic interactions. Formulation H2 (5 % w/v GP) did not show significant thermoresponsive behaviour with respect to the apparent viscosity (Fig. 6b); the higher degree of quaternisation increased solubility and enhanced electrical repulsion between TMC chains to prevent a substantial change in viscosity. These data are in agreement with the literature, demonstrating that the components concentration and polymer characteristics all have an effect over the gelation time and temperature of the formulation [216-218].

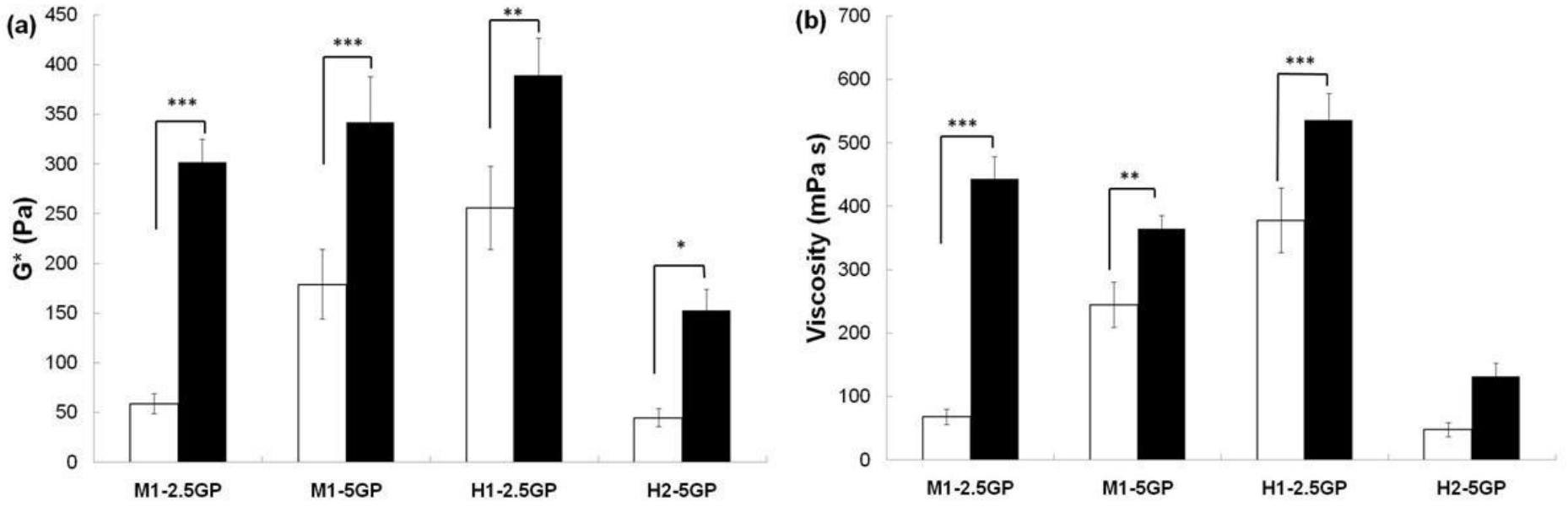

Figure 6. (a) Complex modulus (G*) and (b) apparent viscosity values for TMC/PEG/GP hydrogel formulations at 15 ^{o}C (white) and at 35 ^{o}C (black). Results are given as mean ± SD (n=4): ***p<0.001, **p<0.01, *p<0.05; Tukey-Kramer post-hoc comparison test.

- ## Rheological properties of the hydrogels

Fig. 7 summarises G* and η data – the rheological properties of polymer–mucus mixtures that have a most significant impact on MTR [206] – for hydrogel-mucin mixtures at 15 and at 35 °C. The very significant ($p < 0.001$) increase in G* seen for M1 and for H1 is consistent with mixtures that are capable of exhibiting prolonged residence in the nasal cavity [206]. The complex modulus (G*), which describes the rigidity and overall strength of the gel, is used as a parameter to monitor the effect on MTR. Gels of increasing G* were found to increasingly reduce MTR, due to the inability of the cilia to penetrate effectively into the gel (elastic properties), decreasing the efficiency of energy transfer to the mucus/polymer layer (viscous properties) [206].

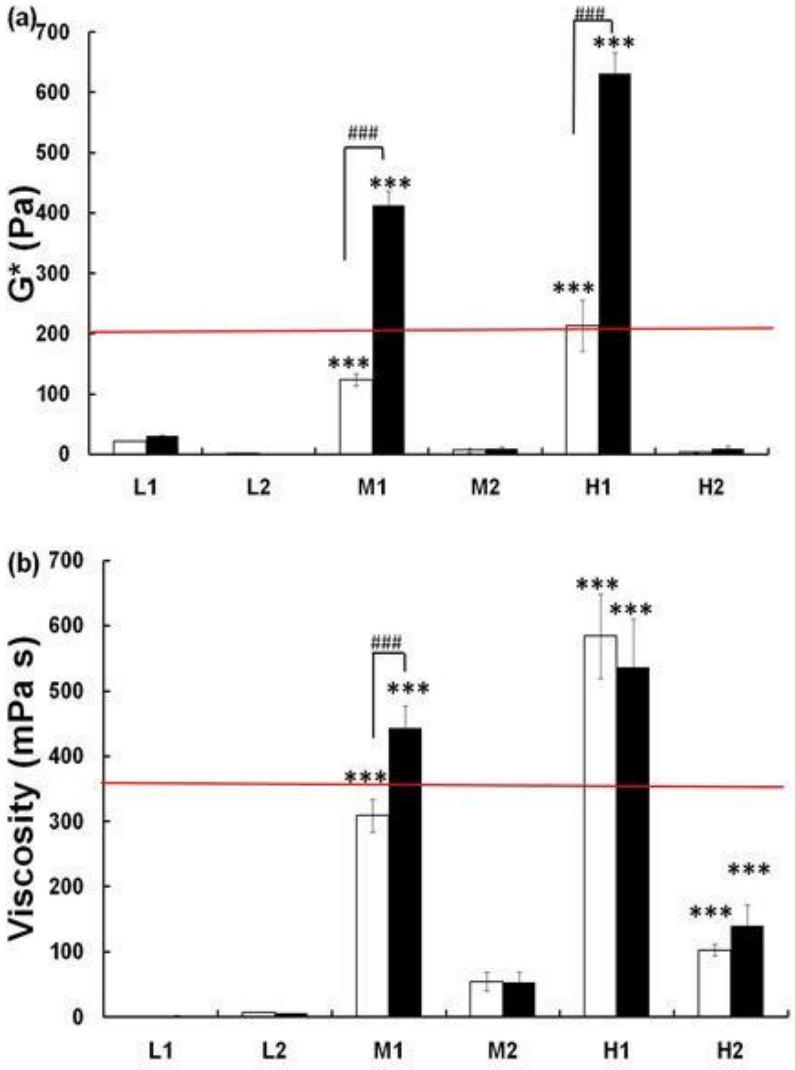

Figure 7. (a) Complex modulus (G*) and (b) apparent viscosity, at 15 °C (white) and 35 °C (black) of TMC/PEG/GP hydrogel-mucin mixtures. All formulations were prepared with 2.5% GP. Values are given as mean ± SD (n=4). Data above the red line indicate (a) G* values required to decrease MTR by at least 80% and (b) η values required to decrease MTR by at least 60% [206]: ###p < 0.001,

comparing 15 °C to 35 °C, ***p < 0.001 with respect to water; Tukey-Kramer post-hoc comparison test.

At 35 °C, the same hydrogel–mucin mixtures displayed apparent viscosity values > 350 mPa s, but at 15 °C only M1 mixtures had viscosities < 350 mPa s; identifying M1 as the material of choice for the formulation of thermosensitive nasal sprays or drops. Hydrogels L1 and L2 appeared to be of little value to nasal delivery since their rheological properties were not significantly different to those of water ($p > 0.05$), at either temperature. Similarly, hydrogels M2 and H2 did not meet the requirements ($G^* > 200$ Pa; $\eta > 350$ mPa s) for use as thermosensitive nasal-delivery systems [206].

- ## Hydrogels–mucin interactions

Oscillation profiles of L1, M1, and H1 and of their mixtures with mucin are presented in Fig. 8, along with those of mucin alone.

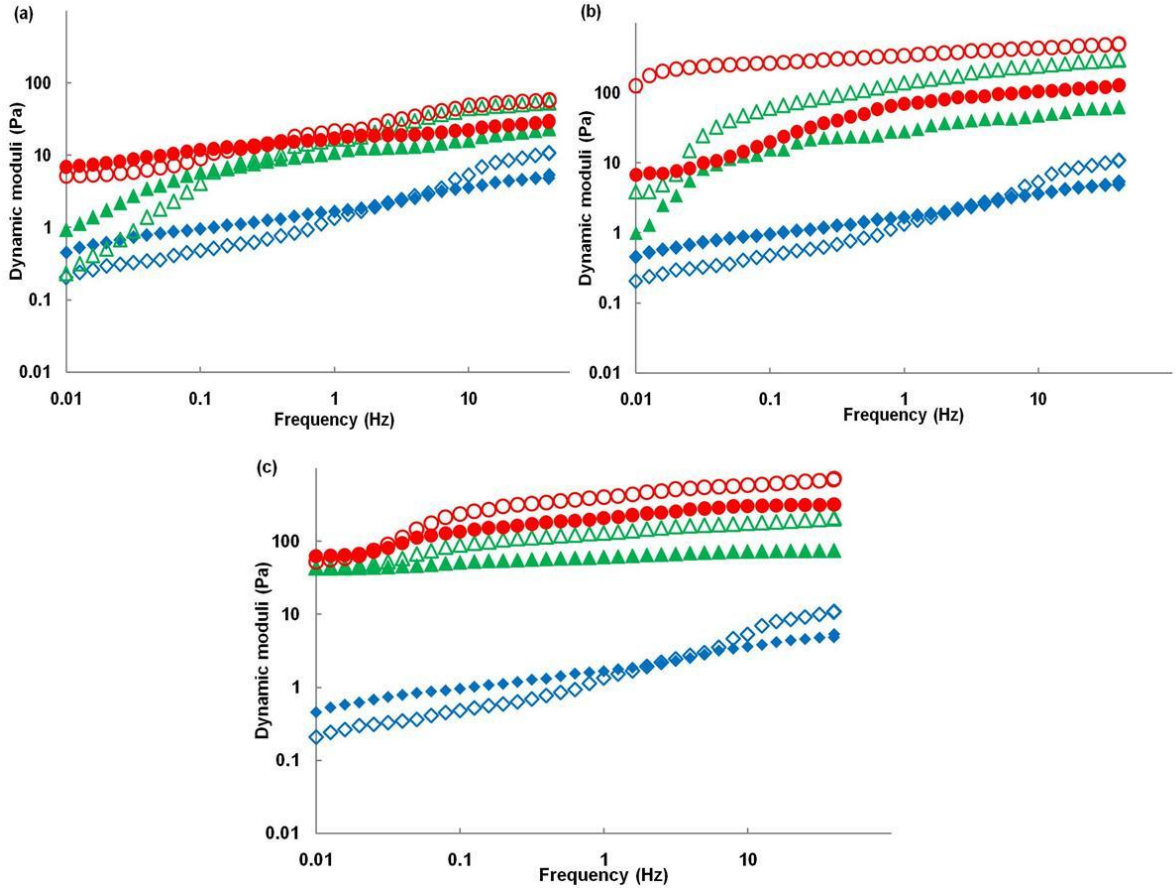

Figure 8. Dynamic oscillation spectra of TMC/PEG/GP hydrogels (all hydrogels containing 2.5 % GP) and of their mixtures with mucin at 35 °C: (a) L1; (b) M1; and, (c) H1 – G' hydrogel–mucin (○); G" hydrogel–mucin (●); G' hydrogel (△); G" hydrogel (▲); G' mucin (◇), G" mucin (◆).

The storage and loss *moduli* of mucin show some frequency dependency, with a cross-over at *ca*. 2 Hz, as is typical of the behaviour of weakly entangled polymeric systems [219]. The observed behaviour of mucin is different to that of physiological mucus, for which G' > G" over the entire frequency range [42]. The oscillation spectra of M1–mucin mixtures (Fig. 8b) show that G' > G" over the entire frequency range, which is consistent with the behaviour of a strongly cross-linked gel [42], consequently indicating that there is substantial interaction between the hydrogel and the mucin. By contrast, L1-mucin mixtures (Fig. 8a) behave as a physically entangled system, exhibiting G" > G' over a broad spectral range along with a substantial decline in G', and to a lesser extent G", at low frequencies [42], therefore showing a lower degree of interaction between the two systems upon mixing. The oscillation spectra of the H1-mucin mixture, Fig. 8c, show a predominance of elastic behaviour (G' > G") with some degree of physical entanglement (G" > G') at lower frequencies. The mixing of H1 with mucin results in a more pronounced increase in G" than in G', which is interpreted as an increase in the fluidity of the system since there is a low degree of entanglement between the longer coiled TMC chains and mucin, decreasing mucoadhesive potential. Comparison of the rheology profiles of L2, M2 and H2 with those of their mixtures with mucin reveals no significant differences in dynamic *moduli*. For these materials the increase in aqueous solubility following the quaternisation of TMC is accompanied by a predominance of viscous properties and a suppression of the elasticity of the hydrogel. Since all materials share the chemical features of chitosan, their capacity to enter into rheologically synergistic relationship with mucin must be a direct consequence of the combined effects of their average molecular weight and degree of quaternisation [53, 220-222].

The addition of mucin to the H1 hydrogel, Fig. 9, effects an increase in G', indicative of the homogeneity of the mixture, and a more pronounced increase in G", which shows that mucin/H1 mixtures are less elastic and more viscous than the parent hydrogel. The relative G' of the mucin/M1 mix, Fig. 9, is consistent with the high compatibility of the constituent materials in their forming of homogeneous mixtures.

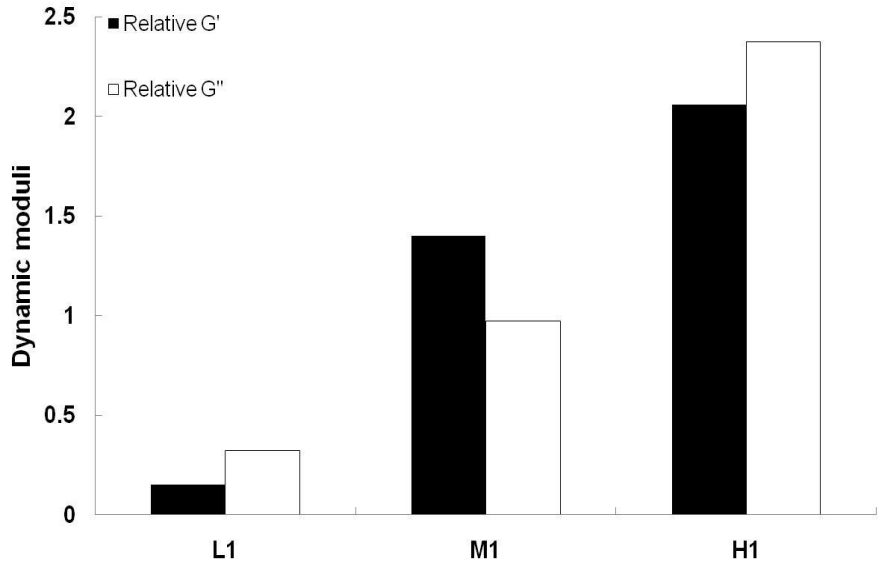

Figure 9. The synergistic effect of TMC/PEG/GP hydrogels-mucin mixtures evaluated using relative G' and G" values at 35 ^{o}C.

2.4.3. Mucoadhesive behaviour

As is prerequisite to good mucoadhesive behaviour, all hydrogels displayed their capacity to hydrate readily and hold high quantities of water (Fig. 10a) [12, 48, 131, 133, 222, 223]. The water-holding capacities of the low degree of quaternisation hydrogels M1 and H1 are comparable with those of poly(acrylic acid), the archetypal mucoadhesive polymer. Complementary work-of-adhesion measurements identify M1 as the hydrogel of choice for employment in mucoadhesive formulations: M1 is the only material that yielded work-of-adhesion values (735 ± 98 µJ) that are comparable with those of poly(acrylic acid) ($p > 0.05$). The work-of-adhesion values determined for hydrogels L1, L2, M2 and H2 were similar ($p > 0.05$) to that obtained for tristearin, the negative control (Fig. 10b). The results correlate with those from rheological investigations, and highlight the complementarity of the techniques in the evaluation of the mucoadhesive potential of a material.

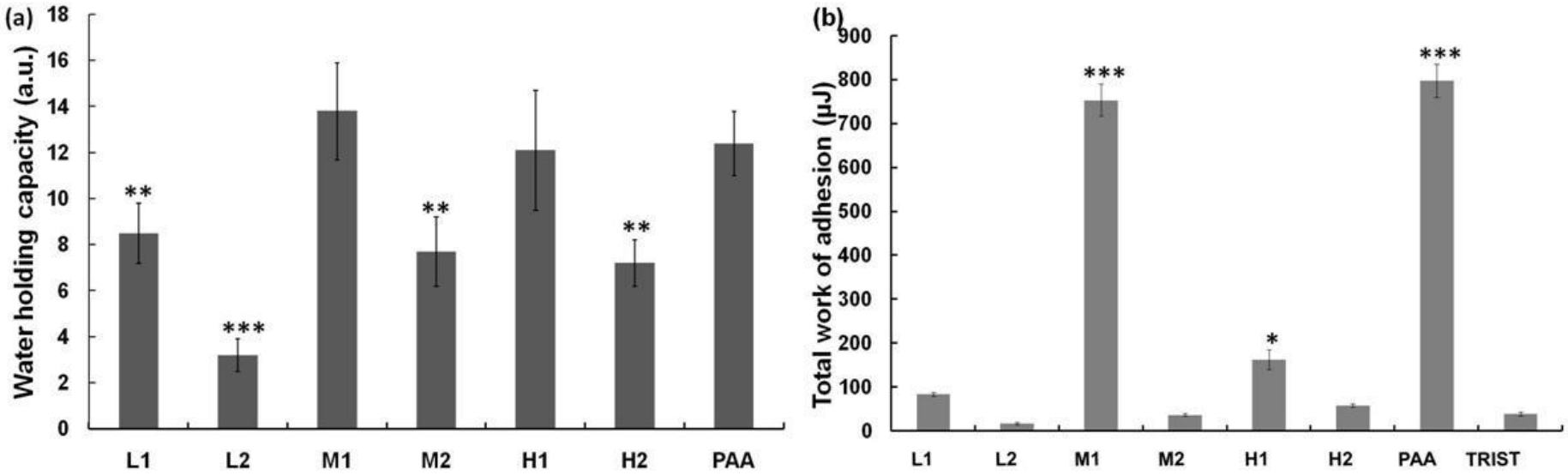

Figure 10. (a) Water holding capacity (WHC; mean ± SD, n = 5) of hydrogel formulations in SNES-mucin solutions: **p < 0.001, ***p < 0.0001 with reference to M1; Tukey-Kramer post-hoc comparison test. (b) Total work of adhesion (TWA; mean ± SD, n = 5) of TMC hydrogels, poly(acrylic acid) (positive control) and tristearin (negative control): ***p < 0.001 and *p < 0.05 with respect to the positive control; Tukey-Kramer post-hoc comparison test

2.4.4. Physicochemical characterisation of hydrogels

As exemplified by infrared spectroscopy of H1 (Fig. 11), hydrogels exhibit the vibrational features of all constituents of the formulation: features associated with PEG are evident at the aliphatic C-H stretch region (*ca*. 2700 cm^{-1}) and also in the skeletal fingerprint region, whereas TMC manifests itself in the hydrogen bonded region (> 3000 cm^{-1}). In H1, the broad absorption arising from hydrogen bonded interactions due to the –NH and –OH functionalities of the TMC constituent of the hydrogel are shifted to higher frequencies relative to those of pure TMC. This shift is consistent with the predominance of intermolecular hydrogen bonding over corresponding intramolecular interactions [224] and confirms the homogeneous nature of the formulation.

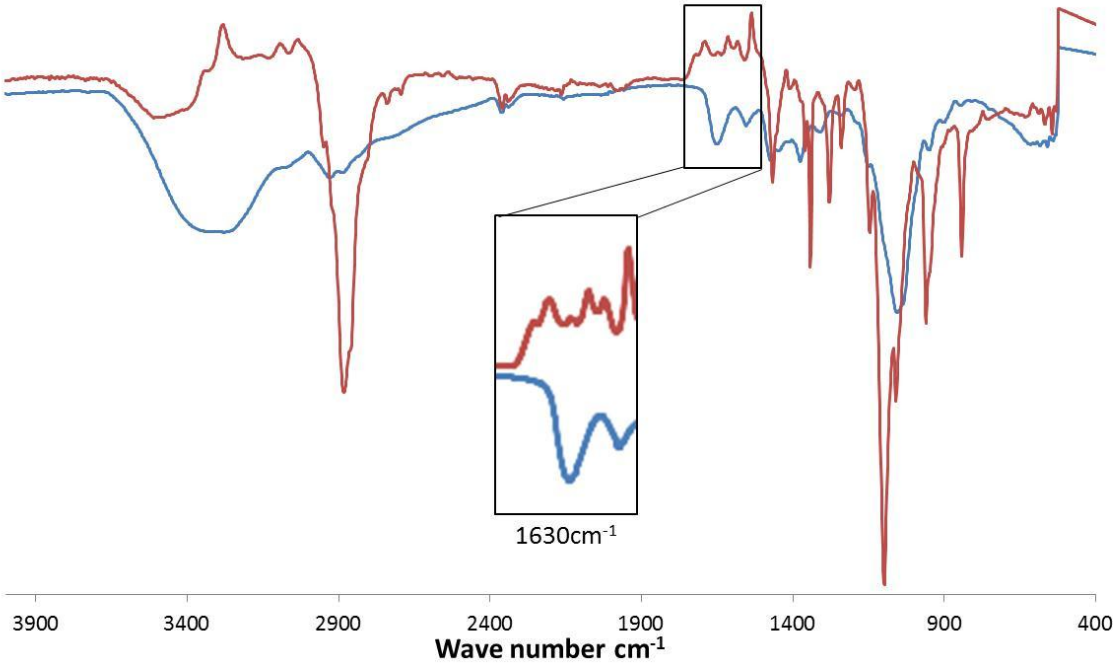

Figure 11. IR spectra of TMC H1 (blue) and TMC(H1)/PEG/GP hydrogel (red).

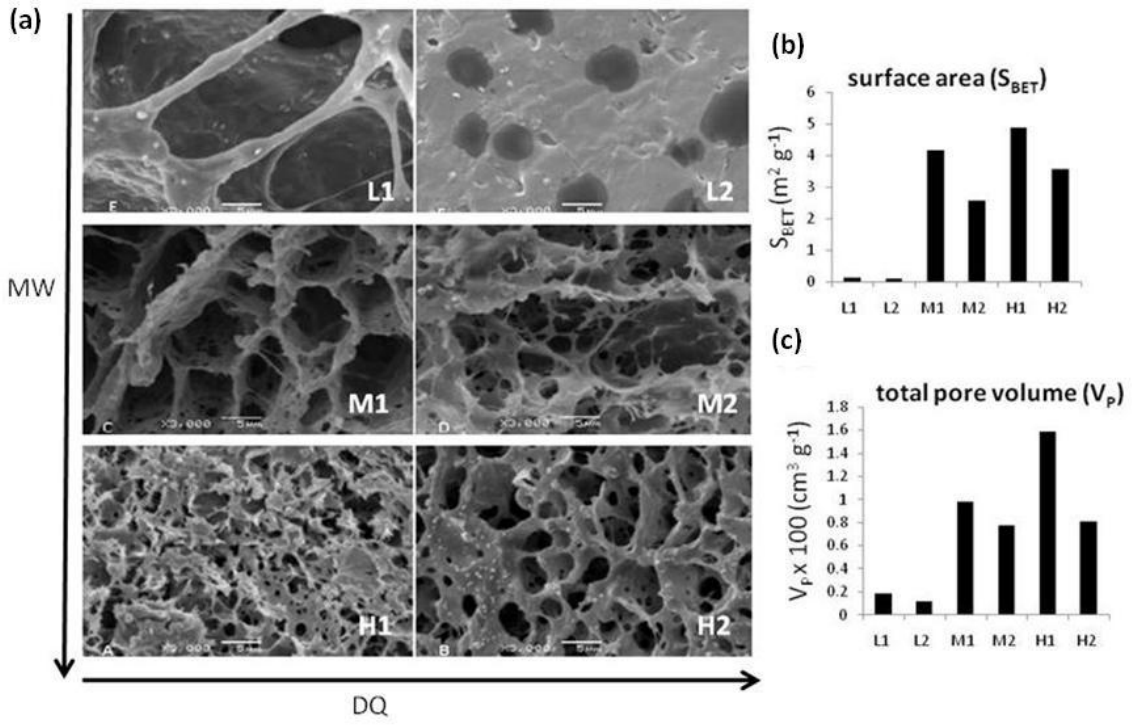

Figure 12. (a) SEM micrographs, (b) surface area (S_{BET}), and (c) total pore volume (VP) of TMC/PEG/GP hydrogel formulations (2.5 % GP). (a)

Surface area analysis, Fig. 12, shows that in a direct relationship with the average molecular weight of each material, S_{BET} (Fig.12b) adopts values that are as low as 0.08 m^2g^{-1} or as high as 4.88 m^2g^{-1}. This trend corresponds with SEM images of pore size, Fig. 10a, and with determinations of pore volume, Fig. 12c: hydrogels that had been dried for SEM imaging exhibited pore diameters varying from *ca*. 4 nm to 1 µm. As expected [225], trends in porosity and S_{BET} data follow those for water holding capacity; hydrogels that hold more water present higher porosity values. With the exception of H1, the mucoadhesive behaviour of the materials also correlated well with trends in internal surface area and porosity. Furthermore, porosity data can help predict the diffusion of drug molecules within the gel [43, 85, 93].

2.5. Conclusion

Co-formulation of poly(ethylene glycol) and glycerophosphate with *N*-trimethyl chitosan of medium average molecular weight and low degree of quaternisation yields an aqueous formulation that exhibits a sol-gel transition at 32.5 °C and within 8 min. The same hydrogel forms rheologically synergistic mixtures with mucus and also exhibits good affinity for mucosal surfaces. The properties of this hydrogel appear to be consistent with its potential use as an *in-situ* thermogelling drug-carrier system for intranasal drug delivery. Further studies are underway to investigate its absorption

enhancing properties and biocompatibility. Positive preliminary results indicate this is a promising formulation.

Chapter Three:A thermosensitive, mucoadhesive intranasal hydrogel based on *N*-trimethyl chitosan: structural integrity, *in vitro* insulin release, cytotoxicity and transport across Calu-3 monolayers.

A thermosensitive, mucoadhesive intranasal hydrogel based on *N*-trimethyl chitosan: structural integrity, *in vitro* insulin release, cytotoxicity and transport across Calu-3 monolayers.

Abstract

An *in situ* thermogelling, mucoadhesive formulation based on *N*-trimethyl chitosan chloride has been evaluated for its potential to affect the transmucosal delivery of insulin *via* the nasal cavity. Spectroscopic and analytical investigations (UV-vis, fluorescence, IR, Raman and SDS-PAGE) have indicated that the incorporated insulin is in monomeric form and that it retains its structural integrity and conformational order over several days. *In vitro* studies at a physiologically relevant temperature (35 °C) have shown that the formulation releases most of its insulin load (*ca*. 70%) in a non-Fickian manner during the timescale over which the gel-to-sol transition (ca. 8 min) takes place, but once gelation is complete the release of the remainder of the therapeutic content follows first order kinetics over at least sixty minutes. Investigations on the effects of the same formulation on a model nasal mucosa (Calu-3 cell monolayer) have shown the capability of the formulation to effect the transient opening of tight junctions.

3.1. Introduction

The impetus for research into transmucosal drug delivery of peptides and proteins is provided by the invasiveness of the parenteral alternative [1]. Consequent to the generally unfavourable transport of macromolecules through mucosal membranes, approaches for enhanced absorption have included: co-administration with protease inhibitors [226]; inclusion of permeation enhancers [227]; modifications of peptide structures to improve metabolic stability or membrane permeation [3]; and, the development of mucoadhesive systems that prolong residence time upon the absorptive surface [228].

Owing to its accessibility, large surface area and thin epithelium, the nasal mucosa may prove useful for the possible delivery of therapeutic macromolecules that cannot withstand the challenges of the gastrointestinal tract. To this end, research efforts have examined the potential use of several types

of formulation, including powders [229], microspheres [230], nanoparticles [231], solutions [232] and gels [4]. The supporting matrix of such formulations is often derived from chitosan, a mucoadhesive polysaccharide that is known to enhance the permeability of the nasal membrane by promoting the transient opening of tight junctions [4, 229, 231, 232].

Towards the *in vitro* testing of such formulations, cultured nasal epithelium provides a useful model for the study of nasal drug absorption in that it allows a preliminary assessment of the permeability, toxicity, metabolism and transport of potential therapeutic agents [233]. A useful surrogate for human nasal epithelia is provided by Calu-3 cells [234, 235] – these are a well characterised, human respiratory tract epithelial cells that can be cultured as confluent monolayers at the air-medium interface [236, 237].

In previous work [146], we have reported the preparation and characterisation of an *in situ* thermogelling formulation based on *N*-trimethyl chitosan chloride (TMC). The formulation, which has been designed for application as intranasal solution, forms a mucoadhesive gel within the timeframe of mucociliary clearance (MCC) to effect prolonged residence at mucosal surfaces [146]. We now extend this work by assessing the capability of these hydrogels to act as controlled-release matrixes for albumin or insulin. Also, by recording the formulation-induced changes in transepithelial electrical resistance (TEER), we use Calu-3 monolayers as an *in vitro* probe of the potential permeation-enhancing capacity of the applied formulation. In parallel, we assess the cytotoxicity of each formulation by monitoring the essential viability of the Calu-3 monolayer substrates.

3.2. Materials

Chitosan (medium viscosity, 400 kDa, DD 84 - 89 *%),* and poly(ethylene) glycol 4000 (PEG) were obtained from Fluka, UK. Glycerophosphate (GP; equimolar mixture of α and β isomers), Bichinchonic acid (BCA) protein kit, Dulbecco's Modified Eagle Medium (Nutrient Mixture F12, Ham's; DMEM/F12), penicillin (10,000 U/mL) / streptomycin (10 mg/mL), fetal bovine serum, non-essential amino acids, l-glutamine, 3-[4,5-dimethylthiazol-2-yl]-2,5-diphenyl tetrazolium bromide (MTT), Hank's Balanced Salt Solution (HBBS), insulin from bovine pancreas, and albumin from chicken egg white, were purchased from Sigma-Aldrich Inc., UK. Methyl iodide and 1-methyl-2-pyrrolidinone were sourced from Acros Organics, Belgium. Dialysis tubing CO 12 – 14000 Da was obtained from Medicell International. Materials used for SDS-PAGE were sourced from Invitrogen Ltd, UK: Novex Tricine SDS Buffer kit and Novex 10-20% Tricine Gel 1.0mm. Human cell line Calu-3

was sourced from ATCC-LGC, UK. All other chemicals were obtained from Fisher Scientific, UK, and used as received.

3.3. Methods

3.3.1. Preparation of thermosensitive and mucoadhesive TMC hydrogel

N-Trimethyl chitosan chloride (degree of quaternisation = 32.8 %) was synthesised from medium molecular weight chitosan as previously described [146]. Albumin (*ca.* 40 kDa) or insulin (*ca.* 5 kDa), both at 3 mg/mL, provided the model molecules for studies of the release of proteins from the hydrogel matrix.

The albumin- or insulin-loaded sol-state hydrogels were formed by mixing GP (12.5 % w/v) with a solution of insulin or albumin (3 mg/mL) in aqueous HCl (0.1M; 1 mL) and then adding (dropwise, stirring) the resulting solution to a pre-prepared solution (4 mL) of TMC (4.5 % w/v) and PEG (6.75 % w/v). The pH of the formulation was in the range 4.8- 5.3. The gelation time and temperature, and the thermosensitivity and viscoelastic properties of the hydrogel were consistent with those reported [146] for corresponding systems prepared in the absence of HCl.

3.3.2. *In vitro* protein release

Uniformly cut dialysis membrane (volume capacity = 3 mL; molecular weight cut-off 12,000-14,000) was used to assess the *in vitro* release of albumin or of insulin from the hydrogel system; prior to filling with each sol-state hydrogel, the artificial membrane was allowed to stand in PBS (pH7.4, 24 h). Each dialysis sac was suspended in SNES-release media (SNES: 7.45 mg mL^{-1} NaCl, 1.29 mg mL^{-1} KCl and 0.32 mg mL^{-1} $CaCl_2.2H_2O$; adjusted to pH 5.5 with 1M aqueous HCl) that had been thermostatted at 35 °C and stirred (70 rpm). Aliquots (100 µL) for the analysis of albumin or insulin content (bichinchoninic acid (BCA) protein assay kit) that had been removed at specified time intervals, over 1 h, were replaced immediately with fresh, warm (35 °C) SNES-release media. Experiments were performed in quadruplicate.

- **Drug release kinetic modelling**

To assess the possible drug-release mechanism data were fitted to the Korsmeyer-Peppas equation[238]:

Equation 4. Korsmeyer-Peppas equation.

$$M_t/M\infty = K\,t^n \quad (1)$$

Where M_t is the amount of drug released at time t; K is the apparent rate constant, which is related to the structure and geometry of the dosage form; M_t/M_∞ is the fractional release of drug at time t; and n is the release exponent, the numerical value of which characterises the mechanism of drug release ($n < 0.45$, Fickian Release; $0.45 < n < 0.89$, non-Fickian Mass Transfer; $n > 0.89$, Case II Transport).

3.3.3. Integrity of released protein

- **SDS Page**

The integrity of released protein, insulin and albumin, from the 60 min *in vitro* study was assessed means of a 10-20 % SDS-PAGE study. The protein standard and samples of released protein were each loaded into individual wells using a micropipette, and the electrophoresis experiment (125 V, 90 mA, 12.5 W) was performed over 75 min. Protein bands were visualised following staining with SimplyBlue SafeStain (1 h, room temperature) and images of dried gels (wiping) were recorded using a scanner.

- **UV-vis, FTIR and Raman analysis**

UV-Vis spectra of insulin solutions (3 mg/mL) in aqueous HCl (0.1 M) were recorded (230-350 nm) using a Unicam UV2 UV-Vis spectrophotometer. To monitor the stability of these solutions, spectra were recorded over one week and second derivative spectra were compared by means of the Friedman test using PASW® Statistics 18 software. Infrared spectra were recorded using a Varian 640-IR FTIR (Varian Inc., Palo Alto, USA; 400-4000 cm, absorbance mode, 4 cm resolution, 32 scans). Fourier Transform Raman (FT-Raman) spectra were recorded using a Thermo Scientific Nicolet 6700, NXR FT-Raman module, CaF_2 beam-splitter, coupled to Omnic 8.0 software. Raman excitation was by means of a A R510 diode pumped Nd:YAG laser operating at 1064 nm; optical filtering reduced the

Rayleigh elastic scattering and, in combination with a CaF_2 beamsplitter and a high sensitivity liquid N_2-cooled Ge-detector, allowed the Raman intensities to be recorded over the range 50-3300 cm in the Stokes side.

3.3.4. Calu-3 cell culture

The differentiated human, mucus-producing, submucosal gland lung carcinoma cell line, Calu-3, were cultivated in flasks (80 cm^3) a using Dulbecco's Modified Eagle's Medium (DMEM)/F12 Ham's 50:50 supplemented with non-essential amino acids (1% w/v), fetal bovine serum (10% w/v) and penicillin and streptomycin (50 µg mL^{-1}) or 0.005% w/v. Cells were maintained in a controlled atmosphere (95 % air, 5 % CO_2) at 37 ˚C. The culture medium was changed every two days until cells were at 80 – 90 % of confluency (*ca*. 7-10 days). After the passage process, cells were seeded at 2 × 10^6 cells per flask.

- **Measurement of transepithelial electrical resistance**

Transepithelial electrical resistance (TEER) of monolayers of cells, seeded at a density of 4 x 10^5 Calu-3 cells cm^{-2}, was measured using Transwell© plates fitted with a microporous (0.4 µm) membrane. Epithelial monolayer confluence, assessed by inspection under the optical microscope, was complete at *ca*.14 days from seeding; growth medium, 1 mL each at the apical and basal chambers of Transwell© inserts, was replenished daily. TEER was monitored using a pair of chopstick electrodes (Millipore, Spain) connected to a MIllicel©-ERS instrument. The baseline resistance was determined from measurements taken at 60 min prior to the replacement of the growth medium with a mixture of the test formulation (hydrogel, or TMC control at 3.6% w/v) and fresh medium. TEER measurements were taken at 15 min intervals over 2 h, after which time the sample in the apical chamber was replaced with fresh medium, and then for a further 2 h to assess recovery following the removal of the test formulation.

- **Transport of the active**

Transwell© inserts containing cell monolayers at confluence were equilibrated with medium (1 mL in each chamber) for 15 min. The medium was then discarded and the inserts were transferred into 12-well plates containing HBSS (pH 7.4; 1.5 mL) that had been supplemented with glucose (15 mM per

well; basal chamber). The monolayers were incubated (37 °C, 10 min) in drug-free transport medium. The test hydrogel (500 µL; pH 4.8- 5.3), or TMC solution (500 µL, 3.6% w/v; pH 4-4.5) each containing albumin or insulin (3 mg/mL), was added to the apical chamber and cells were incubated at 37 ˚C. Aliquots (100 µL) sampled from the basal chamber, at specified time intervals over 2 hr, were replenished with fresh medium. Albumin or insulin transport was evaluated by means of the BCA assay.

- ## Cytotoxicity study

The cytotoxicity of hydrogel formulations and of TMC, PEG and GP solutions in concentrations corresponding to those within the hydrogel formulations was evaluated by means of a 3-[4,5-dimethylthiazol-2-yl]-2,5-diphenyl tetrazolium bromide (MTT) assay on Calu-3 cells that had been seeded at a density of 10^4 cells per well into a 96-well plate and incubated in the culture medium for 2 days. Following removal of the culture medium, cells were exposed to the test solution (500 µL) and incubated for 2 hours at 37 °C; SDS (10 mg/mL) provided the positive control whereas culture medium acted as reference for 100 % cell viability. Subsequent to the removal of the mixture of medium and test solution, cells were washed with PBS, and a freshly prepared solution of MTT in DMEM/F12 (200 µL, 0.5 mg/mL) was added prior to incubation at 37 ˚C for 1 h. After this time, MTT solutions were removed from the wells and DMSO (400 µL) was added to facilitate the dissolution of the formazan crystals that had formed. Following 10 min of continuous agitation, the absorbance was read at 570 nm.

- ## Confocal Light Scanning Microscopy (CLSM)

The Transwell© inserts used for the transport studies were also used for CLSM visualisation. Following the transport study, the monolayers were rinsed apically and basolaterally with sterile PBS, and a solution of propidium iodide (30 µg/mL, in DMEM/F12) was applied apically for 3 min. The solution was then removed, and the support filter cut from the plastic insert and placed between two glass coverslips. The cells were visualised using a Zeiss LSM 510 Meta (Germany) instrument, with propidium iodide excitation at 514 nm. Cells that had been free from dye were decreed viable; an image of damaged cells (incubated with 0.1 % SDS for 2 h) was used as viability comparator. All experiments were carried out in triplicate.

3.3.5. Statistical Analysis

The statistical significance of the differences between the viability of Calu-3 monolayers that had been exposed to the hydrogel or to its components, as compared with the negative control (medium; 100 % cell viability) was tested at the $p < 0.05$ level by one-way analysis of variance (ANOVA) and further by the multiple comparison Tukey-Kramer test.

Statistical significance of differences between protein transport released from solutions and hydrogel systems across Calu 3 monolayers and between TEER values was tested via the Friedman test followed by a Wilcoxon Signed Rank post hoc test using PASW ® Statistics 18 software.

3.4. Results and Discussion

Consistent with the performance requirements for efficient drug delivery through the nose, the thermosensitive semi-rigid gel formulation has been designed such that it gels at *ca.* 33°C (the temperature of the nasal cavity [32]) and within the MCC timescale (*ca*. 8 min from administration [146]) to exhibit rheologically synergistic interactions with nasal mucus, which in turn effect prolonged residence.

3.4.1. *In vitro* release kinetics

The effectiveness of the thermosensitive hydrogel as a drug delivery device appropriate for its proposed use has been assessed by considering the release profiles of incorporated albumin or insulin [85].

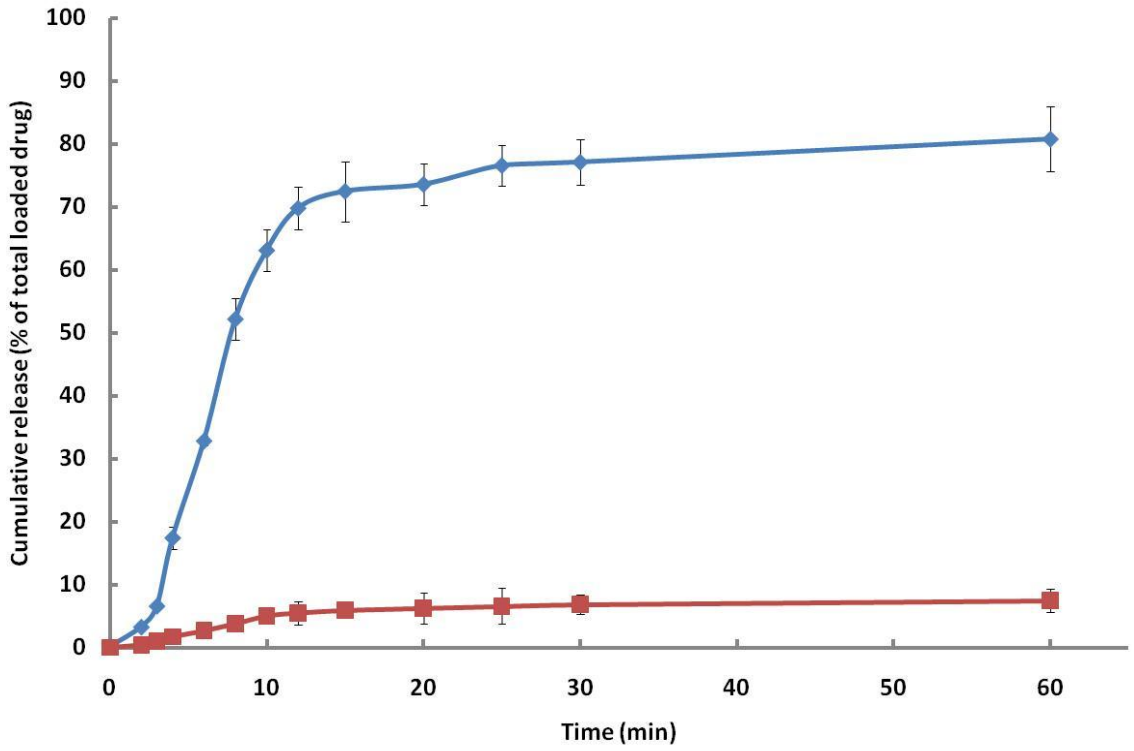

Figure 13. Cumulative release of insulin (◆) and albumin (■) both at concentrations 3mg/mL from TMC/PEG/GP hydrogels. Results are given as mean ± SD (n = 4).

It appears, Fig. 13, that as the hydrogel system moves from the sol to the gel state it fails to entrap all available insulin: the cumulative accumulation of insulin detected in the dialysis medium over the first 12 min of the experiment is *ca*.70 % of that added to the formulation, which, considering the time factor associated with the movement of insulin across the dialysis membrane, appears to correspond with the time that is required to effect gelation at 35 °C (*ca*.8 min). Consistent with the assumption that there is a *ca*.4 min time lag in the movement of insulin through the dialysis membrane, the insulin-release curve in Fig. 13 is characterised by three distinct regions: an initial slow release over the first 4 min of the experiment; a rapid release region over the next 8 min; and, another stage of slow release between 12 and 60 min. It is at this final stage that the release of insulin is assumed to be governed by the gel-state hydrogel. The release profile of albumin also exhibits three distinct regions that are demarcated by the same time points. However, since the total accumulative release of this agent over 60 min is only *ca*.5 % of the available material (with most of that release occurring in the first 12 min), the hydrogel formulation appears to be of little therapeutic relevance as a device for the controlled release of albumin. Consistent with super case II transport (drug diffuses out of the swollen system *via* a mechanism that is determined by the interaction between the polymeric system and the release medium [239]), the data over the time period for the transition from sol to gel (2-12 min; Fig. 13) fit the Korsmeyer-Peppas equation at respective *n* values for insulin and albumin of 1.91 and 1.49. By contrast, the segment of the plot

demarcated by the 12 min and 60 min timepoints is characterised by *n* values of 0.15 (insulin) and 0.17 (albumin), confirming that the release of the protein content of the gel-state system obeys Fickian release [240].

In view of the effect of the porosity of the hydrogel on the rate of diffusion [85, 93, 241, 242] a combination of SEM imaging experiments and BET porosity determinations have been employed to examine the shape, size and distribution of the pores: the hydrogel exhibits pore sizes in the range 4 nm to 100 nm [146], as is typical of such systems [85]. Since respective hydrodynamic radii for insulin and albumin are 1.3 nm and 6.2 nm respectively, the pore size of the hydrogel is not expected to be a significant rate-limiting factor in the diffusion of the insulin but is assumed to play a significant role in the release of albumin.

3.4.2. Protein structural integrity

Insulin is a protein made up of two peptide chains, A (21 amino acid residues) and B (30 residues) which are linked by two disulphide bonds joining cysteine residues A7 and B7 and residues A20 and B19 [243]. Galpin *et al.* [244] have reported that it is the A20/B19 disulphide linkage, which is known to be stable under acidic conditions [31], that is crucial for the maintenance of the biological activity of the molecule. Also, many structure-activity studies have shown that the preservation of certain invariant residues on the surface of the insulin molecule is paramount to the maintenance of its receptor-binding activity. These residues include, but may not be limited to: A1 glycine (Gly^{1}); A4 glutamic acid (Glu^{4}); A5 glutamine (Gln^{5}); A19 tyrosine (Tyr^{19}); A21 asparagine (Asn^{21}); B12 valine (Val^{12}); B16 tyrosine (Tyr^{16}); B22 arginine (Arg^{22}); B23 glycine (Gly^{23}); B24 phenylalanine (Phe^{24}) and B26 tyrosine (Tyr^{26}) [244].

Brange *et al.* [245] have explored the influence of some excipients, formulation environments and pH on insulin stability, reporting that at acidic pH, the amino acid Asn^{21}, the C-terminal residue of the A-chain, is particularly labile to hydrolytic action. The same workers suggested that the uncharged carboxyl moiety at the C-terminal effects the deamidation at A21 *via* a proton transfer to the amide group and a subsequent nucleophilic attack by the thus generated carboxylate ion [245]. Since the rate of deamidation is dependent upon pH and temperature, the normal formulation practice is to adopt experimental protocols that impact minimally upon degradation, such that the impact upon the therapeutic effect is also minimal. In addition, the maintenance of the stereochemistry of the molecule is of importance, as is exemplified by the work of Elkordy *et al.* [246] who have assessed

the effects of a peptide's secondary structure upon biological activity. Despite this potential disruption to the structural integrity of the insulin molecule, the acidic dissolution of insulin during aqueous formulation is common practice amongst researchers working towards the development of intranasal dosage forms for the treatment of diabetes, Table 12.

Table 12. Examples of *in vivo* and *in vitro* studies investigating drug delivery systems containing insulin.

Nature of formulation	*In vitro* studies	*In vivo* studies	Reference
Porcine insulin was dissolved into a solution of chitosan in aqueous hydrochloric acid, pH 4.	Rabbit nasal mucosa employed in permeation studies using Valia-Chien diffusion chambers.	Intranasal administration of the insulin/chitosan solutions, 10 IU/kg insulin, to male Sprague Dawley rats: increasing the concentration of chitosan increased glucose-lowering capacity. Solutions of 1.5 % chitosan lowered serum glucose levels to *ca.* 20 % of initial value, which was in contrast to the effect induced by the subcutaneous control (*ca.* 40 % reduction).	[247]
Bovine insulin was dissolved in 0.1 M HCl and adjusted to pH 4.5 with NaOH before adding to gels of Poloxamer (P), Poloxamer-chitosan (P-CS) or Poloxamer-chitosan/glutaraldehyde/glycine (P-CS/GA/GY).	Drug release was determined *via* diffusion through a dialysis membrane and tested using the Bradford method.	Intranasal administration to male Wistar rats of polymeric gels containing 10 IU/kg insulin: Blood glucose levels decreased to *ca*. 45, 48 and 55 % in rats respectively administered with P, P-CS, and P-CS/GA/GY formulations, as compared with a *ca.* 35 % reduction achieved with the sc control.	[248]
A thermosensitive hydrogel was formed by adding sequentially recombinant human insulin and *α,β*-Glycerophosphate.to a solution of N-[(2-hydroxy-3-trimethylammonium)propyl] chitosan chloride (HTCC) and poly(ethylene glycol) in 0.1 M lactic acid.	Drug release was monitored by the Bradford method.	Intranasal administration of the thermosensitive HTCC-PEG gel, 10 IU/kg insulin, to male Sprague Dawley rats effected a *ca.* 40 % reduction to blood glucose after 4 hours from administration. A sc control effected the same percentage reduction after 1 hour from administration.	[4]
A nanoparticulate dosage form was prepared by adding a solution of porcine insulin in aqueous tripolyphosphate to a pre-prepared solution of PEG-grafted chitosan in acetic acid.	Drug release was monitored by the Bradford method using supernatant collected from nanoparticles incubated in aqueous media.	Intranasal administration of insulin-PEG-g-chitosan suspension and insulin-PEG-g-chitosan nanoparticles, both at 5 IU/kg insulin, to female New Zealand rabbits lowered respective blood glucose levels to 68 % and 54 % of the basal level; a control intranasal insulin solution effected a <20 % decrease.	[249]
Solutions (pH 4).of semi-synthetic human sodium insulin mixed with each of a range of chitosan salts were prepared by dissolving in aqueous saline.		Intranasal administration, 4 IU/kg insulin, to male Wistar rats effected variable baseline reductions to blood glucose levels over the range of *ca.* 50 % to *ca.* 26 %, depending on the nature of the chitosan salt.	[250]

Owing to the complexity of the insulin molecule, the assessment of the effects of the formulation strategy upon the molecular structure demands not only the application of a combination of spectroscopic investigations and analytical techniques [246, 251, 252] but also of evaluations of biological activity.

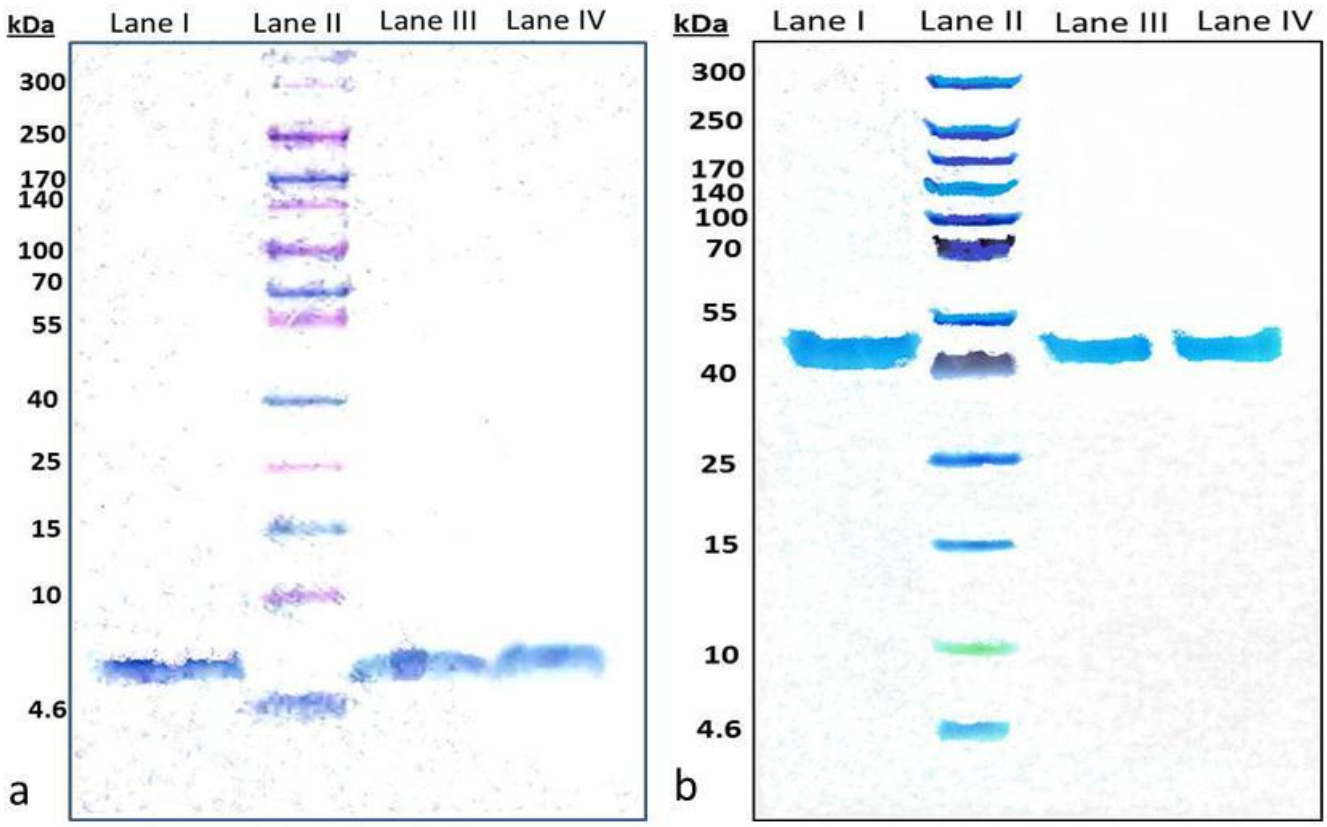

Figure 14. SimplyBlue SafeStain SDS-PAGE gel of (a) insulin and (b) albumin. Lanes I, II, III and IV are respectively: the protein solution; the molecular weight markers; protein loaded into the hydrogel, and the protein in the release medium after 60 min.

The application of sodium dodecyl sulfate polyacrylamide gel electrophoresis SDS PAGE has allowed the assessment of the effect of 0.1M HCl solution on the chain length of the insulin, Fig. 14a, and of the albumin, Fig. 14b, used in this work. The SDS-PAGE results compare the electrophoresis behaviour of the loaded protein active within the hydrogel formulation with that of the released active after 60 min and that of the commercial protein solution that has been used for loading. The molecular weight ladder (Lane II) shows that as expected, the commercial insulin solution (*ca.* 5 kDa;Fig. 14a, Lane I) falls between the 4.6 and the 10 kDa markers and the albumin solution (*ca.* 45 kDa; Fig. 14b, Lane I) falls between the 40 and 55 kDa marker. The loaded and released actives, respectively Lanes III and IV for insulin and albumin, show well-defined bands that correspond with

respective bands in Lane I. This matching of bands at *ca.* 5 kDa and *ca.* 45 kDa and the absence of new bands are both indicative of the preservation of the integrity of the mass and size of insulin and albumin, further suggesting that the experimental protocol adopted for the formulation inhibits the deamidation at residue 21, at least within the sensitivity limits of the SDS-PAGE technique [252]. Owing to the low amounts of albumin released from the hydrogel formulation, the release of this protein was not investigated further.

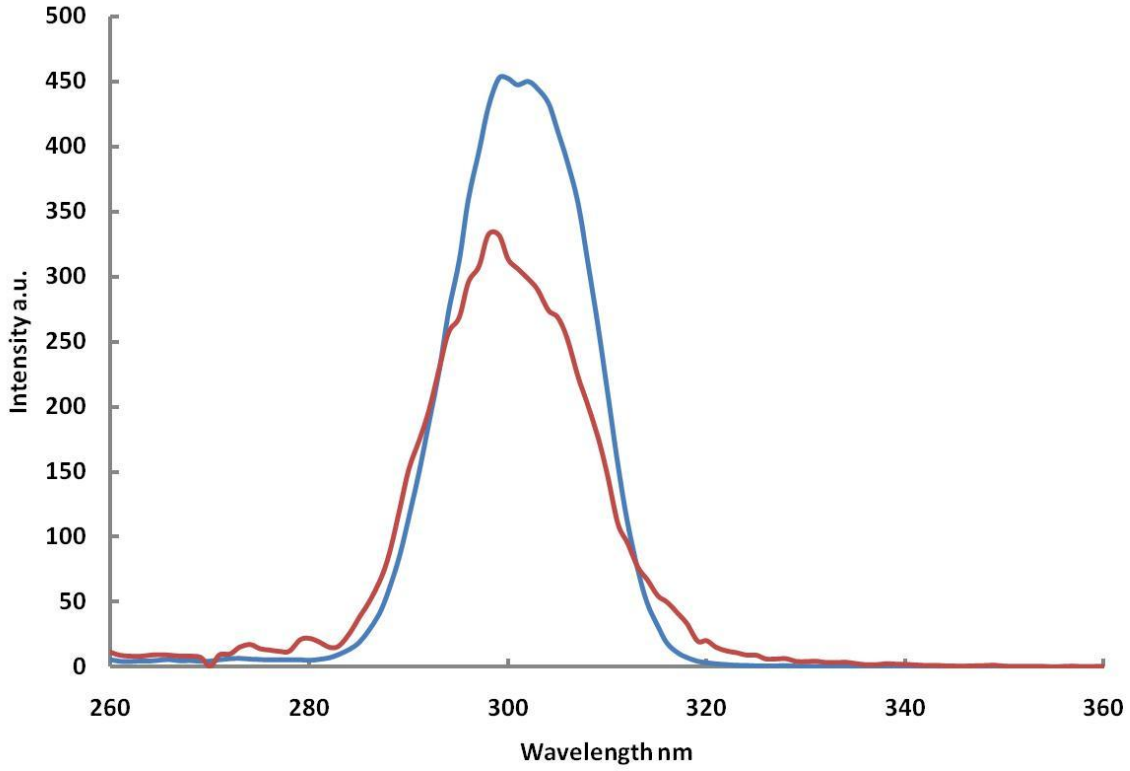

Figure 15. Fluorescence emission spectra of the native insulin (blue) in 0.02M HCl (aq) and released (red) insulin from the peptide hydrogel in SNES (the two solutions are not of equal concentrations).

The protonation of insulin following its dissolution in 0.02M aqueous HCl is manifested by a shift in the fluorescence emission maximum from 304 nm [253] to 297 nm, Fig. 15**.** Since tyrosine (4-hydroxyphenylalanine) is the only amino acid residue present in insulin that is both fluorescent and susceptible to protonation by HCl, it is assumed that that the shift in the fluorescence maximum is consequent to the reduction in the electron-donating effect of the p-hydroxyl moiety of this residue following protonation. The fluorescence emission spectrum of insulin in SNES was slightly broader, with evidence for fine structure (with a distinctly weak contribution from phenalanine at 282 nm), but exhibited the same absorption maximum (297 nm) as the protonated insulin. The fine structure is attributed to differences in the folding of the protein in the two media.

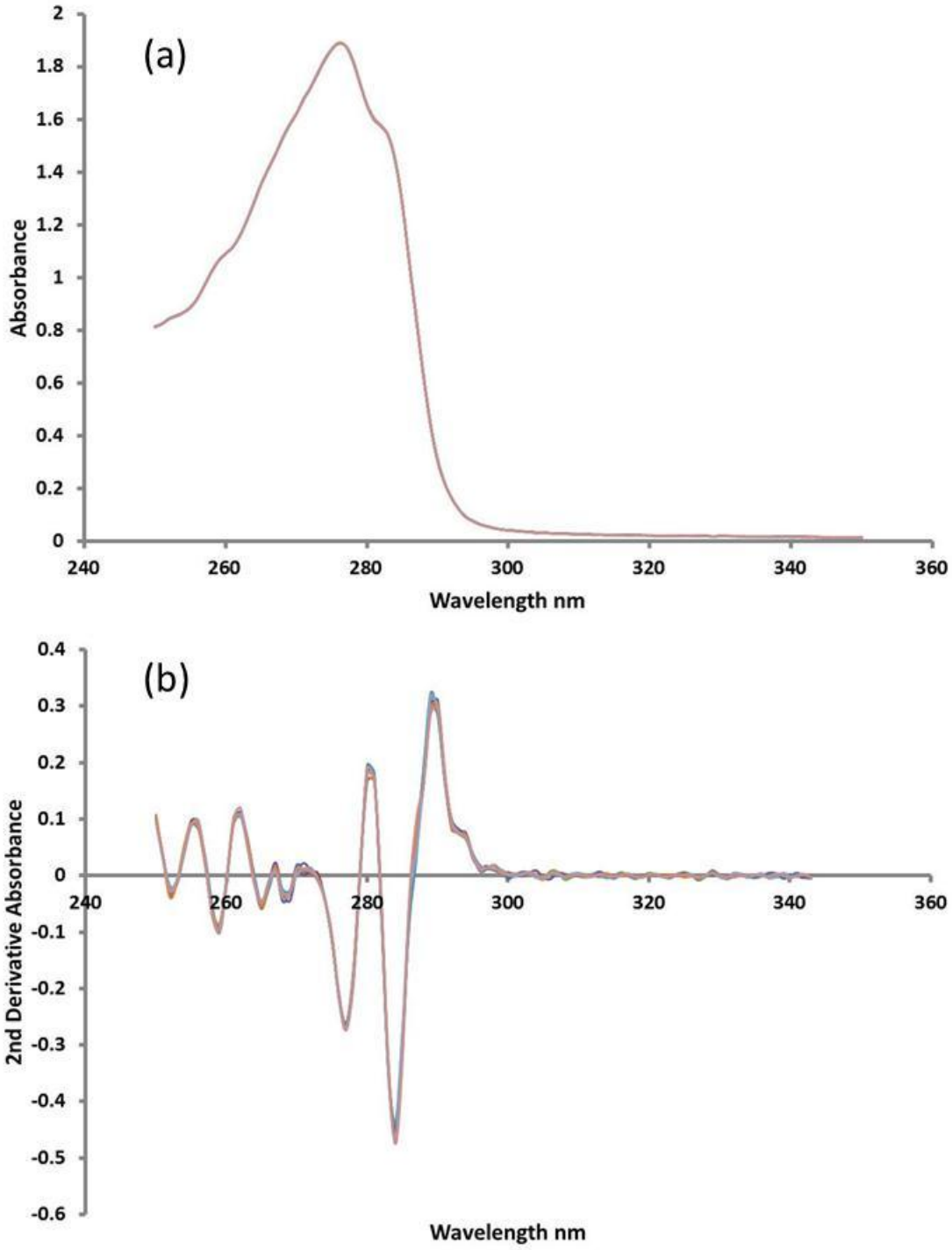

Figure 16. (a) UV-vis spectra and (b) Second derivative UV-vis spectra of insulin in 0.02M HCl(aq.) solution, monitored over a period of one week: time points: freshly prepared; at two hours from preparation; then at 36, 48, 60, 72, 84 and 96 hours from preparation. The spectra are super-imposable (chi-square = 0.773 (7); P = 0.998).

Although insulin in 0.02 M HCl(aq.) solution is in its therapeutically preferred monomeric state [254, 255], the observed UV absorption maximum (279 nm, Fig. 16(a)) is at a lower wavelength than that of monomeric insulin in ethanolic solution (305nm) [256]. Since there is no contribution from

aggregation phenomena, this shift is consistent with the reduction in the auxochromic contribution of the p-hydroxyl group following the protonation of tyrosine. Monitored over a period of one week, the UV-Vis spectra of insulin in 0.02 M HCl(aq.) solution did not exhibit any variations in their absorption maxima or in their extinction coefficient (Fig. 16(b)), as would have been expected for samples that aggregate or precipitate out of solution. The same set of experiments also confirmed the hydrolytic stability of the peptide bonds at the tyrosine and phenylalanine positions, since the hydrolysis of those bonds would have been marked by shifts in the positions and intensities of the absorption maxima consequent to the liberation of these amino acids or due to their presence as terminal groups in insulin fragments.

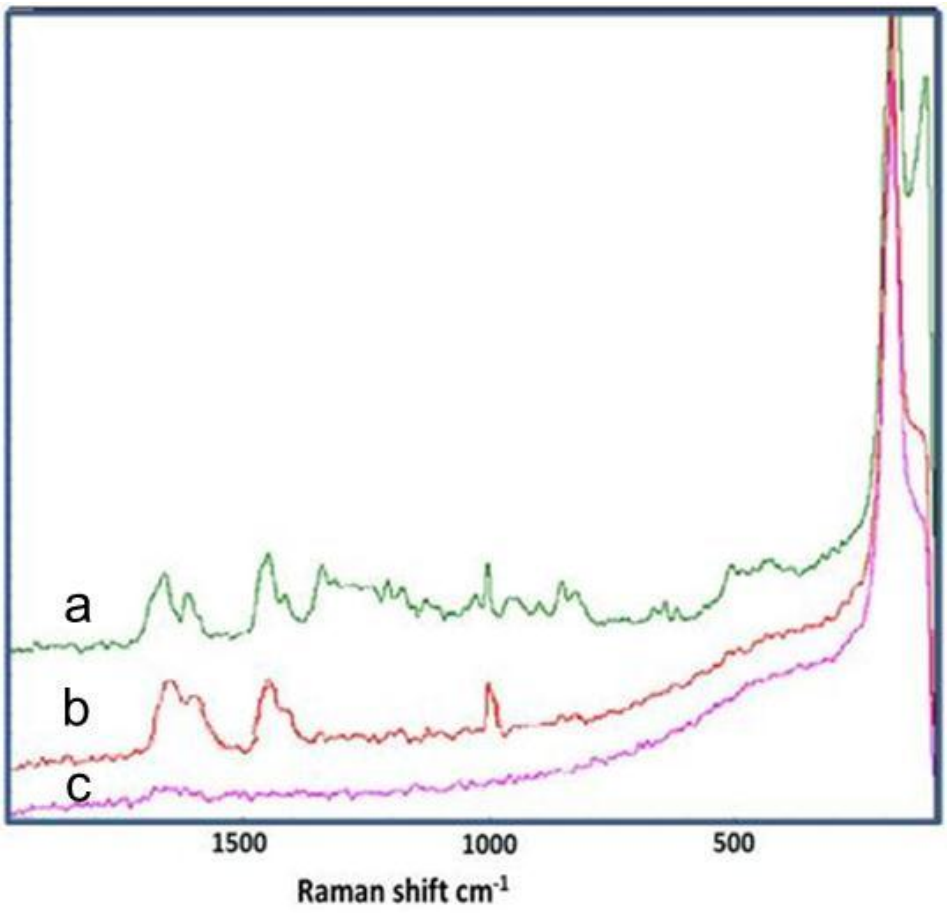

Figure 17. FT-Raman spectra of (a) insulin solid (green); (b) insulin 3 mg/mL in 0.02 M HCl (aq) (red) and (c) 0.02 M HCl (aq) (pink).

Table 13. Raman assignments of insulin spectral features (from [257]).

Frequency cm^{-1}	Assignment
516	*v*(S – S)
626	Phe
646	Tyr
673	*v*(C –S) of C – S – S – C
726	Skeletal bending
770	Skeletal bending
834	Tyr
855	Tyr
898	*v*(C – C)
962	*v*(C – C)
1007	Phe
1035	Phe
1130	*v*(C – N)
1180	Tyr
1210	Tyr and Phe
1267	Amide III (α – helical)
1319	CH deformation
1341	CH deformation
1450	CH_2 deformation
1616	Tyr
1663	Amide I (α – helical structure)

The amounts of insulin released from the hydrogel formulation were sufficiently high to allow the acquisition of FT-Raman and FT-IR spectroscopic data (minimum required concentration, 3-5 mg/ml [258]). The structural changes that differentiate insulin that had been dissolved in 0.02 M HCl from the solid sample, Fig. 17. and Table 13, are manifested by changes in the Raman spectra. Insulin in solution is characterised by the disappearance of the insulin bands between 500 and 800 cm^{-1} and by the decrease in the intensities of absorptions between *ca.* 800 – 950 cm^{-1} and of those between *ca.* 1050 – 1400 cm^{-1}. While the distinct bands that are characteristic of the phenylalanine residue (*ca.* 1000 cm^{-1}), the CH_2 deformation band (1400 – 1500 cm^{-1}), and the tyrosine and amide I (*α*-helical structure) (1600 – 1700 cm^{-1}) are evident in both spectra, the loss of some the *α*-helical structure following the dissolution of insulin is suggested by the almost complete disappearance of the amide III vibration (N-H bending, 1250-1350 cm^{-1}). The preservation of the amide I stretch (mainly C=O, with some contribution from C-N; 1645-1660 cm^{-1}) is consistent with the preservation of some of the *α*-helical structure [246].

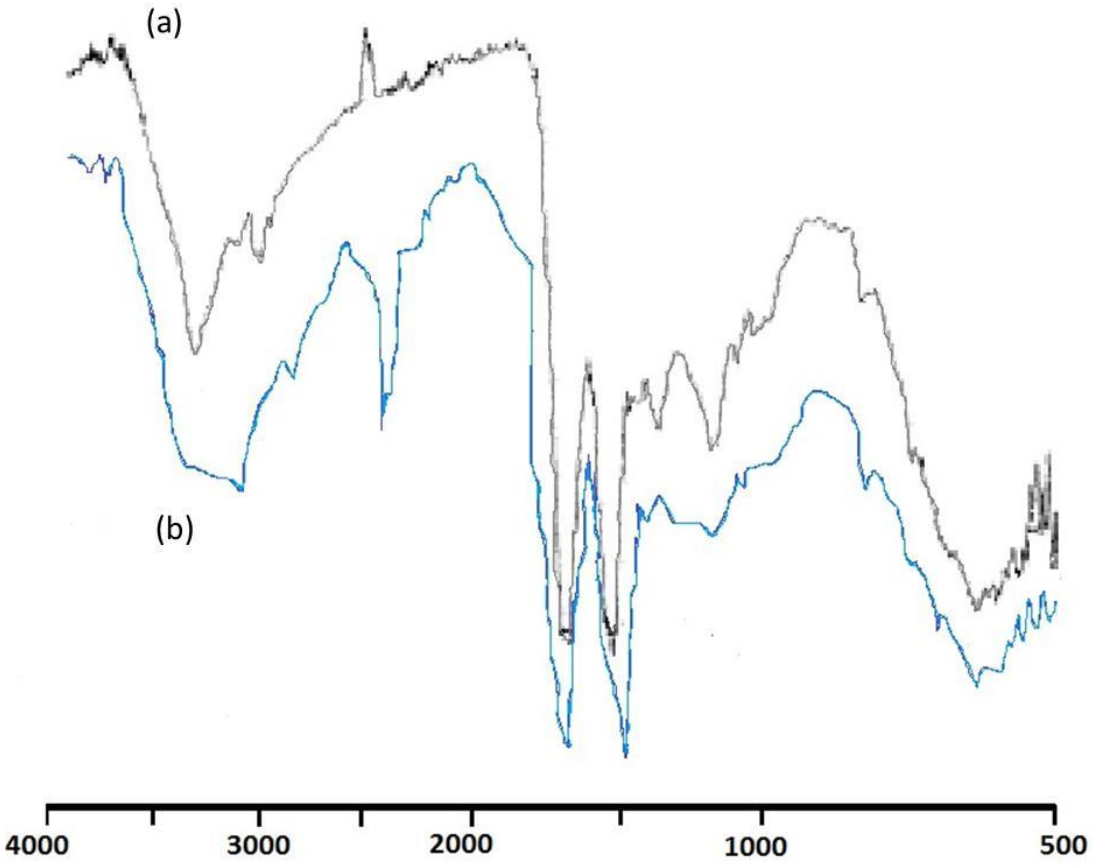

Figure 18. FTIR spectra of (a) insulin solid, and (b) insulin 3 mg/mL in 0.02M HCl (aq).

Infrared spectroscopic data further support the suggested Raman-evidenced changes in the features of the amide III band and are consistent with the preservation of those of the amide I vibrations (in aqueous HCl, this band coincides with the 1645 cm^{-1} bending vibration of water), Fig. 18. Solid bovine insulin displays characteristic absorptions at 1650 cm^{-1} (amide I); 1540 cm^{-1} (amide II); 1396 cm^{-1}, 1452 cm^{-1} (carboxyl) and 1242 cm^{-1} (amide III) [259]. While most of these features are preserved in the spectra of the acidified solution of insulin, marked differences in the region 1000 – 1500 cm^{-1} reflect changes at the structural moiety that is responsible for the amide III (complex bands dependent on the details of the force field, the nature of side chains and the extent of hydrogen bonding) absorption. Changes in the shape and position of the amide II band, which arises from the combined effects of the N-H in-plane bending vibration and the C-N stretching vibration, further support the hypothesis that only some of the α-helical structure is lost. The amide A band (mainly N-H stretching vibration, *ca*. 3500 cm^{-1}) and amide B (about 3100 cm^{-1}), which originate from a Fermi resonance between the first overtone of amide II and the N-H stretching vibration, also reflect the suggested changes in the structure of insulin, Fig. 18. As is consistent with the presence of water, in HCl solution the presence of the amide A band**,** which does not depend on backbone

conformation but is very sensitive to the strength of hydrogen bonding [260] , is only witnessed as a shoulder that exhibits the same profile as the amide A absorption. Similarly, the amide B band is superimposed on the broad band that is characteristic of the presence of liquid-state water.

The impact of protonation by aqueous HCl and the associated structural changes imposed upon insulin can only be assessed through evaluations of the clinical effectiveness of this molecule.

3.4.5. Cell Culture

- **TEER and protein transport**

Tight junction integrity was assessed by monitoring the variations in TEER across the Calu-3 monolayers following exposure to the hydrogel or to its respective TMC solution. Consistent with previous reports [261], both TMC and the hydrogel induced dramatic but transient reductions in TEER: maximal reductions in TEER (respectively 55 % and 43 %, Fig. 19, which were shown to be statistically significantly different to one another, $p<0.00$) were observed at 120 min (the time-point at which the applied formulations were removed).

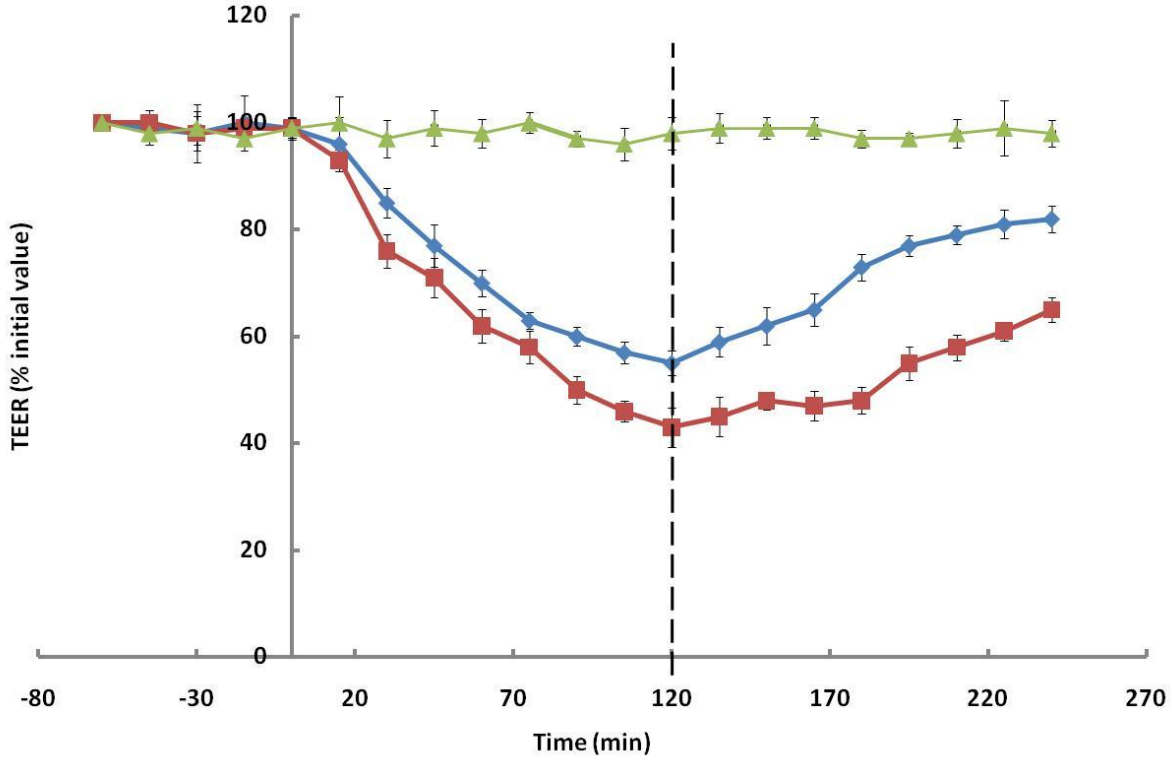

Figure 19. Effect of 3.6 % w/v TMC solution (■) and TMC/PEG/GP hydrogel (◆) on TEER values of Calu-3 monolayers compared to the medium control (▲). Data presented are a mean ± SD (n = 4). Dotted line at 120 min is the time point where TMC and TMC/PEG/GP hydrogel samples were removed from the monolayers and the following 120 min demarcates the recovery period.

It has been suggested that the capability of TMC to open tight junctions transiently is attributable to the disruption of the F-actin cytoskeleton protein through interactions involving the positive charges at the C-2 position of the molecular structure [262]. The combination of TMC polymers with glycerophosphate is known [232] to reduce the capacity of TMC to open tight junctions, which in turn impacts upon the efficiency of absorption enhancement.

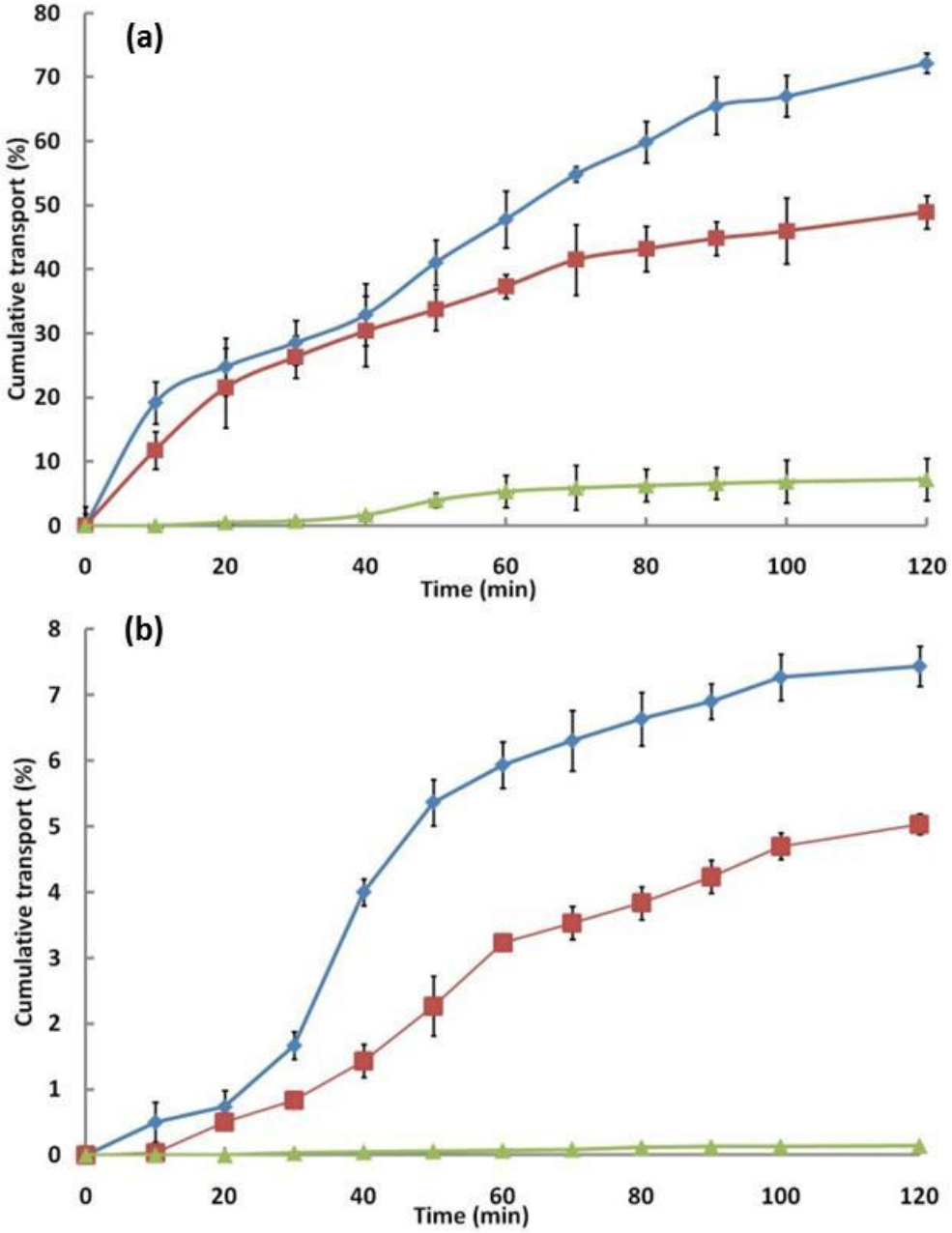

Figure 20. Cumulative transport of (a) insulin and (b) albumin (3 mg/ mL)from a 3.6 % w/v TMC solution (◆), the TMC/PEG/GP hydrogel (■) and from an aqueous protein solution (▲). Results are presented as means ± SD (n = 4) and statistical analysis has shown significantly different transport between all TMC solutions, their respective hydrogels and the protein solutions.

Data for the transport of proteins through Calu-3 cell monolayers treated with hydrogel or TMC formulations, or with an aqueous solution of each test protein, Fig. 20, show that TMC has a more pronounced penetration-enhancing effect: 7.4% of the available albumin and 72.2 % of the available insulin were seen to be transported across the monolayer over 2 h. This, however, may be reflective of a TMC-induced decrease in cell viability and/or of the disruption in the confluency of the monolayer. Over the same experimental period, the application of the hydrogel formulation effected a marked enhancement in the efficiency of protein transport as compared with corresponding solutions of each protein (respectively for albumin and insulin: 5 % and 49 % *vs*. 0.14 % and 73 %).

- ## Cytotoxicity

Even at short-term (2 h) exposure, the MTT assay unmasked the considerable toxicity associated with each of the separate components of the formulation: at concentration levels consistent with the hydrogel formulation, respective cell viabilities for TMC, PEG and GP are 40 %, 39 % and 46 %, Fig. 21. The observed 60 % reduction in cell viability induced by the 36 mg/mL solution of TMC (32.8 % DQ) is in marked contrast with reports which suggest that TMC has little or no cytototoxic effect [208, 263, 264], and supports the findings of Amidi *et al*. [234] who showed that a 20 mg/mL solution of TMC (25 % DQ) reduces Calu-3 cell viability by approximately 30%. The observation that formulations of chitosan exhibit lower cytotoxicity than each of its components (88 % cell viability, not significantly different from the medium control; Fig. 21) is in accord with the findings of Kim *et al.* [218], who observed the toxic effects of GP solutions on cancer cells and also demonstrated the increased viability of cells treated with a thermosensitive hydrogel that had been formulated from chitosan and GP relative to that of cells treated with GP alone.

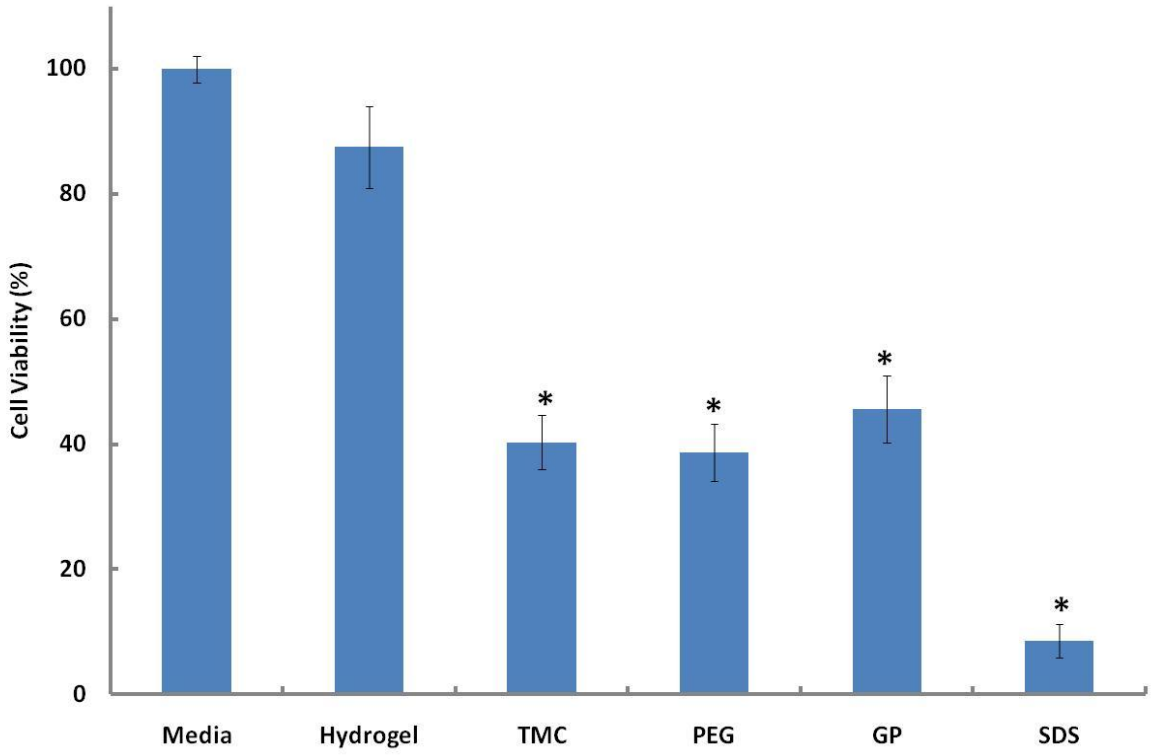

Figure 21. Cytotoxicity assay of TMC/PEG/GP hydrogel and its individual components at the corresponding concentrations on Calu-3 monolayers. Results are presented as means ± SD (n = 4). * p < 0.001 with respect to medium, 100% viability; Tukey-Kramer post-hoc comparison test.

Towards a further evaluation of cytotoxicity, the hydrogel and each of its components were investigated for their effect on Calu-3 cell viability though staining with propidium iodide (a membrane-impermeant dye) and subsequent imaging with CLSM. The images confirmed that incubation with TMC solution causes considerable damage to the monolayer, as is demonstrated by the visualised uptake of propidium iodide by the nuclei of Calu-3 cells, Fig. 22a, but this damage is not as pronounced as that caused by SDS (Fig. 22c). The degree of cell-wall disruption in monolayers that had been treated with the hydrogel (Fig. 22b) was similar to that of controls that had been treated with DMEM/F12 (Fig. 22d). These observations are consistent with the hypothesis that the reduction in TEER seen in monolayers that had been treated with the hydrogel was not related to cell-membrane damage, as may have been the case for TMC-treated monolayers, and support the assertion that the hydrogel promotes the paracellular transport of insulin *via* the opening of tight junctions.

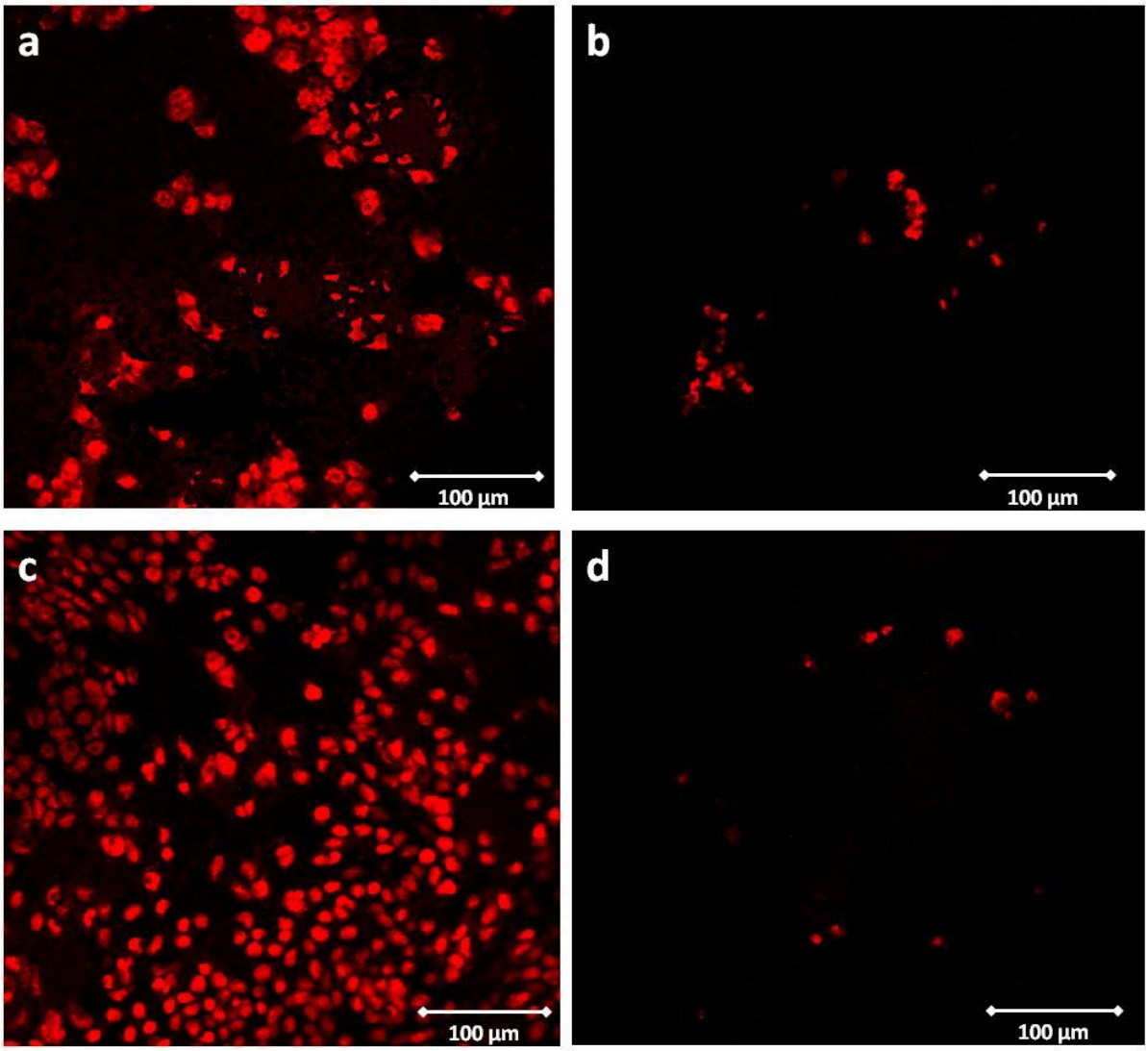

Figure 22. CLSM images of Calu-3 cells stained with propidium iodide after 2 hours of treatment with (a) 3.6 % w/v TMC solution, (b) TMC/PEG/GP hydrogel, (c) 0.1 % SDS solution and (d) DMEM/F12.

3.5. Conclusion

An insulin-loaded, mucoadhesive thermogel formulation based on *N*-trimethyl chitosan has been identified as a candidate vehicle for the nasal delivery of insulin, since *in vitro* evaluation have shown that the formulation combines the capacity to effect the opening of modelled tight junctions with the capability to release its therapeutic content under conditions that mimic those of the nasal environment.

Chapter Four: An *in situ* thermogelling nasal formulation for the intranasal delivery of insulin: *in vivo* assessment of nasal clearance and controlled release profile

An *in situ* thermogelling nasal formulation for the intranasal delivery of insulin: *in vivo* assessment of nasal clearance and controlled release profile.

Abstract

The *in vivo* potential of a readily accessible *in situ* thermogelling nasal formulation of *N*-trimethyl chitosan chloride, glycerophosphate and poly(ethylene glycol) to act as a once-a-day dosage form for the intranasal delivery of insulin has been demonstrated in the rat model. The retention upon the absorptive nasal membrane was evaluated to show potentially 60 % of the hydrogel formulation still in place after 2 h. The pharmacological activity of the controlled released insulin was demonstrated to exert its glucose-lowering effect over *ca*. 24 hours.

4.1. Introduction

The impetus for the considerable research activities towards the development of an intranasal system for the delivery of insulin [17, 230-232, 250, 265-269] is provided by the site-specific features of the mucosal epithelium: relatively low barrier to penetration by macromolecular actives, low enzymatic activity, avoidance of the first-pass effect, and relative ease of administration [5, 30, 137]. The main barrier to the efficient nasal delivery of actives is presented by the mucociliary clearance (MCC) [30, 270] – nasal cilia beat in a coordinated fashion to transport the mucus to the nasopharynx where it is eliminated by swallowing. Additionally, the absorption of macromolecular drugs, such as insulin, is inhibited by the tight junctions that are located between epithelial cells [265].

The main formulation strategy towards the improvement of the residence time of nasal-delivery systems involves the use of mucoadhesive agents that disrupt the normal ciliary rhythm, and consequently MCC [3]. Zaki *et al.* have shown [105] that the nasal administration of a poly(acrylic acid) mucoadhesive agent (Carbopol 934P) results in the *in situ* formation of a gel that is capable of prolonging the transport time of co-formulated metoclopramide from 10 min (control solution) to 52 min (mucoadhesive gel) while maintaining mucosal integrity over two weeks of sequential

administration. The weak correlation between consistency index (a measure of gel viscosity) and MCC (a measure of *in vivo* mucoadhesiveness) led to the suggestion that the observed enhancement in residence time was more likely attributable to the bioadhesive properties of the polymer rather than the changes in viscosity induced by the gel [105]. Majithiya *et al.* [59] have suggested that of primary importance in the adhesion of Carbopol to nasal mucosa is the formation of hydrogen bonds between the carboxylic acid functionalities of the mucoadhesive and the oxygen atoms of oligosaccharide chains at the mucus membrane.

In vivo work (rat model) by Morimoto *et al.* [267] using aqueous gels of insulin and poly(acrylic acid) (PAA) has demonstrated the glucose-lowering effect of these formulations. The enhancement in the nasal absorption of therapeutic agents effected by poly(acrylic acid) has been suggested to be due to the combined effects of its mucoadhesiveness, its effects on viscosity and, more importantly, on this material forcing the temporary opening of tight junctions as it swells by extracting water from the local environment [137].

Chitosan, a material that is also capable of effecting the transient opening of tight junctions [271, 272], has also received considerable interest in the quest for the development of intranasal hydrogels for the delivery of insulin [4, 5, 17, 117, 265, 269, 273-278]. Chitosan is known to induce the translocation of occludin and of ZO-1 from plasma membranes to cytoplasm, thereby facilitating the partial alteration of the cytoskeleton and in turn the opening of tight junctions. Both the increasing effectiveness of chitosan at opening tight junctions and its capacity to establish strong mucoadhesive interactions are generally accepted to be enhanced by increases in the molecular weight and/or degree of deacetylation [5].

Chitosan has been combined with poly(vinyl alcohol) to form a thermosensitive *in situ* gelling system for the nasal delivery of insulin, which has been shown to exhibit a prolonged hypoglycaemic affect (maximum reduction of blood glucose of *ca*. 40 % at 4 hours from administration) as compared with the subcutaneous insulin control which induced a very similar reduction in blood glucose but over a much shorter timescale (1 hour). The potential advantage of the chitosan/poly(vinyl alcohol) system over subcutaneous delivery becomes apparent by considering the claim that a gradual decrease in blood glucose inhibits the over-hypoglycaemic potential of a dosage form [265]. Chung *et al.* [269] have reported a cross-linked chitosan gel (chitosan cross-linked using glutaraldehyde, interpenetrating with Poloxamer and glycine) that displays an even more prolonged hypoglycaemic effect (*ca*. 5 hours). Work by Yu *et al*. [232] has

shown the concentration-dependent penetration enhancing effects of chitosan in the intranasal delivery of insulin [232].

The enhanced permeability imparted to nasal mucosa by thiolated or quaternised derivatives of chitosan, especially *N*-trimethyl chitosan chloride (TMC), has been shown to be a function of the degree of functionalisation [5, 146]. TMC fulfils two further pre-requisites to efficient nasal delivery, namely: good mucoadhesive behaviour, and rheological synergy with mucus [146]. Accordingly, du Plessis *et al*. [17] have reported that the nasal co-administration of insulin and chitosan in solution effect a twofold increase in the intranasal absorption of insulin, while an equivalent solution of insulin and highly quaternised (60 %) TMC enhances absorption threefold, both as compared with a control solution of pure insulin.

In view of the promise of TMC as a carrier matrix for the intranasal delivery of insulin, we have formulated an *in situ* thermogelling hydrogel, which has been shown by *in vitro* studies to be biocompatible and to exhibit several pre-requisite properties for the intranasal delivery of this therapeutic agent, namely: a viscosity profile that is within the MCC-inhibiting range; mucoadhesive behaviour that is comparable with that of poly(acrylic acid) (PAA; the archetypal mucoadhesive polymer) [146]; and, the capacity to effect the opening of tight junctions.

We now report the results from studies that have been designed to assess the *in vivo* (rat model) effects of the formulation on MCC and also those of parallel studies designed to monitor the hypoglycaemic effect induced as a result of the intranasal release of insulin from the same formulation.

4.2. Materials

Orange FluoSpheres© aqueous suspension (1.0 µm; 2 % w/v) was purchased from Invitrogen, Paisley UK. Upon dilution, the FluoSpheres© gave a linear fluorescence response up to a concentration on 0.02 mg/mL. Streptozocin, sodium pentobarbital, bovine insulin and the glucose Trinder kit were obtained from Sigma (St. Louis, MO, USA).

4.3. Methods

4.3.1. Preparation of formulations

N-Trimethyl chitosan chloride (degree of quaternisation, 32.8 %) was synthesised from medium molecular weight chitosan as previously described [28].

The insulin-loaded, sol-state hydrogel (pH 4.8-5.3) was formed by dissolving *α,β*-glycerophosphate (GP) (12.5 % w/v) into a solution of insulin in aqueous HCl (0.1M; 1 mL) and then adding (dropwise, stirring) this solution to a pre-prepared aqueous solution of TMC (4 mL, 4.5 %w/v) and PEG (6.75 %w/v).

Insulin-loaded TMC solutions (4.5 %w/v; pH 4.0-4.5), insulin solution (0.1M HCl: water in a ratio 1:4, pH 4.5-5.0) and TMC solutions (4.5 %w/v; pH 4.0-4.5) were all formulated to a final insulin concentration of 250 IU/mL; control hydrogels were formulated with no insulin content.

4.3.2. *In vivo* studies

- **Nasal clearance studies in rats**

Animals were supplied by the Department of Pharmacology of the Beirut Arab University, where this series of experiments was conducted. Animal care and handling were performed in accordance with the regulations and guidelines stipulated by the Ethical Review Committee at Beirut Arab University, Lebanon and endorsed by the ethical committee of the University of Portsmouth, UK.

Male, Sprague-Dawley rats each weighing 200-300 g were used to measure the *in vivo* rate of mucociliary clearance according to the method of Donovan *et al.* [79]. Rats were housed in an environment of controlled temperature (21 ± 2°C) and humidity (50–70 %). For MCC measurements, rats were rendered mildly sedated (by the intraperitoneal injection of sodium pentobarbital, 50 mg/kg) before instillation (right nostril) of hydrogel suspension (25 µL) that had been loaded with FluoSpheres© (1 % w/v). The FluoSpheres© exiting the nasal cavity were collected by swabbing the back of the oral cavity of the rat using moistened foam-tipped applicators. Swabs were taken at two minute intervals for the first 30 min and then every 5 min for the following 90 min. The FluoSpheres© were removed from the applicators by washing (distilled water, 4 mL) and the fluorescence of the resulting suspension was determined using a JASCO spectrophotometer FP-

6200 (excitation 540 nm and emission 560 nm). The mass of FluoSpheres© in the sample was then calculated from a previously constructed standard curve. Controls were provided by a FluoSphere© suspension in normal saline (25 µL, 1 % w/v); each experiment was conducted in triplicate.

The clearance of fluorescent particles in solution and in hydrogel from the nasal cavity is expressed as the percentage loss of the total FluoSphere© loaded as a function of time, and as a percentage of the total mass recovered at the end of the 120 min experiment period. Since clearance during the first 2 min is not controlled by ciliary motility [79], initial clearance rates (k) were obtained from the monoexponential fit of data obtained between 2 and 30 min [279]. The time needed for 90 % of the total mass recovered from the nasal cavity to clear (t_{90}) was also calculated. Student's *t*-test and ANOVA were used to determine statistical differences at the $p < 0.05$ level.

- ## Induction of diabetes

Animals were supplied by the Department of Pharmaceutical Sciences of the University of Padua, where this series of experiments was conducted. Animal care and handling were performed in accordance with the provisions of the European Economic Community Council Directive 86/209 (recognised and adopted by the Italian Government with the approval decree D.M. No. 230/95-B) and the NIH publication No. 85-23, revised 1985.

Twenty four male Wistar rats, each weighing 200–300 g (pubescent), were housed as pairs in plastic cages. The cages were kept in an air-conditioned room (21 ± 2 °C, 50–70 % relative humidity) that was maintained at a 12 h light-dark cycle. The animals had free access to basal diet and water for one week prior to the induction of diabetes by means of a single intra-peritoneal administration of streptozocin (STZ, 45 mg/kg, in 0.9 % aqueous NaCl). For blood-glucose testing, a few drops of blood were extracted from the tail and tested for glucose concentration using the glucose Trinder Kit according to manufacturer´s instructions: a rat was considered diabetic if its fasting plasma glucose level exceeded 10 mmol/L (or 1.8 mg/mL); only diabetic rats with plasma glucose levels in the range 1.8 – 5.0 mg/mL were utilised in further work.

- ***In vivo* testing of hypoglycaemic effect of formulations**

For the intranasal testing of formulations and controls, diabetic rats were randomly separated into 6 groups (n=4) for treatment as shown in table 14.

Table 14. Groups of rats and the dosage forms that were administered.

Group	Formulation	Insulin dose IU/kg
1	Intranasal hydrogel solution	0
2	Intranasal hydrogel solution with insulin	10
3	Intranasal TMC solution	0
4	Intranasal TMC solution loaded with insulin	10
5	Intranasal insulin solution	10
6	Subcutaneous injection (100 % bioavailability) [232]	1

Formulations (10 µL, 2.5 IU; equivalent to 10 IU/kg assuming an average weight of 250 g per animal) [232] were administered into the right nostril of each rat (not anaesthetised) using a micropipette. Four rats received the sub-cutaneous injection (1 IU/kg). Blood samples (4 drops, *ca.* 100 µL) were collected in heparinised tubes prior to administration and then at specified intervals post dosing: 30, 60, 90, 150, 210, 270, 330, 390 min. During this time rats were caged in pairs in the air-conditioned environment described above and were allowed free access to food and water. The blood was phase separated by centrifugation (4000 rpm, 5 min) and the serum glucose level was determined, after dilution in distilled water (1:10), using the glucose Trinder Kit [280]. This experiment was repeated using another 20 freshly induced diabetic rats that were allocated to receive formulations as per groups 2, 4, 5 and 6 (table 1) (n=5). The blood samples were collected at time intervals: 0, 30, 60, 150, 270, 390, 520, 1320, 1800, 2740 min in the same way as before.

The minimum blood glucose concentration (C_{min}), and time to reach C_{min} (T_{min}) were noted and the area above the serum glucose levels vs time curve (AAC) was calculated using the trapezoidal rule in Microsoft Excel, where the limits of integration were the start and end point of experimentation. For groups 2, 4, and 5, calculations were determined from the longer experiment of *ca.* 2 days, whereas for groups 1, 3 and 6 were calculated over the *ca.* 6 h period. The data collected allowed the estimation of the pharmacodynamic availability of nasally administered insulin, F_{dyn} [4, 232, 281]:

Equation 5. Pharmacodynamic availability.

$$F_{dyn} = \frac{AAC_{in} \times Dose_{sc}}{AAC_{sc} \times Dose_{in}} \times 100\ \% \quad (1)$$

Intranasal and subcutaneous administration are respectively denoted by subscripts *in* and *sc*. Mean values of C_{min}, T_{min}, AAC and F_{dyn} with standard deviations (SD) were calculated for each group. Student's *t*-test and ANOVA were used to determine statistical difference. Differences were considered to be significant for values of $p < 0.05$.

Statistical significance of differences between the hypoglycaemic effect achieved by the intranasal formulations and the subcutaneous injection was tested via the Friedman test followed by a Wilcoxon Signed Rank post hoc test using PASW ® Statistics 18 software.

4.4. Results and Discussion

The design of the intranasal *in situ* thermogelling TMC hydrogel is such that it can be instilled in the sol state (drops or spray), and once in the nasal cavity undergo gelation to form a mucoadhesive viscous body [146]. To assess the mucoadhesive behaviour of this formulation, MCC was determined by monitoring the clearance of fluorescent microspheres (FluoSphere©) that had been mixed with the hydrogel and administered intranasally to rats.

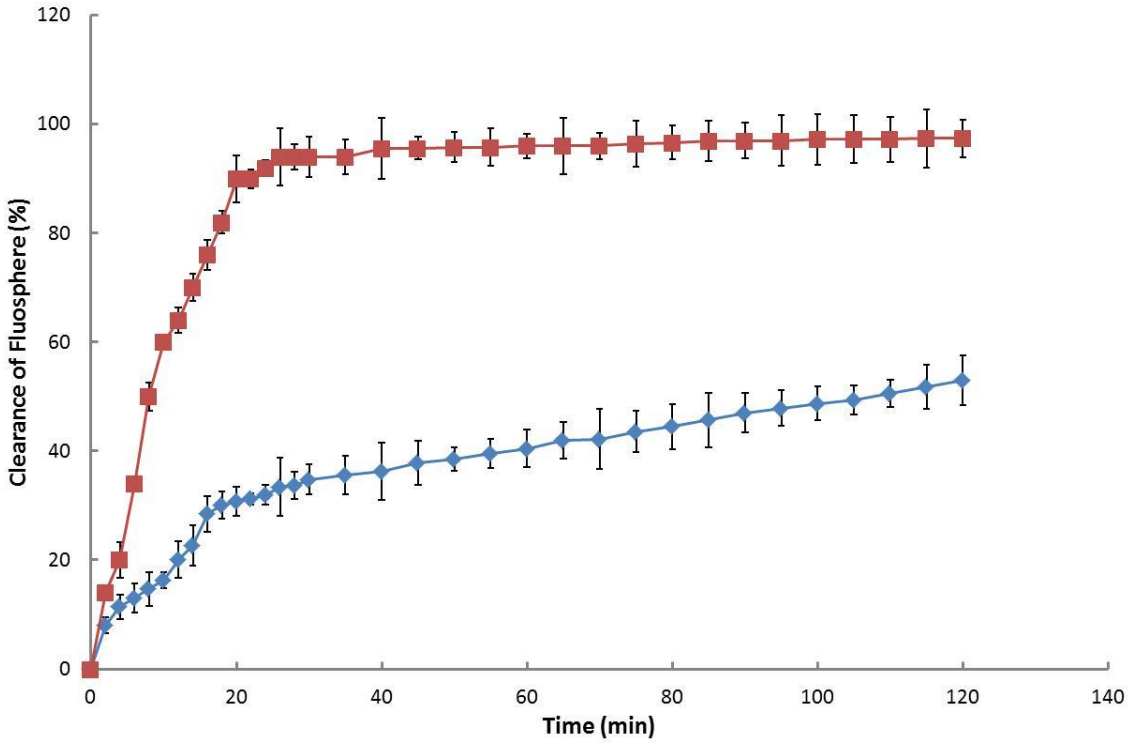

Figure 23. The recovery or clearance of 1 % w/v FluoSphere© following the intranasal administration of (■) FluoSphere© suspension and (◆) TMC/PEG/GP hydrogel. Mean ± SD, n=3.

The control experiment (intranasal instillation of an aqueous suspension of FluoSphere©) has shown that the microspheres clearing time is consistent with that expected from a normally functioning MCC: *ca*. 90% is cleared within 20 min, Fig. 23; the reported clearance rate for nasal mucus in the rat is 15-20 min [30, 270]. The hydrogel exhibited a significant capability to reduce the rate of MCC: FluoSphere© clearance following application from the hydrogel formulation was significantly slower than that for the control, with only *ca*. 30 % of the FluoSphere© content been cleared over 20 min. This rate of MCC clearance became even slower after 20 min, presumably as a consequence of the formulation being in its gel state (at the temperature of the nasal cavity the sol-to-gel transition occurs within ca. 8 min [146]): at 120 min following intranasal administration *ca*. 50 % of the administered FluoSphere© content is still in the nasal cavity as is consistent with the bioadhesive nature of TMC [131, 146, 203] and the viscous nature of the hydrogel formulation.

The determination of the hypoglycaemic activity profile of diabetic rats following the intranasal delivery of insulin by means of the thermosensitive TMC hydrogel involved comparison with the corresponding profile of subcutaneously injected insulin from a control group (F_{dyn} of 100 %; 1 IU/kg). For both test samples and controls, the dosages of insulin administered to the rats were consistent with those normally applied for the evaluation of insulin-delivery systems [4, 232, 282].

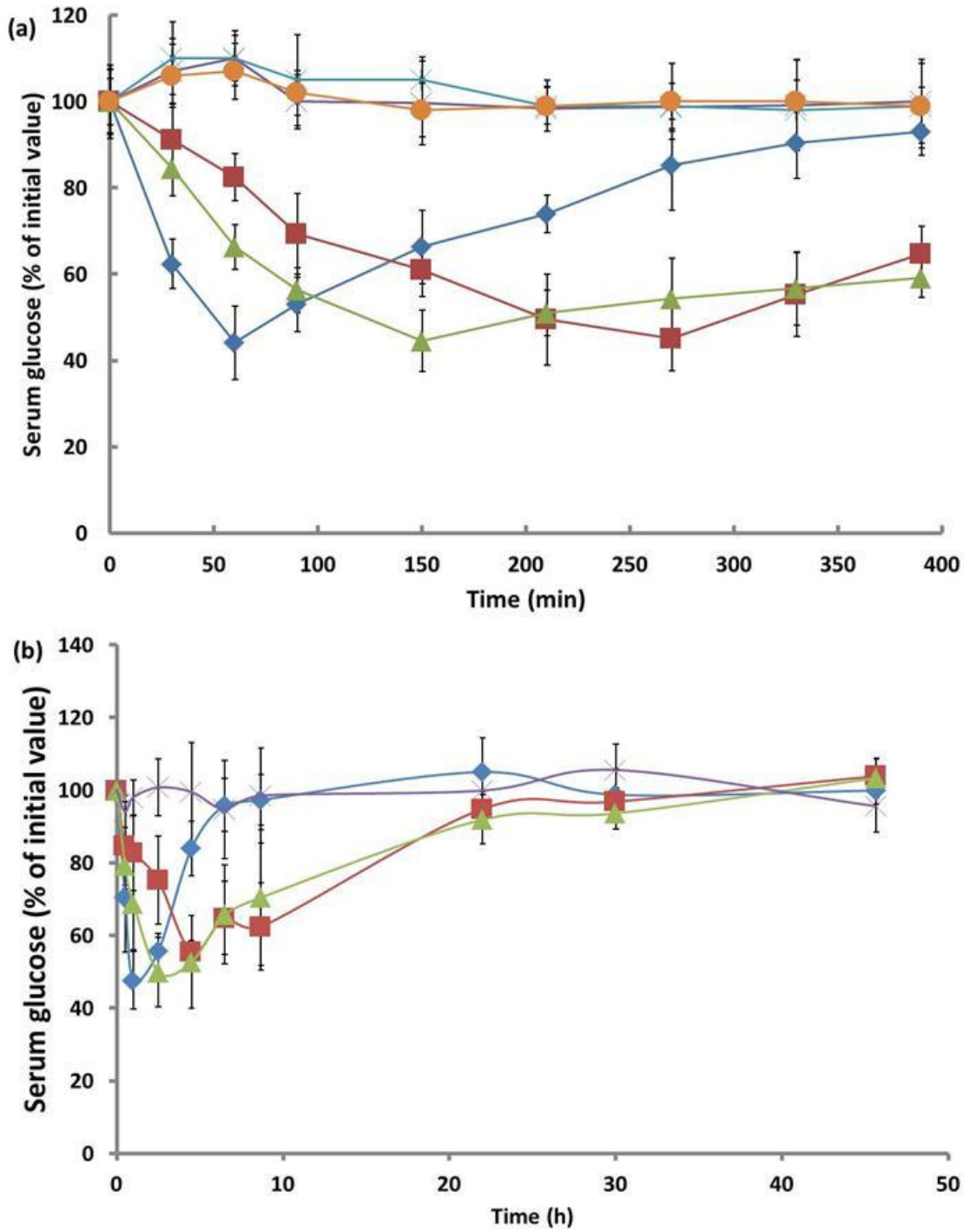

Figure 24. Serum glucose levels over (a) 6 hour and (b) 2 day period of rats following administration of: (■) insulin hydrogel; (▲) insulin TMC solution; (X) insulin solution; (X) hydrogel; (●) TMC solution, and (◆) insulin subcutaneous injection. Mean ± SD, n=5.

The averaged serum glucose profiles are presented in Fig. 24 (a) and (b). As expected, the nasal administration of insulin-free formulations failed to effect a reduction to overall serum-glucose levels. Nasally administered insulin solution also failed to induce a serum-glucose lowering effect. In fact, over the first 60 min, these formulations effected a slight elevation in glucose levels

(relative to the basal level), Fig. 24 (a), which are assumed to mark the stress-induced physiologically reactive response induced by the handling of the animals. The serum glucose concentration in control-group animals (sc injection) reached its lowest values (C_{min} = (47.6 ± 7.9) % of the basal value, Table 15) at *ca*. 1 h from insulin administration, after which time it began to increase at a near-constant rate until it returned to almost its original value (97.4 %) after *ca.* 9 h (Fig. 24 (b)). The serum glucose profile of animals that had been administered insulin using TMC solution exhibited a similar C_{min} ((49.6 ± 9.5) %), which was reached 90 min later (*ca*. 150 min from administration) than that of the control. The return to basal levels was slow with levels returning to their basal state towards at *ca*. 24 hours. Hence, it may be claimed that the TMC preparation is a promising candidate for further evaluation in the controlled release of nasally administered insulin. The hydrogel delivery system also achieved a C_{min} ((55.1 ± 3.0) %) that is almost comparable with that of the sc injection or the TMC solution since no statistical difference was observed between the sc, TMC solution or the hydrogel system, but this minimum was achieved at *ca*. 270 min (respectively 210 min and 120 min later than those seen following the sc injection or the nasal administration of the TMC solution). The subsequent increase in serum glucose was observed to occur at similar rate to that observed with the TMC solution, returning to basal glucose concentration at *ca*. 24 hours. However, it must be registered that one of the rats that had been administered with intranasal TMC solution died at 9 h from administration – while the reasons for the death of the animal are not known, this event highlights the need for the further toxicological evaluation of the formulation.

Calculated with reference to the sc injection group, the pharmacodynamic availability (F_{dyn}) of insulin that had been delivered intranasally *via* hydrogel or in TMC solution was not statistically different (respectively (17.1 ± 2.4) % and (16.8 ± 4.1) %), and much higher than that achieved with insulin solution (0.1 ± 0.0) %. Since there was no statistically significant variation in age, weight or basal serum glucose levels in the diabetic rats employed for this investigation, it is assumed that the administered insulin formulations were responsible for the induced hypoglycaemic response [269].

Table 15. The pharmacodynamic parameters of insulin administered to diabetic rats (* over 2740 min and † over 390 min).

Formulation	T_{min} (min)	C_{min} (% initial value)	AAC † (% glucose.min)	AAC * (% glucose.min)	F_{dyn} (%)
Insulin s.c.*	60	47.6 ± 7.9	13252 ± 1261	22059 ± 9303	100.0 ± 42.1
Insulin hydrogel*	270	55.1 ± 3.0	11538 ± 2842	37752 ± 5294	17.1 ± 2.4
Insulin TMC solution*	150	49.6 ± 9.5	15467 ± 3203	37072 ± 10542	16.8 ± 4.1
Insulin solution†	210	98.3 ± 5.2	141 ± 32		0.1 ± 0.0
Hydrogel†	330	98.0 ± 6.9	270 ± 57		0.2 ± 0.0
TMC solution†	150	98.0 ± 6.2	210 ± 48		0.2 ± 0.0

The F_{dyn} value, Table 15, determined for the intranasal administration of insulin into rats using the TMC hydrogel is similar to those reported for the administration of insulin using chitosan solution (15.4 %) [232], and somewhat superior to those reported for a chitosan gel (9.3–18.0 %) [269], for a chitosan/PVA gel (8.8%) [265] and for a derivatised chitosan (HTCC)-PEG hydrogel (3.2–7.3 % dependent upon PEG concentration) [4]. The observed prolonged lowering of glucose levels, manifested by the pharmacodynamic availability of insulin from TMC solution and the TMC hydrogel formulation, is consistent with earlier observations that have demonstrated the capability of TMC to disrupt the integrity of Calu-3 monolayers [261].

Barichello *et al.* [282] have shown that the sc administration into healthy rats of insulin in Pluronic F127 gels or in gels containing insulin-PGLA nanoparticles effects a prolonged hypoglycaemic effect which is analogous to that effected by the TMC hydrogel formulation (C_{min} of *ca*. 40 % at 3 h; serum glucose levels at *ca*. 60 % of basal at 6 h from administration). Dyer *et al.* [266] have reported that insulin-loaded chitosan nanoparticles, exhibit a C_{min} of 50–60 % at *ca*. 2 h and possess a F_{dyn} of *ca*. 37 %, which does not offer any advantage over chitosan intranasal insulin solution (C_{min} of *ca*. 40 % after approx. 90 min, and an F_{dyn} of *ca*. 48 %). The nanoparticulate format appears to possess greater transmucosal penetrative capacity than the TMC hydrogel presented here, but neither surpasses the absorption enhancing characteristics of the insulin-TMC intranasal solution. However, owing to the relatively low pH (4.0–4.5) inherent to this formulation, its therapeutic relevance remains to be tested [17, 262].

4.5. Conclusion

In vivo experiments in the rat model have demonstrated that an *in situ* thermogelling nasal formulation of TMC is capable of residing at the nasal mucosa over time scales that far exceed those of mucus turnover. The same formulation has also been shown to be capable of affecting the controlled delivery of insulin, as is demonstrated by the observed *in vivo* reduction in blood glucose over *ca.* 24 hours. The data highlight the potential of the device as a once-a-day dosage form for the delivery of insulin through the nasal route.

Chapter Five: Future Work

Future Work

By the very nature of hydrogel systems, and as has been highlighted by the gel format of this sol-gel TMC/PEG/GP example, controlled drug release is the kinetic profile to be expected. This concept does not marry well with the established belief of nasal systems to have a fast therapeutic action. Small, highly potent drug entities may compensate for the sustained release from hydrogel networks, whereas larger drugs requiring a substantial concentration to be absorbed so as to exert a pharmacological response are potentially not well suited to the hydrogel intranasal administration. The system demonstrated here has shown some favourable characteristics for the potential use as a vehicle for the delivery of small proteins, such as biocompatibility, mucoadhesivity and a penetration enhancing effect. Further optimisation of the formulation through the reformulation to a nanogel may improve the uptake of the loaded insulin through additional active transport mechanisms across mucosal membranes. The subsequent absorption profile may render the formulation as a quicker acting hypoglycaemic system that would adhere more closely to the fast action expected of nasal drug delivery systems. In achieving this, the goal to improving the current invasive therapies for glucose control may be more successfully met, since a short/intermediate acting insulin spray may act as a replacement to the frequent pre-prandial injections that feature commonly in diabetic regimens.

Whilst retaining the formulation in the current thermosensitive format, the development of an on-demand pulsatile release system that modulates insulin release in response to physiological demand through coupling with a glucose sensor is a possibility. This system could be appropriately designed as an injectable sol-gel system that forms a gel implant within the body and acts as an artificial pancreas; monitoring glucose levels and subsequently releasing insulin appropriate to the glucose concentration recorded. This system could be tailored to act as a controlled delivery device replacing the need for long acting insulin injections and providing the basal insulin levels required when glucose levels are stable and relatively low. The in-built monitoring system registers the increased

glucose levels post-prandial triggering a conformational change to the hydrogel implant to allow more rapid release of the loaded insulin for a responsive hypoglycaemic effect.

The further work is therefore two-tiered, with one aspect directed towards the further development of the formulation so it is fit for purpose to the nasal mucosal membrane, and another that involves diversifying the application of the hydrogel to another administration route.

References

[1] C. Prego, M. Garcia, D. Torres, M.J. Alonso, Transmucosal macromolecular drug delivery, J Control Release, 101 (2005) 151-162.
[2] T. Furubayashi, D. Inoue, A. Kamaguchi, Y. Higashi, T. Sakane, Influence of formulation viscosity on drug absorption following nasal application in rats, Drug Metab Pharmacokinet, 22 (2007) 206-211.
[3] X.P. Duan, S.R. Mao, New strategies to improve the intranasal absorption of insulin, Drug Discovery Today, 15 (2010) 416-427.
[4] J. Wu, W. Wei, L.-Y. Wang, Z.-G. Su, G.-H.S. Ma, A thermosensitive hydrogel based on quaternized chitosan and poly(ethylene glycol) for nasal drug delivery system, Biomaterials, 28 (2007) 2220-2232.
[5] B. Luppi, F. Bigucci, T. Cerchiara, V. Zecchi, Chitosan-based hydrogels for nasal drug delivery: from inserts to nanoparticles, Expert Opin Drug Deliv, 7 (2010) 811-828.
[6] H. Tandel, K. Florence, A. Misra, Protein and Peptide Delivery through Respiratory Pathway, in: Challenges in Delivery of Therapeutic Genomics and Proteomics, Elsevier, London, 2011, pp. 429-479.
[7] Y. Sudhakar, K. Kuotsu, A.K. Bandyopadhyay, Buccal bioadhesive drug delivery -- A promising option for orally less efficient drugs, J Control Release, 114 (2006) 15-40.
[8] N. Salamat-Miller, M. Chittchang, T.P. Johnston, The use of mucoadhesive polymers in buccal drug delivery, Adv Drug Deliv Rev, 57 (2005) 1666-1691.
[9] S. Rossi, M. Marciello, M.C. Bonferoni, F. Ferrari, G. Sandri, C. Dacarro, P. Grisoli, C. Caramella, Thermally sensitive gels based on chitosan derivatives for the treatment of oral mucositis, Eur J Pharm Biopharm, 74 (2010) 248-254.
[10] N.A. Nafee, F.A. Ismail, N.A. Boraie, L.M. Mortada, Mucoadhesive buccal patches of miconazole nitrate: *in vitro/in vivo* performance and effect of ageing, Int J Pharm, 264 (2003) 1-14.
[11] B.-L. Guo, Q.-Y. Gao, Preparation and properties of a pH/temperature-responsive carboxymethyl chitosan/poly(*N*-isopropylacrylamide)semi-IPN hydrogel for oral delivery of drugs, Carbohyd Res, 342 (2007) 2416-2422.
[12] C.B. He, F.Y. Cui, L.C. Yin, F. Qian, C. Tang, C.H. Yin, A polymeric composite carrier for oral delivery of peptide drugs: bilaminated hydrogel film loaded with nanoparticles, Eur Polym J, 45 (2009) 368-376.
[13] A. Bernkop-Schnurch, M.E. Krajicek, Mucoadhesive polymers as platforms for peroral peptide delivery and absorption: synthesis and evaluation of different chitosan-EDTA conjugates, J Control Release, 50 (1998) 215-223.
[14] C. Valenta, The use of mucoadhesive polymers in vaginal delivery, Advanced Drug Deliv Rev, 57 (2005) 1692-1712.
[15] L. Perioli, V. Ambrogi, L. Venezia, C. Pagano, M. Ricci, C. Rossi, Chitosan and a modified chitosan as agents to improve performances of mucoadhesive vaginal gels, Colloids and Surfaces B: Biointerfaces, 66 (2008) 141-145.
[16] M.C. Bonferoni, G. Sandri, S. Rossi, F. Ferrari, S. Gibin, C. Caramella, Chitosan citrate as multifunctional polymer for vaginal delivery - Evaluation of penetration enhancement and peptidase inhibition properties, Eur J Pharm Sci, 33 (2008) 166-176.
[17] L. du Plessis, A. Kotze, H. Junginger, Nasal and rectal delivery of insulin with chitosan and N-trimethyl chitosan chloride, Drug Deliv, 17 (2010) 399-407.
[18] Y. Cao, C. Zhang, W. Shen, Z. Cheng, L. Yu, Q. Ping, Poly*(N*-isopropylacrylamide)-chitosan as thermosensitive *in situ* gel-forming system for ocular drug delivery, J Control Release, 120 (2007) 186-194.
[19] K. Hosny, Preparation and evaluation of thermosensitive liposomal hydrogel for enhanced transcorneal permeation of ofloxacin, AAPS Pharm Sci Tech, 10 (2009) 1336-1342.
[20] B.C. Baudner, D.T. O'Hagan, Bioadhesive delivery systems for mucosal vaccine delivery, J Drug Targeting, 18 (2010) 752-770.
[21] A. Ludwig, The use of mucoadhesive polymers in ocular drug delivery, Adv Drug Deliv Rev, 57 (2005) 1595-1639.

[22] H. Fujishima, I. Toda, M. Yamada, N. Sato, K. Tsubota, Corneal temperature in patients with dry eye evaluated by infrared radiation thermometry, British J Opthalmol, 80 (1996) 29-32.
[23] J.W. Lee, J.H. Park, J.R. Robinson, Bioadhesive-based dosage forms: the next generation, J Pharm Sci, 89 (2000) 850-866.
[24] J.A. Nicolazzo, B.L. Reed, B.C. Finnin, Buccal penetration enhancers - How do they really work?, J Control Release, 105 (2005) 1-15.
[25] T.A. Spierings, M.C. Peters, A.J. Plasschaert, Surface temperature of oral tissues. A review, J Biol Buccale, 12 (1984) 91-99.
[26] D.J. Aframan, T. Davidowitz, R. Benoliel, The distribution of oral mucosal pH values in healthy saliva secretors, Oral diseases, 12 (2006) 420-423.
[27] J. Blanchette, N. Kavimandan, N.A. Peppas, Principles of transmucosal delivery of therapeutic agents, Biomedicine & Pharmacotherapy, 58 (2004) 142-151.
[28] B.J. Aungst, Oral mucosal permeation enhancement: possibilities and limitations, in: M.J. Rathbone (Ed.) Oral mucosal delivery, Marcel Dekker, New York, 1996 pp. 65-83.
[29] Y.W. Chien, Oral drug delivery and delivery systems, in: Y.W. Chien (Ed.) Novel drug delivery systems, Marcel Dekker, New York, 1992, pp. 139-196.
[30] A. Pires, A. Fortuna, G. Alves, A. Falcao, Intranasal drug delivery: How, why and what for?, J Pharm Pharmaceut Sci, 12 (2009) 288-311.
[31] N. Mygind, R. Dahl, Anatomy, physiology and function of the nasal cavities in health and disease, Adv Drug Deliv Rev, 29 (1998) 3-12.
[32] D. Elad, M. Wolf, T. Keck, Air-conditioning in the human nasal cavity, Respir Physiol Neurobiol, 163 (2008) 121-127.
[33] M.S. Quraishi, N.S. Jones, J. Mason, The rheology of nasal mucus: a review, Clin Otolaryngology Allied Sci, 23 (1998) 403-413.
[34] G. Pilcer, K. Amighi, Formulation strategy and use of excipients in pulmonary drug delivery, Int J Pharm, 392 (2010) 1-19.
[35] Z. Borrill, C. Starkey, J. Vestbo, D. Singh, Reproducibility of exhaled breath condensate pH in chronic obstructive pulmonary disease, Eur Respir J, 25 (2005) 269-274.
[36] P. Cole, Respiratory mucosal vascular responses, air conditioning and thermoregulation, J Laryngol Otol, 68 (1954) 1-10.
[37] J. Yu, Y.W. Chien, Pulmonary drug delivery: Physiological and mechanistic aspects, Crit Rev in Therapeut Drug Carrier Sys, 14 (1997) 395-453.
[38] P.R. Byron, Respiratory drug delivery, in, CRC Press, Boca Raton, FL, 1990.
[39] J. Das Neves, M.F. Bahia, Gels as vaginal drug delivery systems, Int J Pharm, 318 (2006) 1-14.
[40] C. Valenta, The use of mucoadhesive polymers in vaginal delivery, Adv Drug Deliv Rev, 57 (2005) 1692-1712.
[41] A.L. Rashad, W.L. Toffler, N. Wolf, K. Thoraburg, E.P. Kirk, G. Ellis, W.E. Whitehead, Vaginal $P0_2$ in healthy women and in women infected with Trichomonas vaginalis: Potential implications for metronidazole therapy, American J Obstet Gynecol, 166 (1992) 620-624.
[42] F. Madsen, K. Eberth, J.D. Smart, A rheological assessment of the nature of interactions between mucoadhesive polymers and a homogenised mucus gel, Biomaterials, 19 (1998) 1083-1092.
[43] G.P. Andrews, T.P. Laverty, D.S. Jones, Mucoadhesive polymeric platforms for controlled drug delivery, Eur J Pharm Biopharm, 71 (2009) 505-518.
[44] P. Sriamornsak, N. Wattanakorn, Rheological synergy in aqueous mixtures of pectin and mucin, Carbohyd Polym, 74 (2008) 474-481.
[45] J.K. Vasir, K. Tambwekar, S. Garg, Bioadhesive microspheres as a controlled drug delivery system, Int J Pharm, 255 (2003) 13-32.
[46] M. Ishida, N. Nambu, T. Nagai, Ointment-type oral mucosal dosage form of Carbopol containing prednisolone for treatment of aptha., Chem Pharm Bull, 31 (1983) 1010-1014.
[47] E. Hagesaether, S.A. Sande, *In vitro* measurements of mucoadhesive properties of six types of pectin, Drug Dev Ind Pharm, 33 (2007) 417-425.

[48] A. Jintapattanakit, S. Mao, T. Kissel, V.B. Junyaprasert, Physicochemical properties and biocompatibility of *N*-trimethyl chitosan: Effect of quaternization and dimethylation, Eur J Pharm Biopharm, 70 (2008) 563-571.
[49] D. Duchene, G. Ponchel, Principle and investigation of the bioadhesion mechanism of solid dosage forms, Biomaterials, 13 (1992) 709-714.
[50] J. Xiang, L. Xiaoling, Investigation of correlations between mucoadhesion and surface energy properties of mucoadhesives, J Appl Polym Sci, 102 (2006) 2608-2615.
[51] D. Solomonidou, K. Cremer, M. Krumme, J. Kreuter, Effect of carbomer concentration and degree of neutralisation on the mucoadhesive properties of polymer films, J Biomater Sci Polym Ed, 12 (2001) 1191-1205.
[52] N.A. Peppas, P.A. Buri, Surface interfacial and molecular aspects of polymer bioadhesion on soft tissues, J Control Release, 2 (1985) 257-275.
[53] F. Madsen, K. Eberth, J.D. Smart, A rheological examination of the mucoadhesive/mucus interaction: the effect of mucoadhesive type and concentration, J Control Release, 50 (1998) 167-178.
[54] G.P. Andrews, T.P. Laverty, D.S. Jones, Mucoadhesive polymeric platforms for controlled drug delivery, Eur J Pharm Biopharm, 71 (2009) 505-518.
[55] J.D. Smart, I.W. Kellaway, H.E. Worthington, An *in vitro* investigation of mucosa-adhesive materials for use in controlled drug delivery, J Pharm Pharmacol, 36 (1984) 295-299.
[56] A.G. Mikos, N.A. Peppas, Systems for controlled release of drugs. V: Bioadhesive systems, STP Pharma Sci, 19 (1986) 705-715.
[57] S.H. Leung, J.R. Robinson, The contribution of anionic polymer structural features to mucoadhesion, J Control Release, 5 (1988) 223-230.
[58] C. Wong, K. Yuen, K. Peh, An *in-vitro* method for buccal adhesion studies: importance of instrument variables, Int J Pharm, 180 (1999) 47-57.
[59] R.J. Majithiya, P.K. Ghosh, M.L. Umrethia, R.S.R. Murthy, Thermosensitive-mucoadhesive gel for nasal delivery of sumatriptan, AAPS Pharm Sci Tech, 7 (2006).
[60] E.E. Hassan, J.M. Gallo, A simple rheological method for the in vitro assessment of mucin-polymer bioadhesive bond strength, Pharm Res, 7 (1990) 491-495.
[61] R.G. Riley, J.D. Smart, J. Tsibouklis, P.W. Dettmar, F. Hampson, J.A. Davis, G. Kelly, W.R. Wilber, An investigation of mucus/polymer theological synergism using synthesised and characterised poly(acrylic acid)s, Int J Pharm, 217 (2001) 87-100.
[62] L. Mayol, F. Quaglia, A. Borzacchiello, L. Ambrosio, M.I. La Rotonda, A novel poloxamers/hyaluronic acid *in situ* forming hydrogel for drug delivery: rheological, mucoadhesive and *in vitro* release properties, Eur J Pharm Biopharm, 70 (2008) 199-206.
[63] S. Tamburic, D.M. Craig, A comparison of different *in vitro* methods for measuring mucoadhesive performance, Eur J Pharm Biopharm, 44 (1997) 159-167.
[64] S. Rossi, M.C. Bonferoni, G. Lippoli, M. Bertoni, F. Ferrari, C. Caramella, U. Conte, Influence of mucin type on polymer-mucin rheological interactions, Biomaterials, 16 (1995) 1073-1079.
[65] J. Kocevar-Nared, J. Kristl, J. Smid-Korbar, Comparative rheological investigation of crude gastric mucin and natural gastric mucus, Biomaterials, 18 (1997) 677-681.
[66] H.K. Batchelor, D. Banning, P.W. Dettmar, F.C. Hampson, I.G. Jolliffe, D.Q.M. Craig, An *in vitro* mucosal model for prediction of the bioadhesion of alginate solutions to the oesophagus, Int J Pharm, 238 (2002) 123-132.
[67] E. Jabbari, N. Wisniewski, N.A. Peppas, Evidence of mucoadhesion by chain interpretation at a poly(acrylic acid)/mucin interface using ATR-FTIR spectroscopy, J Control Release, 26 (1993) 99-108.
[68] M.M. Patel, J.D. Smart, T.G. Nevell, P. Eaton, R.J. Ewen, J. Tsibouklis, Mucin/poly(carboxylic acid) interactions: a spectroscopic investigation of mucoadhesion, Biomacromol, 4 (2003) 1184-1190.
[69] P. Sriamornsak, N. Wattanakorn, J. Nunthanid, S. Puttipipatkhachorn, Mucoadhesion of pectin as evidence by wettability and chain interpenetration, Carbohyd Polym, 74 (2008) 458-467.

[70] L. Joergensen, B. Klosgen, A.C. Simonsen, J. Borch, E. Hagesaether, New insights into the mucoadhesion of pectins by AFM roughness parameters in combination with SPR, Int J Pharm, 411 (2011) 162-168.
[71] P. Esposito, I. Colombo, M. Lovrecich, Investigation of surface properties of some polymers by thermodynamic and mechanical approach: possibility of predicting mucoadhesion and biocompatibility, Biomaterials, 15 (1994) 177-182.
[72] C.-M. Lehr, J.A. Bouwstra, H.E. Bodde, H.E. Junginger, A surface energy analysis of mucoadhesion: contact angle measurements on polycarbophil and pig intestinal mucosa in physiologically relevant fluids, Pharm Res, 9 (1992) 70-75.
[73] H. Takeuchi, J. Thongborisute, Y. Matsui, H. Sugihara, H. Yamamoto, Y. Kawashima, Novel mucoadhesion tests for polymers and polymer-coated particles to design optimal mucoadhesive drug delivery systems, Adv Drug Deliv Rev, 57 (2005) 1583-1594.
[74] W. Sajomsang, U.R. Ruktanonchai, P. Gonil, O. Nuchuchua, Mucoadhesive property and biocompatibility of methylated *N*-aryl chitosan derivatives, Carbohyd Polym, 78 (2009) 945-952.
[75] J. Cleary, L. Bromberg, E. Magner, Adhesion of polyether-modified poly(acrylic acid) to mucin, Langmuir, 20 (2004) 9755-9762.
[76] R.J. Soane, M. Frier, A.C. Perkins, N.S. Jones, S.S. Davis, L. Illum, Evaluation of the clearance characteristics of bioadhesive systems in humans, Int J Pharm, 178 (1999) 55-65.
[77] J.L. Richardson, J. Whetstone, N.F. Fisher, P. Watts, N.F. Farraj, M. Hinchcliffe, L. Benedetti, L. Illum, Gamma scintigraphy as a novel method to study the distribution and retention of a bioadhesive vaginal delivery system in sheep., J Control Release, 42 (1996) 133-142.
[78] K. Albrecht, M. Greindl, C. Kremser, C. Wolf, P. Debbage, A. Bernkop-Schnurch, Comparative *in vivo* mucoadhesion studies of thiomer formulations using magnetic resonance imaging and fluorescence detection, J Control Release, 115 (2006) 78-84.
[79] M.D. Donovan, Z. Mengping, Drug effects on *in vivo* nasal clearance in rats, Int J Pharm, 116 (1995) 77-86.
[80] R.G. Riley, J.D. Smart, J. Tsibouklis, P.W. Dettmar, F. Hampson, A. Davis, G. Kelly, W.R. Wilber, The gastrointestinal transit profile of C14-labelled poly(acrylic acids): an *in vivo* study, Biomaterials, 22 (2001) 1861-1867.
[81] M. Roldo, E. Barbu, J.F. Brown, D.W. Laight, J.D. Smart, J. Tsibouklis, Orally administered, colon-specific mucoadhesive azopolymer particles for the treatment of inflammatory bowel disease: an *in vivo* study, J Biomed Materials Res, 79A (2006) 706-715.
[82] S.K. Maurya, K. Pathak, V. Bali, Therapeutic potential of mucoadhesive drug delivery systems - An updated patent review, Recent Pat Drug Deliv Formulation, 4 (2010) 256-265.
[83] D. Dodou, P. Breedveld, P.A. Wieringa, Mucoadhesives in the gastrointestinal tract: revisiting the literature for novel applications, Eur J Pharm Biopharm, 60 (2005) 1-16.
[84] O. Wichterle, D. Lim, Hydrophilic gels for biological use, Nature, 185 (1960) 117-118.
[85] N. Bhattarai, J. Gunn, M. Zhang, Chitosan-based hydrogels for controlled, localized drug delivery, Adv Drug Deliv Rev, 62 (2010) 83-99.
[86] G. Kavanagh, S.B. Ross-Murphy, Rheological characterisation of polymer gels, Prog Polym Sci, 23 (1998) 533-562.
[87] J. Berger, M. Reist, J.M. Mayer, O. Felt, R. Gurny, Structure and interactions in chitosan hydrogels formed by complexation or aggregation for biomedical applications, Eur J Pharm Biopharm, 57 (2004) 35-52.
[88] M. Hamidi, A. Azadi, P. Rafiei, Hydrogel nanoparticles in drug delivery, Adv Drug Deliv Rev, 60 (2008) 1638-1649.
[89] M. Dash, F. Chiellini, R. Ottenbrite, E. Chiellini, Chitosan - A versatile semi-synthetic polymer in biomedical applications Prog Polym Sci, 36 (2011) 981-1014.
[90] N. Hunt, A. Smith, U. Gbureck, R. Shelton, L. Grover, Encapsulation of fibroblasts causes accelerated alginate hydrogel degradation, acta Biomaterialia, 6(2010) 3649-3656.

[91] T. Boontheekul, H. Kong, D. Mooney, Controlling alginate gel degradation utilising partial oxidation and bimodal molecular weight distribution, Biomaterials, 26 (2005) 2455-2465.
[92] H. Kong, E. Alsberg, D. Kaigler, K. Lee, D. Mooney, Controlling degradation of hydrogels via the size of cross-linked junctions, Adv Mater, 16 (2004) 1917.
[93] C.-C. Lin, A.T. Metters, Hydrogels in controlled release formulations: Network design and mathematical modeling, Adv Drug Deliv Rev, 58 (2006) 1379-1408.
[94] S. Lu, L. Mingzhu, B. Ni, An injectable oxidised carboxymethylcellulose/*N*-succinyl-chitosan hydrogel, Chem Engineering J, 160 (2010) 779-787.
[95] M. St'astny, D. Plocova, T. Etrych, M. Kovar, K. Ulbrich, B. Rihova, HPMA-hydrogels containing cytostatic drugs. Kinetics of the drug release and *in vivo* efficacy, J Control Release, 81 (2002) 101-111.
[96] M. Konishi, Y. Tabata, M. Kariya, H. Hosseinkhani, A. Suzuki, K. Fukuhara, M. Mandai, K. Takakura, S. Fujii, *In vivo* anti-tumour effect of dual release of cisplatin and adriamycin from biodegradeable gelatin hydrogel, J Control Release, 103 (2005) 7-19.
[97] V.V. Khutoryanskiy, Hydrogen-bonded interpolymer complexes as materials for pharmaceutical applications, Int J Pharm, 334 (2007) 15-26.
[98] C. Chun, S.M. Lee, S.Y. Kim, H.K. Yang, S.C. Song, Thermosensitive poly(organophosphazene)-paclitaxel conjugate gels for antitumour applications, Biomaterials, 30 (2009) 2349-2360.
[99] D.S. Benoit, C.R. Nuttelman, S.D. Collins, K.S. Anseth, Synthesis and characterisation of a fluvastatin-releasing hydrogel delivery system to modulate hMSC differentiation and function for bone regeneration, Biomaterials, 27 (2006) 6102-6110.
[100] T.R. Hoare, D.S. Kohane, Hydrogels in drug delivery: progress and challenges, Polymer, 49 (2008) 1993-2007.
[101] C.R. Nuttelman, M.C. Tripodi, K.S. Anseth, Dexamethasone-functionalised gels induce osteogenic differentiation of encapsulated hMSCs, J Biomed Materials Res, 76 (2006) 183-195.
[102] K. Morimoto, T. Takeeda, Y. Nakamoto, Effective vaginal absorption of insulin in diabetic rats and rabbits using polyacrylic acid aqueous gel bases, Int J Pharm, 12 (1982).
[103] O. Yu-Kyoung, P. Jeong-Sook, Y. Ho, K. Chong-Kook, Enhanced mucosal and systemic immune responses to a vaginal vaccine coadministered with RANTES expressing plasmid DNA using in situ-gelling mucoadhesive delivery system, Vaccine, 21 (2003) 1980-1988.
[104] E. Ghelardi, A. Tavanti, A. Lupetti, F. Celandroni, E. Boldrini, M. Campa, S. Senesi, Control of Candida albicans murine vaginitis by topical administration of polycarbophil-econazole complex, Antimicrob Agents Chemother, 42 (1998) 2434-2436.
[105] N.M. Zaki, G.A. Awad, N.D. Mortada, S.S. Abd ElHady, Enhanced bioavailability of metoclopramide HCl by intranasal administration of a mucoadhesive *in situ* gel with modulated rheological and mucociliary transport properties, Eur J Pharm Sci, 32 (2007) 296-307.
[106] J. Cassidy, B. Berner, K. Chan, V. John, S. Toon, B. Holt, M. Rowland, Human transbuccal absorption of diclofenac sodium from a prototype hydrogel delivery device, Pharm Res, 10 (1993) 126-129.
[107] K. Lindell, S. Engstrom, In vitro release of timolol maleate from an in situ gelling polymer system, Int J Pharm, 95 (1993) 219-228.
[108] M. Dhiman, P. Yedurkar, K.K. Sawant, Formulation, characterisation and in vitro evaluation of bioadhesive gels containing 5-fluorouracil, Pharm Dev Technol, 13 (2008) 15-25.
[109] Y. Ozsoy, T. Tuncel, A. Can, N. Akev, S. Birteksoz, A. Gerceker, *In vivo* studies on nasal preparations of ciprofloxacin hydrochloride, Pharmazie, 55 (2000) 607-609.
[110] L. Mayol, M. Biondi, F. Quaglia, S. Fusco, A. Borzacchiello, L. Ambrosio, M.I. La Rotonda, Injectable thermally responsive mucoadhesive gel for sustained protein delivery, Biomacromol, 12 (2011) 28-33.
[111] D. Shastri, S. Prajapati, L. Patel, Thermoreversible mucoadhesive opthalmic *in situ* hydrogel: Design and optimisation using a combination of polymers, Acta Pharma, 60 (2010) 349-360.

[112] F. Khan, R.S. Tare, R.O.C. Oreffo, M. Bradley, Versatile biocompatible polymer hydrogels: scaffolds for cell growth, Angewandte Chemie, 121 (2009) 996-1000.
[113] N. Bhattarai, H.R. Ramay, J. Gunn, F.A. Matsen, M. Zhang, PEG-grafted chitosan as an injectable thermosensitive hydrogel for sustained protein release, J Control Release, 103 (2005) 609-624.
[114] H.S. Yoo, Photo-cross-linkage and thermo-responsive hydrogels containing chitosan and Pluronic for sustained release of human growth hormone (hGH), J Biomater Sci Polym Ed, 18 (2007) 1429-1441.
[115] A.K. Azab, V. Doviner, B. Orkin, J. Kleinstern, M. Srebnik, A. Nissan, A. Rubinstein, Biocompatibility evaluation of cross-linked chitosan hydrogels after subcutaneous and intraperitoneal implantation in the rat, J Biomed Materials Res, 83A (2007) 412-422.
[116] V.R. Patel, M. Amiji, Preparation and characterisation of freeze-dried chitosan-poly(ethylene oxide) hydrogels for site-specific antibiotic delivery to the stomach, Pharm Res, 13 (1996) 588-593.
[117] J. Varshosaz, S. H., A. Heidari, Nasal delivery of insulin using bioadhesive chitosan gels, Drug Deliv, 13 (2006) 31-38.
[118] S. Chelladurai, M. Mishra, B. Mishra, Design and evaluation of bioadhesive in-situ nasal gel of ketorolac tromethamine, Chem Pharm Bull, 56 (2008) 1596-1599.
[119] N. Rasool, T. Yasin, J.Y.Y. Heng, Z. Akhter, Synthesis and characterisation of novel pH-, ionic strength and temperature- sensitive hydrogel for insulin delivery, Polymer, 51 (2010) 1687-1693.
[120] Y. Shechter, M. Mironchik, R. S., H. Tsubery, K. Sasson, Y. Marcus, M. Fridkin, Reversible pegylation of insulin facilitates its prolonged action *in vivo*, Eur J Pharm Biopharm, 70 (2008) 19-28.
[121] A. Yamamoto, E. Hayakawa, L. V.H., Insulin and proinsulin proteolysis in mucosal homogenates of the albino rabbit: implications in peptide delivery from nonoral routes, Life Sci, 47 (1990) 2465-2474.
[122] Z. Shao, K. R., A.K. Mitra, Cyclodextrins as nasal absorption promoters of insulin: mechanistic evaluations, Pharm Res, 9 (1992) 1157-1163.
[123] S. Takatsuka, T. Kitazawa, T. Morita, Y. Horikiri, H. Yoshino, Enhancement of intestinal absorption of poorly absorbed hydrophilic compounds by simultaneous use of mucolytic agent and non-ionic surfactant, Eur J Pharm Biopharm, 62 (2006) 52-58.
[124] J.A. Nicolazzo, B.L. Reed, B.C. Finnin, Assessment of the effects of sodium dodecyl sulfate on the buccal permeability of caffeine and estradiol, J Pharm Sci, 93 (2004) 431-440.
[125] C.L. Froebe, F.A. Simion, R.H. Rhein, R.H. Cagan, A. Kligman, Stratum corneum lipid removal by surfactants:relation to in vitro irritation, Dermatologica, 181 (1990) 277-283.
[126] A.F. Kotze, H.L. Luessen, B.J. deLeeuw, B.G. deBoer, J.C. Verhoef, H.E. Junginger, *N*-trimethyl chitosan chloride as a potential absorption enhancer across mucosal surfaces: *In vitro* evaluation in intestinal epithelial cells (Caco-2), Pharm Res, 14 (1997) 1197-1202.
[127] M. Morishita, I. Morishita, K. Takayama, Y. Machida, T. Nagai, Site-dependent effect of aprotinin, sodium caprate, Na_2EDTA and sodium glycocholate on intestinal absorption of insulin, Biol Pharm Bull, 16 (1993) 68-72.
[128] N. Fefelova, Z. Nurkeeva, G. Mun, V. Khutoryanskiy, Mucoadhesive interactions of amphiphilic cationic copolymers based on [2-(methacryloyloxy)ethyl]triethylammonium chloride, Int J Pharm, 339 (2007) 25-32.
[129] M. Roldo, D.G. Fatouros, Chitosan derivative based hydrogels as drug delivery platforms: applications in drug delivery and tissue engineering, in: Active implants and scaffolds for tissue regeneration, Springer, 2011, pp. 351-376.
[130] W. Boonyo, H.E. Junginger, N. Waranuch, A. Polnok, T. Pitaksuteepong, Chitosan and trimethyl chitosan chloride (TMC) as adjuvants for inducing immune repsonses to ovalbumin in mice following nasal administration, J Control Release, 121 (2007) 168-175.
[131] D. Snyman, J.H. Hamman, A.F. Kotze, Evaluation of the mucoadhesive properties of *N*-trimethyl chitosan chloride, Drug Dev Ind Pharm, 29 (2003) 61-69.
[132] A. Bernkop-Schnurch, F. Gabor, M. Szostak, W. Lubitz, An adhesive drug delivery system based on K99-fimbrae, Eur J Pharm Sci, 3 (1995) 293-299.

[133] M. Roldo, M. Hornof, P. Caliceti, A. Bernkop-Schnurch, Mucoadhesive thiolated chitosans as platforms for oral controlled drug delivery: synthesis and in vitro evaluation, Eur J Pharm Biopharm, 57 (2004) 115-121.
[134] S. Sajeesh, C. Vauthier, C. Gueutin, G. Ponchel, C.P. Sharma, Thiol functionalised polymethacrylic acid-based hydrogel microparticles for oral insulin delivery, Acta Biomaterialia, 6 (2010) 3072-3080.
[135] C.D. Pritchard, T.M. O'Shea, D.J. Siegwart, E. Calo, D.G. Anderson, F.M. Reynolds, J.A. Thomas, J.R. Slotkin, E.J. Woodard, R. Langer, An injectable thiol-acrylate poly(ethylene glycol) hydrogel for sustained release of methylprednisolone sodium succinate, Biomaterials, 32 (2011).
[136] A.A. Aimetti, A.J. Machen, K.S. Anseth, Poly(ethylene glycol) hydrogels formed by thiol-ene photopolymerisation for enzyme-responsive protein delivery, Biomaterials, 30 (2009) 6048-6054.
[137] L. Jiang, L. Gao, X. Wang, L. Tang, J. Ma, The application of mucoadhesive polymers in nasal drug delivery, Drug Dev Ind Pharm, 36 (2010) 323-336.
[138] W. Rencher, Bioadhesive pharmaceutical carrier, US5192802, 1993.
[139] B. Mehta, R. Shah, M. Doshi, Novel stomatological gel, US20050214230, 2005.
[140] A. Fernandez, A. Garcia, R. Martin, M. Olaechea, J. Munoz, A. Gascon, Semi-solid mucoadhesive formulations, US20060240111, 2006.
[141] M. Prinin, Bioadhesive gel based on hydroxyethylcellulose, US20070031479S, 2007.
[142] G. Bottoni, P. Maffei, A. Sforzini, M. Federici, C. Caramella, S. Rossi, V. Claudio, Mucoadhesive xyloglucan containing formulations useful in medical devices and in pharceutical formulations, US20090081133, 2009.
[143] C. Perman, R. Skwieczynski, Aqueous gel formulations containing immune response modifiers, US20090163532, 2009.
[144] E. Tijsma, M. Gonzalez, N. Schalffhausen, E. Tenbroeck, Protective gel based on chitosan and oxidised polysaccharide, US2009027034, 2009.
[145] M. Gonzalez, E. Tijsma, N. Schalffhausen, Thiolated chitosan gel, US20090269417, 2009.
[146] H. Nazar, D.G. Fatouros, S.M. van der Merwe, N. Bouropoulos, G. Avgouropoulos, J. Tsibouklis, M. Roldo, Thermosensitive hydrogels for nasal drug delivery: The formulation and characterisation of systems based on *N*-trimethyl chitosan chloride, Eur J Pharm Biopharm, 77 (2011) 225-232.
[147] S. Khan, K. Patil, N. Bobade, P. Yeole, R. Gaikwad, Formulation of intranasal mucoadhesive temperature-mediated in situ gel containing ropinirole and evaluation of brain targeting efficiency in rats, J Drug Targeting, 18 (2010) 223-234.
[148] P. Ved, K. Kim, Poly(ethylene oxide/propylene oxide) copolymer thermo-reversible gelling system for the enhancement of intranasal zidovudine delivery to the brain, Int J Pharm, 411 (2011) 1-9.
[149] M. Nguyen, D. Lee, Bioadhesive PAA-PEG-PAA triblock copolymer hydrogels for dryg delivery in oral cavity, Macromolecular Res, 18 (2010) 284-288.
[150] P. Gupta, K. Vermani, S. Garg, Hydrogels: from controlled release to pH-responsive drug delivery, Drug Discovery Today, 7 (2002) 569-579.
[151] G. Sharma, M. Srikanth, M. Uhumwangho, K. Phani Kumar, K. Ramana Murthy, Recent trends in pulsatile drug delivery systems - A review, Int J Drug Deliv 2(2010) 200-212.
[152] W. Qi, X. Yan, L. Duan, Y. Yang, J. Li, Glucose-sensitive microcapsules from gluteraldehyde cross-linked hemoglobin and glucose oxidase, Biomacromol, 10 (2009) 1212-1216.
[153] R. Yin, K. Wang, J. Han, J. Nie, Photo-crosslinked glucose-sensitive hydrogels based on methacrylate modified dextran-concanavalin and PEG dimethacrylate, Carbohyd Polym, 82 (2010) 412-418.
[154] X. Jin, X. Zhang, Z. Wu, D. Teng, X. Zhang, Y. Wang, e. al, Amphiphilic random glycopolymer based on phenylboronic acid: Synthesis, characterisation, and potential as glucose-sensitive matrix, Biomacromol, 10 (2009) 1337-1345.

[155] D. Jason, R. Matthew, K. Santoshkumar, W. Yinan, K. Sapna, G. Leonides, e. al, Glucose responsive hydrogel networks based on protein recognition, Macromolecular Bioscience, 9 (2009) 864-868.
[156] D. Roy, J. Cambre, B. Sumerlin, Future perspectives and recent advances in stimuli-responsive materials, Prog Polym Sci, 35 (2010) 278-301.
[157] T. Miyata, N. Asami, T. Uragami, A reversibly antigen-responsive hydrogel, Nature, 399 (1999) 766-769.
[158] M. Kurisawa, N. Yui, Dual-stimuli-responsive drug release from interpenetrating polymer network-structured hydrogels of gelatin and dextran, J Control Release, 54 (1998) 191-200.
[159] L. Wang, M. Liu, C. Gao, L. Ma, D. Cui, A pH-, thermo-, and glucose-, triple-responsive hydrogels: Synthesis and controlled drug delivery, Reactive and Functional Polymers, 70 (2010) 159-167.
[160] A. Gutowska, J.S. Bark, I.C. Kwon, Y.H. Bae, Y. Cha, S.W. Kim, Squeezing hydrogels for controlled drug delivery, J Control Release, 48 (1997) 141-148.
[161] S. Koutsopoulos, L.D. Unsworth, Y. Nagai, S. Zhang, Controlled release of functional proteins through designer self-assembling peptide nanofiber hydrogel scaffold, PNAS, 106 (2009) 4623-4628.
[162] Y. Nagai, L.D. Unsworth, S. Koutsopoulos, S. Zhang, Slow release of molecules in self-assembling peptide nanofiber scaffold, J Control Release, 115 (2006) 18-25.
[163] A. Altunbas, S.J. Lee, S.A. Rajasekaran, J.P. Schneider, D.J. Pochan, Encapsulation of curcumin in self-assembling peptide hydrogels as injectable drug delivery vehicles, Biomaterials, 32 (2011) 5906-5914.
[164] H. Renliang, Q. Wei, F. Libin, R. Su, Z. He, Self assembling peptide polysaccharide hybrid hydrogel as a potential carrier for drug delivery, Soft Matter, 7 (2011) 6222-6230.
[165] S. Zhang, Emerging biological materials through molecular self-assembly, Biotechnol. Advances, 20 (2002) 321-339.
[166] W. Wang, H. Wang, C. Ren, J. Wang, M. Tan, J. Shen, Z. Yang, P.G. Wang, L. Wang, A saccharide-based supramolecular hydrogel for cell culture, Carbohyd Res, 346 (2011) 1013-1017.
[167] J. Chen, K. Park, Synthesis and characterisation of superporous hydrogel composites, J Control Release, 65 (2000) 73-82.
[168] F.A. Dorkoosh, J. Brusse, J.C. Verhoef, G. Borchard, M. Rafiee-Tehrani, H.E. Junginger, Preparation and NMR characterisation of superporous hydrogels (SPH) and SPH composities, Polymer, 41 (2000) 8213-8220.
[169] C. Tang, C. Yin, Y. Pei, M. Zhang, L. Wu, New superporous hydrogels composites based on aqueous Carbopol solution (SPHCcs): synthesis, characterisation and in vitro bioadhesive force studies, Eur Polym J, 41 (2005).
[170] L. Yin, L. Fei, F. Cui, C. Tang, C. Yin, Superporous hydrogels containing poly(acrylic acid-co-acrylamide)/O-carboxymethyl chitosan intepenetrating polymer networks, Biomaterials, 28 (2007) 1258-1266.
[171] F.A. Dorkoosh, J.C. Verhoef, G. Borchard, M. Rafiee-Tehrani, H.E. Junginger, Development and characterisation of a novel peroral peptide drug delivery system, J Control Release, 71 (2001) 307-318.
[172] F.A. Dorkoosh, G. Borchard, M. Rafiee-Tehrani, J.C. Verhoef, H.E. Junginger, Evaluation of superporous hydrogel (SPH) and SPH composite in porcine intestine *ex-vivo*: assessment of drug transport, morphology effect, and mechanical fixation to intestinal wall, Eur J Pharm Biopharm, 53 (2002) 161-166.
[173] D. Kim, K. Park, Swelling and mechanical properties of superporous hydrogels of poly(acrylamide-co-acrylic acid/polyethylenimine interpenetrating polymer networks, Polymer, 45 (2004) 189-196.
[174] L. Yin, J. Ding, J. Zhang, C. He, C. Tang, C. Yin, Polymer integrity related absorption mechanism of superporous hydrogel containing intepenetrating polymer networks for oral delivery of insulin, Biomaterials, 31 (2010) 3347-3356.

[175] L. Verestiuc, O. Nastasescu, E. Barbu, I. Sarvaiya, K.L. Green, J. Tsibouklis, Functionalised chitosan-NIPAM/HEMA hybrid polymer network as inserts for ocular drug delivery: synthesis, in-vitro assessment and in-vivo evaluation, J Biomed Materials Res, 77A (2006) 726-735.
[176] R. Pelton, Temperature-sensitive aqueous microgels, Advances in Colloid and Interface Science, 85 (2000) 1-35.
[177] M. Malsten, H. Bysell, P. Hansson, Biomacromolecules in microgels - Opportunities and challenges for drug delivery, Curr Opin Colloid Interface Sci, 15 (2010) 435-444.
[178] M.M. Yallapu, M. Jaggi, S.C. Chauhan, Design and engineering of nanogels for cancer treatment, Drug Discovery Today, 16 (2011) 457-463.
[179] S.V. Vinogradov, Polyplex nanogel formulations for frug delivery of cytotoxic nucleoside analogs, J Control Release, 107 (2005) 143-157.
[180] Y. Shin, J.H. Chang, J. Liu, R. Williford, Y.-K. Shin, G.J. Exarhos, Hybrid nanogels for sustainable positive thermosensitive drug release, J Control Release, 73 (2001) 1-6.
[181] N.V. Nukolova, H.S. Oberoi, S.M. Cohen, A.V. Kabanov, T.K. Bronich, Folate-decorated nangels for targeted therapy of overian cancer, Biomaterials, 32 (2011) 5417-5426.
[182] N. Li, J. Wang, X. Yang, L. Li, Novel nanogels as drug delivery systems for poorly soluble anticancer drugs, Colloids and Surfaces B: Biointerfaces, 83 (2011) 237-244.
[183] M. Kettel, F. Dierkes, K. Schasfer, M. Moeller, A. Pich, Aqueous nanogels modified with cylclodextrin, Polymer, 52 (2011) 1917-1924.
[184] E. Barbu, L. Verestiuc, M. Iancu, A. Jatariu, A. Lungu, J. Tsibouklis, Hybrid polymeric hydrogels for ocular drug delivery: nanoparticulate systems from copolymers of acrylic acid-functionalised chitosan and *N*-isopropylacrylamide or 2-hydroxyethyl methacrylate, Nanotechnol, 20 (2009).
[185] M.I. Ugwoke, R.U. Agu, N. Verbeke, R. Kinget, Nasal mucoadhesive drug delivery: Background, applications, trends and future perspectives, Adv Drug Deliv Rev, 57 (2005) 1640-1665.
[186] R.U. Agu, H.V. Dang, M. Jorissen, T. Willems, R. Kinget, N. Verbeke, Nasal absorption enhancement strategies for therapeutic peptides: an in vitro study using cultured human nasal epithelium, Int J Pharm, 237 (2002) 179-191.
[187] M. Amidi, S.G. Romeijn, G. Borchard, H.E. Junginger, W.E. Hennink, W. Jiskoot, Preparation and characterization of protein-loaded N-trimethyl chitosan nanoparticles as nasal delivery system, J Control Release, 111 (2006) 107-116.
[188] E.S. Khafagy, M. Morishita, K. Isowa, J. Imai, K. Takayama, Effect of cell-penetrating peptides on the nasal absorption of insulin, J Control Release, 133 (2009) 103-108.
[189] T. Kissel, U. Werner, Nasal delivery of peptides: An *in vitro* cell culture model for the investigation of transport and metabolism in human nasal epithelium, J Control Release, 53 (1998) 195-203.
[190] J. Wang, Y. Tabata, K. Morimoto, Aminated gelatin microspheres as a nasal delivery system for peptide drugs: Evaluation of in vitro release and in vivo insulin absorption in rats, J Control Release, 113 (2006) 31-37.
[191] M.I. Ugwoke, N. Verbeke, R. Kinget, The biopharmaceutical aspects of nasal mucoadhesive drug delivery, J Pharm Pharmacol, 53 (2001) 3-21.
[192] N. Uchida, Y. Maitani, Y. Machida, M. Nakagaki, T. Nagai, Influence of bile-salts on the permability of insulin through the nasal-mucus of rabbits in comparison with dextran derivatives Int J Pharm, 74 (1991) 95-103.
[193] L. Mayo, F. Quaglia, A. Borzacchiello, L. Ambrosio, M.I. La Rotonda, A novel poloxamers/hyaluronic acid in situ forming hydrogel for drug delivery: rheological, mucoadhesive and in vitro release properties, Eur J Pharm Biopharm, 70 (2008) 199-206.
[194] S. Charlton, N. Jones, S. Davis, L. Illum, , Distribution and clearance of bioadhesive formulations from the olfactory region in man: Effect of polymer type and nasal delivery device, Eur J Pharm Sci, 30 (2007) 295-302.
[195] J. Berger, A. Reist, A. Chenite, O. Felt-Baeyens, J.M. Mayer, R. Gurny, Pseudo-thermosetting chitosan hydrogels for biomedical application, Int J Pharm, 288 (2005) 197-206.

[196] H.Q. Chen, M.W. Fan, Novel thermally sensitive pH-dependent chitosan/carboxymethyl cellulose hydrogels, J Bioactive Compatible Polym, 23 (2008) 38-48.
[197] M.N.V.R. Kumar, R.A.A. Muzzarelli, C. Muzzarelli, H. Sashiwa, A.J. Domb, Chitosan Chemistry and Pharmaceutical Perspectives, Chem Rev, 104 (2004) 6017-6084.
[198] L.S. Nair, T. Starnes, J.W.K. Ko, C.T. Laurencin, Development of injectable thermogelling chitosan-inorganic phosphate solutions for biomedical applications, Biomacromol, 8 (2007) 3779-3785.
[199] S.M. van der Merwe, J.C. Verhoef, J.H.M. Verheijden, A.F. Kotzé, H.E. Junginger, Trimethylated chitosan as polymeric absorption enhancer for improved peroral delivery of peptide drugs, Eur J Pharm Biopharm, 58 (2004) 225-235.
[200] A. Chenite, M. Buschmann, D. Wang, C. Chaput, N. Kandani, Rheological characterisation of thermogelling chitosan/glycerol-phosphate solutions, Carbohyd Polym, 46 (2001) 39-47.
[201] Y. Chang, L. Xiao, Y. Du, Preparation and properties of a novel thermosensitive *N*-trimethyl chitosan hydrogel, Polym Bull, 63 (2009) 531-545.
[202] A.B. Sieval, M. Thanou, A.F. Kotze, J.E. Verhoef, J. Brussee, H.E. Junginger, Preparation and NMR characterization of highly substituted *N*-trimethyl chitosan chloride, Carbohydr Polym, 36 (1998) 157-165.
[203] F. Chen, Z.R. Zhang, Y. Huang, Evaluation and modification of *N*-trimethyl chitosan chloride nanoparticles as protein carriers, Int J Pharm, 336 (2007) 166-173.
[204] J. Wu, Z.G. Su, G.H. Ma, A thermo- and pH-sensitive hydrogel composed of quaternized chitosan/glycerophosphate, Int J Pharm, 315 (2006) 1-11.
[205] Q.X. Ji, Q.S. Zhao, J. Deng, R. Lu, A novel injectable chlorhexidine thermosensitive hydrogel for periodontal application: preparation, antibacterial activity and toxicity evaluation, J Materials Sci-Materials in Medicine, 21 (2010) 2435-2442.
[206] A.J. Shah, M.D. Donovan, Formulating gels for decreased mucociliary transport using rheological properties: polyacrylic acids, AAPS Pharm Sci Tech, 8 (2007) article 33.
[207] J.H. Hamman, A.F. Kotze, Effect of the type of base and number of reaction steps on the degree of quaternization and molecular weight of *N*-trimethyl chitosan chloride, Drug Dev Ind Pharm, 27 (2001) 373-380.
[208] M. Thanou, A.F. Kotze, T. Scharringhausen, H.L. Luessen, A.G. de Boer, J.C. Verhoef, H.E. Junginger, Effect of degree of quaternization of *N*-trimethyl chitosan chloride for enhanced transport of hydrophilic compounds across intestinal Caco-2 cell monolayers, J Control Release, 64 (2000) 15-25.
[209] H. Chung, H. Dong, Synthesis and characterisation of Pluronic grafted chitosan copolymer as a novel injectable biomaterial, Curr Appl Phys, 5 (2005) 485-488.
[210] I.K. Han, Y.B. Kim, H.S. Kang, D. Sul, W.W. Jung, H.J. Cho, Y.K. Oh, Thermosensitive and mucoadhesive delivery systems of mucosal vaccines, Methods, 38 (2006) 106-111.
[211] M. Hasegawa, A. Isogai, F. Onabe, M. Usuda, R.H. Atalla, Characterization of cellulose chitosan blend films, J Appl Polym Sci, 45 (1992) 1873-1879.
[212] C.E. Orrego, N. Salgado, J.S. Valencia, G.I. Giraldo, O.H. Giraldo, C.A. Cardona, Novel chitosan membranes as support for lipases immobilization: characterization aspects, Carbohyd Polym, 79 (2010) 9-16.
[213] W. Groenewoud, Characterisation of polymers by thermal analysis, 1st ed., Elsevier Science, Amsterdam, 2001.
[214] S. Kumar, J. Dutta, P.K. Dutta, Preparation and characterization of *N*-heterocyclic chitosan derivative based gels for biomedical applications, Int J Biol Macromol, 45 (2009) 330-337.
[215] S. Green, M. Roldo, D. Douroumis, N. Bouropoulos, D. Lamprou, D.G. Fatouros, Chitosan derivatives alter release profiles of model compounds from calcium phosphate implants, Carbohyd Res, 344 (2009) 901-907.
[216] F. Ganji, M.J. Abdekhodaie, A. Ramanzi, Gelation time and degradation rate of chitosan-based injectable hydrogel, J Sol-Gel Sci Techn, 42 (2007) 47-53.

[217] Q.X. Ji, J. Deng, X.M. Xing, C.Q. Yuan, X.B. Yu, Q.C. Xu, J. Yue, Biocompatibility of chitosan-based injectable thermosensitive hydrogel and its effects on dog periodontal tissue regeneration, Carbohydr Polym, 82 (2010) 1153-1160.
[218] S. Kim, S.K. Nishimoto, J.D. Bumgardner, W.O. Haggard, M.W. Gaber, Y. Yang, A chitosan/β-glycerophosphate thermo-sensitive gel for the delivery of ellagic acid for the treatment of brain cancer, Biomaterials, 31 (2010) 4157-4166.
[219] P. Sriamornsak, N. Wattanakorn, Rheological synergy in aqueous mixtures of pectin and mucin, Carbohyd Polym, 74 (2008).
[220] S.A. Mortazavi, B.G. Carpenter, J.D. Smart, An investigation of the rheological behavior of the mucoadhesive mucosal interface, Int J Pharm, 83 (1992) 221-225.
[221] S.A. Mortazavi, B.G. Carpenter, J.D. Smart, A comparative-study on the role played by mucus glycoproteins in the rheological behavior of the mucoadhesive mucosal interface, Int J Pharm, 94 (1993) 195-201.
[222] S.A. Mortazavi, J.D. Smart, Factors influencing gel-strengthening at the mucoadhesive-mucus interface, J Pharm Pharmacol, 46 (1994) 86-90.
[223] Q.Z. Li, D.Z. Yang, G.P. Ma, Q. Xu, X.M. Chen, F.M. Lu, J. Nie, Synthesis and characterization of chitosan-based hydrogels, Int J Biol Macromol, 44 (2009) 121-127.
[224] L.M. Harwood, T.D.W. Claridge, Introduction to Organic Spectroscopy, Oxford University Press, Great Britain, 1996.
[225] B.B. Mandal, S. Kapoor, S.C. Kundu, Silk fibroin/polyacrylamide semi-interpenetrating network hydrogels for controlled drug release, Biomaterials, 30 (2009) 2826-2836.
[226] A. Bernkop-Schnurch, The use of inhibitory agents to overcome the enzymatic barrier to perorally administered therapeutic peptides and proteins, J Control Release, 52 (1998) 1-16.
[227] B.J. Aungst, Intestinal permeation enhancers, J Pharm Sci, 89 (2000) 429-442.
[228] S. Khan, K. Patil, N. Bobade, P. Yeole, R. Gaikwad, Formulation of intranasal mucoadhesive temperature-mediated *in situ* gel containing ropinirole and evaluation of brain targeting efficiency in rats, J Drug Targeting, 18 (2010) 223-234.
[229] Y.H. Cheng, A.M. Dyer, I. Jabbal-Gill, M. Hinchcliffe, R. Nankervis, A. Smith, P. Watts, Intranasal delivery of recombinant human growth hormone (somatropin) in sheep using chitosan-based powder formulations, Eur J Pharm Sci, 26 (2005) 9-15.
[230] J. Wang, Y. Tabata, K. Morimoto, Aminated gelatin microspheres as a nasal delivery system for peptide drugs: Evaluation of *in vitro* release and *in vivo* insulin absorption in rats, J Control Release, 113 (2006) 31-37.
[231] X.G. Zhang, H.J. Zhang, Z.M. Wu, Z. Wang, H.M. Niu, C.X. Li, Nasal absorption enhancement of insulin using PEG-grafted chitosan nanoparticles, Eur J Pharm Biopharm, 68 (2008) 526-534.
[232] S.Y. Yu, Y. Zhao, F.L. Wu, X. Zhang, W.L. Lu, H. Zhang, Q. Zhang, Nasal insulin delivery in the chitosan solution: *in vitro* and *in vivo* studies, Int J Pharm, 281 (2004) 11-23.
[233] R.U. Agu, H.V. Dang, M. Jorissen, T. Willems, R. Kinget, N. Verbeke, Nasal absorption enhancement strategies for therapeutic peptides: an *in vitro* study using cultured human nasal epithelium, Int J Pharm, 237 (2002) 179-191.
[234] M. Amidi, S.G. Romeijn, G. Borchard, H.E. Junginger, W.E. Hennink, W. Jiskoot, Preparation and characterization of protein-loaded *N*-trimethyl chitosan nanoparticles as nasal delivery system, J Control Release, 111 (2006) 107-116.
[235] C. Witschi, R.J. Mrsny, *In vitro* evaluation of microparticles and polymer gels for use as nasal platforms for protein delivery, Pharm Res, 16 (1999) 382-390.
[236] B.Q. Shen, W.E. Finkbeiner, J.J. Wine, R.J. Mrsny, J.H. Widdicombe, Calu-3: A human airway epithelial cell line that shows cAMP-dependent Cl- secretion, Am J Physiol, 266 (1994) L493-L501.
[237] D. Cremaschi, C. Porta, R. Ghirardelli, Endocytosis of polypeptides in rabbit nasal respiratory mucosa, News in Physiological Sciences, 12 (1997) 219-225.
[238] R.W. Korsmeyer, R. Gurny, E. Doelker, P. Buri, N.A. Peppas, Mechanisms of solute release from porous hydrophilic polymers, Int J Pharm, 15 (1983) 25-35.

[239] P.I. Lee, C.J. Kim, Probing the mechanisms of drug release from hydrogels, J Control Release, 16 (1991) 229-236.
[240] R.W. Korsmeyer, R. Gurny, E. Doelker, P. Buri, N.A. Peppas, Mechanisms of solute release from porous hydrophilic polymers, Int J Pharm, 15 (1983) 25-35.
[241] I. Molina, S.M. Li, M.B. Martinez, M. Vert, Protein release from physically crosslinked hydrogels of the PLA/PEO/PLA triblock copolymer-type, Biomaterials, 22 (2001) 363-369.
[242] S. Gordon, A. Saupe, W. McBurney, T. Rades, S. Hook, Comparison of chitosan nanoparticles and chitosan hydrogels for vaccine delivery, J Pharm Pharmacol, 60 (2008) 1591-1600.
[243] C. Ortiz, D. Zhang, Y. Xie, J. Davisson, D. Ben-Amotz, Identification of insulin variants using Raman spectroscopy, Analytical Biochem, 332 (2004) 245-252.
[244] I.J. Galpin, G. Hancock, W. Kenner, B.A. Morgan, The synthesis of an insulin active site analogue, Tetrahedron, 39 (1983) 149-158.
[245] J. Brange, L. Langkjaer, Chemical stability of insulin. 3. Influence of excipients, formulation, and pH, Acta Pharm Nord, 4 (1992) 149-158.
[246] A.A. Elkordy, R.T. Forbes, B.W. Barry, Study of protein conformational stability and integrity using calorimetry and FT-Raman spectroscopy correlated with enzymatic activity, Eur J Pharm Sci, 33 (2008) 177-190

[247] S.Y. Yu, Y. Zhao, F.L. Wu, X. Zhang, W.L. Lu, H. Zhang, Q. Zhang, Nasal insulin delivery in the chitosan solution: in vitro and in vivo studies, Int J Pharm, 281 (2004) 11-23.
[248] T.-W. Chung, D.-Z. Liu, J.-S. Yang, Effects of interpenetration of thermo-sensitive gels by crosslinking of chitosan on nasal delivery of insulin: *In vitro* characterisation and *in vivo* study, Carbohyd Polym, 82 (2010) 316-322.
[249] X. Zhang, H. Zhang, Z.M. Wu, Z. Wang, H. Niu, C.X. Li, Nasal absorption anhancement of insulin using PEG-grafted chitosan particles, Eur J Pharm Biopharm, 68 (2007) 526-534.
[250] T.J. Aspden, L. Illum, O. Skaugrud, Chitosan as a nasal delivery system: evaluation of insulin absorption enhancement and effect on nasal membrane integrity using rat models, Eur J Pharm Sci, 4 (1996) 23-31.
[251] L. Jorgensen, C. Vermehren, S. Bjerregaard, S. Froekjaer, Secondary structure alterations in insulin and growth hormone water-in-oil emulsions, Int J Pharm, 254 (2003) 7-10.
[252] J.L.E. Reubsaet, J.H. Beijnen, A. Bult, R.J. van Maanen, J.A. Danielle Marchal, W.J.M. Underberg, Analytical techniques to study the degradtion of proteins and peptides: chemical instability, J Pharmaceutical and Biomed Anal, 17 (1998) 955-978.
[253] F.W.J. Teale, The ultraviolet fluorescence of proteins in neutral solution, Biochem J, 76 (1960) 381-388.
[254] C. Binder, Artificial systems for insulin delivery, Raven Press, New York, 1983.
[255] J. Brange, G. Dodson, B. Xiao, Designing insulin for diabetes therapy by protein engineering, Curr Opin Struct Biol, 1 (1991) 934-940.
[256] V.L. Lassalle, M.L. Ferreira, Experimental problems in the application of UV/visible based methods as the quantification tool for the entrapped/released insulin from PGLA carriers, J Chem Technol Biotechnol, 84 (2009) 1267-1273.
[257] N.-Y. Yu, C.S. Liu, D.C. O'Shea, Laser Raman spectroscopy and the conformation of insulin and proinsulin, J Mol Biol, 70 (1972) 117-132.
[258] M.A.H. Capelle, R. Gurny, T. Arvinte, High throughput screening of protein formulation stability: Practical considerations, Eur J Pharm Biopharm, 65 (2007) 131-148.
[259] M. Gumusderelioglu, H. Turkoglu, Biomodification of non-woven polyester fabrics by insulin and RGD for use in serum-free cultivation of tissue cells, Biomaterials, 23 (2002) 3927-3935.
[260] S. Krimm, J. Bandekar, Vibrational spectroscopy and conformation of peptides, polypeptides and proteins, Adv Protein Chem, 38 (1986) 181-364

[261] J.K. Sahni, S. Chopra, F.J. Ahmad, R.K. Khar, Potential prospects of chitosan derivative trimethyl chitosan chloride (TMC) as a polymeric absorption enhancer: synthesis, characterisation and applications, J Pharm Pharmacol, 60 (2008) 1111-1119.
[262] J.K. Sahni, S. Chopra, F.J. Ahmad, R.K. Khar, Potential prospects of chitosan derivative trimethyl chitosan chloride (TMC) as a polymeric absorption enhancer: synthesis, characterization and applications, J Pharm Pharmacol, 60 (2008) 1111-1119.
[263] M. Thanou, J.C. Verhoef, H.E. Junginger, Chitosan and its derivatives as intestinal absorption enhancers, Adv Drug Deliv Rev, 50 (2001) S91-S101.
[264] M.M. Thanou, J.C. Verhoef, S.G. Romeijn, J.F. Nagelkerke, F. Merkus, H.E. Junginger, Effects of *N*-trimethyl chitosan chloride, a novel absorption enhancer, on Caco-2 intestinal epithelia and the ciliary beat frequency of chicken embryo trachea, Int J Pharm, 185 (1999) 73-82.
[265] A.K. Agrawal, P.N. Gupta, A. Khanna, R.K. Sharma, H.K. Chandrawanshi, N. Gupta, U.K. Patil, S.K. Yadav, Development and characterisation of *in situ* gel system for nasal insulin delivery, Pharmazie, 65 (2010) 188-193.
[266] A.M. Dyer, M. Hinchcliffe, P. Watts, J. Castile, I. Jabbal-Gill, R. Nankervis, A. Smith, L. Illum, Nasal delivery of insulin using novel chitosan based formulations: A comparative study in two animal models between simple chitosan formulations and chitosan nanoparticles, Pharm Res, 19 (2002) 998-1008.
[267] K. Morimoto, K. Morisaka, A. Kamada, Enhancement of nasal absorption of insulin and calcitonin using polyacrylic acid gel, J Pharm Pharmacol, 37 (1985) 134-136.
[268] R. D'Souza, S. Mutalik, M. Venkatesh, S. Vidyasagar, N. Udupa, Nasal insulin gel as an alternate to parenteral insulin: formulation, preclinical and clinical studies, AAPS Pharm Sci Tech, 6 (2005).
[269] T.-W. Chung, D.-Z. Liu, J.-S. Yang, Effects of interpenetration of thermosensitive gels by cross-linking of chitosan on nasal delivery of insulin: *In vitro* charactersation and in vivo study, Carbohyd Polym, 82 (2010) 316-322.
[270] L. Illum, Nasal drug delivery: possibilities, problems and solutions, J Control Release, 87 (2003) 187-198.
[271] P. Artusson, T. Lindmark, S.S. Davis, L. Illum, Effect of chitosan on the permeability of monolayers of intestinal epithelial cells (Caco-2), Pharm Res, 11 (1994) 1358-1361.
[272] H.L. Luessen, B.J. De-Leeuw, M. Langemeyer, A.G. De Boer, J.C. Verhoef, H.E. Unginger, Mucoadhesive polymers in peroral peptide drug delivery. IV. Carbomer and chitosan improve the intestinal absorption of the peptide drug buserelin in vivo, Pharm Res, 13 (1996) 1668-1672.
[273] S.B. Rao, C.P. Sharma, Use of chitosan as a biomaterial: studies on its safety and hemostatic potential, J Biomed Materials Res, 34 (1997) 21-28.
[274] R. Chen, H.C. Chen, Chitin enzymology-chitinase, Adv Chtin Sci, 3 (1998) 16-23.
[275] C. Muzzarelli, Human enzymatic activities related to the therapeutic administration of chitin derivatives, Cell Mol Life Sci, 53 (1997) 131-140.
[276] S. Hirano, H. Seino, Y. Akiyama, I. Nonaka, Biocomaptibility of chitosan by oral and intravenous administrations, Poly Eng Sci, 59 (1988) 897-901.
[277] S. Hirano, Y. Noishiki, The blood compatibility of chitosan and N-acylchitosans, J Biomed Materials Res, 19 (1985) 413-417.
[278] C.-M. Lehr, J.A. Bouwstra, E.H. Schacht, *In-vitro* evaluation of mucoadhesive properties of chitosan and some other natural polymers, Int J Pharm, 78 (1992) 43-48.
[279] M. Zhou, M. Donovan, Intranasal mucociliary clearance of putative bioadhesive polymer gels, Int J Pharm, 135 (1996) 115-125.
[280] P. Caliceti, F.M. Veronese, S. Lora, Polyphosphazene microspheres for insulin delivery, Int J Pharm, 211 (2000) 57-65.
[281] A.H. Krauland, V.M. Leitner, V. Grabovac, A.B. Schnch, *In vivo* evaluation of a nasal insulin delivery system based on thiolated chitosan, J Pharm Sci, 95 (2006) 2463-2472.

[282] J.M. Barichello, M. Morishita, K.T.T. Nagai, Absorption of insulin from Pluronic F-127 gels following subcutaneous administration in rats, Int J Pharm, 184 (1999) 189-198.